1-1-2018

Brønsted Acid Catalyzed Carbon-Carbon Bond Forming Reactions

Jiangyue Miao
University of Denver

Brønsted Acid Catalyzed Carbon-Carbon Bond Forming Reactions

Abstract

The focus of this research project lies in the development of new methodology in the field of Brønsted acid catalysis enabling rapid synthesis of medicinally relevant compounds. It is foreseen that small molecule sulfonic acids evaluated in this research project will unveil new asymmetric carbon carbon bond forming reactions between substrates hitherto unexplored with Brønsted acid catalysis. It has been established that strong Brønsted acids, such as phosphoric acids, are capable of mediating highly selective transformations operating through unique mechanistic manifolds.

Specific focus for the sulfonic acid catalysts was geared towards asymmetric coupling reactions with synthetically useful precursors such as azlactones. We have discovered a novel coupling reaction between azlactones and acetals with Brønsted acid catalysis, with simple and universal purification procedure, pure products were isolated with some diastereoselectivities.

The implementation of Newman-Kwart rearrangement afforded desired mono-protic BINOL based sulfonic acid was successfully performed. This will be followed by evaluating sulfonic acid catalytic efficiencies towards asymmetric coupling reactions.

The total synthesis of latifolian A through application of a chiral sulfonic acid catalyzed Friedel–Crafts cyclization reaction as a key synthetic step was designed. This is an ongoing investigation but is promising in the new treatment of Alzheimer's that have potential benefits in medicinal chemistry.

Document Type

Dissertation

Degree Name

Ph.D.

Department

Chemistry and Biochemistry

First Advisor

Bryan J. Cowen, Ph.D.

Keywords

Aldol reactions, Brønsted acid catalysis, Carbon-carbon bond forming, Diastereoselectivity, Sulfonic acids

Subject Categories

Biochemistry | Chemistry | Organic Chemistry

Brønsted Acid Catalyzed Carbon-Carbon Bond Forming Reactions

_____

A Dissertation

Presented to

the Faculty of Natural Sciences and Mathematics

University of Denver

_____

In Partial Fulfillment

of the Requirements for the Degree

Doctor of Philosophy

_____

by

Jiangyue Miao

November 2018

Advisor: Dr. Bryan J. Cowen

Author: Jiangyue Miao
Title: Brønsted Acid Catalyzed Carbon-Carbon Bond Forming Reactions
Advisor: Dr. Bryan J. Cowen
Degree Date: November 2018

ABSTRACT

The focus of this research project lies in the development of new methodology in the field of Brønsted acid catalysis enabling rapid synthesis of medicinally relevant compounds. It is foreseen that small molecule sulfonic acids evaluated in this research project will unveil new asymmetric carbon carbon bond forming reactions between substrates hitherto unexplored with Brønsted acid catalysis. It has been established that strong Brønsted acids, such as phosphoric acids, are capable of mediating highly selective transformations operating through unique mechanistic manifolds.

Specific focus for the sulfonic acid catalysts was geared towards asymmetric coupling reactions with synthetically useful precursors such as azlactones. We have discovered a novel coupling reaction between azlactones and acetals with Brønsted acid catalysis, with simple and universal purification procedure, pure products were isolated with some diastereoselectivities.

The implementation of Newman-Kwart rearrangement afforded desired mono-protic BINOL based sulfonic acid was successfully performed. This will be followed by evaluating sulfonic acid catalytic efficiencies towards asymmetric coupling reactions.

The total synthesis of latifolian A through application of a chiral sulfonic acid catalyzed Friedel–Crafts cyclization reaction as a key synthetic step was designed. This is an ongoing investigation but is promising in the new treatment of Alzheimer's that have potential benefits in medicinal chemistry.

ACKNOWLEDGEMENTS

First and foremost, I would like to thank my advisor, Dr. Bryan Cowen, for the opportunity he gave me to join his group. This experience has been rewarding on many levels, I cannot thank him enough for his incredible support, patience and understanding over the last few years, not to mention the irreplaceable knowledge from him.

I would also like to thank all the other professors and mentors at the University of Denver, their dedication in teaching and scientific enthusiasm had a profound influence during my career as a graduate student. A special thanks to all the graduate students, past and present, for showing me support and friendship over the years. I will cherish the memory of my stay in DU and great times I had with my labmates.

This journey would not have been possible without the support of my family, I am especially grateful to my husband, Zhelin Yu, and my parents, who supported me unconditionally. I always knew that you believed in me and wanted the best for me, thank you for listening, offering me advice, and supporting me through this entire process.

TABLE OF CONTENTS

LIST OF FIGURES

LIST OF ABBEVIATIONS AND ACRONYMS

Å	Ångstrom
α	alpha
β	beta
Δ	heat
°C	degrees Celsius
Ac	acetyl
aq.	aqueous
Ar	aryl
BBr_3	boron tribromide
BINOL	1,1'-bi-2-naphthol
Boc	tert-butyloxycarbonyl
calcd	calculated
cat.	catalyst (or catalytic amount)
$CHCl_3$	chloroform
$CDCl_3$	deuterated chloroform
C_6D_6	deuterated benzene
CH_3CN	acetonitrile
Cs_2CO_3	cesium carbonate
CSA	camphorsulfonic acid
DCM	dichloromethane
DMAP	4-dimethylaminopyridine
DMF	dimethylformamide
DMSO	dimethyl sulfoxide
dr	diastereomeric ratio
Et	ethyl
EtOAc	ethyl acetate
Et_2O	diethyl ether

ee	enantiomeric excess
eq.	equivalent
FDA	U.S. food and drug administration
g	gram(s)
h	hour(s)
HRMS	high-resolution mass spectrum
HCl	hydrochloric acid
JNK-3	c-Jun N-terminal kinase 3
KOH	potassium hydroxide
$LiAlH_4$	lithium aluminum hydride
LED	light emitting diode
LUMO	lowest unoccupied molecular orbital
m-CPBA	meta-chloroperoxybenzoic acid
Me	methyl
mg	milligram(s)
µl	microliter
ml	milliliter
M	molar
mmol	millimole
mol	mole
min	minute(s)
$MgSO_4$	magnesium sulfate
MRI	magnetic resonance imaging
MS	molecular sieves
NaH	sodium hydride
NaCl	sodium chloride
$NaBH_4$	sodium borohydride
$NaHCO_3$	sodium bicarbonate
NaOH	sodium hydroxide

Na_2SO_4	sodium sulfate
NMDA	N-methyl-D-aspartate
NMR	nuclear magnetic resonance
NEt_3	triethylamine
Ph	phenyl
PPh_3	triphenylphosphine
Pr	propyl
PET	positron emission tomography
r.t.	room temperature
R-TRIP	3,3′-bis(2,4,6-triisopropylphenyl)-1,1′-binaphthyl-2,2′-diyl hydrogen phosphate
sat.	saturated
SiO_2	silicon dioxide
SPINOL	1,1’-spirobiindane-7,7’-diol
STRIP	6,6′- bis(2,4,6-triisopropylphenyl)-1,1′-spirobiindan-7,7′-diyl hydrogen phosphate
TADDOL	α, α, α’, α’-tetraaryl-1,3-dioxolan- 4,5-dimethanol
TLC	thin-layer chromatography
TFA	trifluoroacetic acid
TFAA	trifluoroacetic anhydride
TsOH	para-toluenesulfonic acid
THF	tetrahydrofuran
TMS	trimethylsilane
TMSCl	trimethylsilyl chloride
TBDPSCl	tert-butyldiphenylchlorosilane
UV	ultraviolet

CHAPTER ONE: REVIEW OF BRØNSTED ACID REACTIONS AND CATALYTIC STEREOSELECTIVITY RESEARCH

1.1 Introduction and Background of Brønsted Acid Catalysts

In 1923, chemists Johannes Nicolaus Brønsted and Thomas Martin Lowry independently proposed acid and base theory based on the abilities of chemical compounds to either donate or accept protons [1] [2]. In this theory, acids are defined as proton donors which release the hydrogen cation in aqueous solution; whereas bases are defined as proton acceptors which take protons in aqueous solution. When an acid and a base react with each other, the acid forms its conjugate base, and the base forms its conjugate acid by proton transfer. The fundamental concept of Brønsted–Lowry acid-base theory can be expressed in terms of an equilibrium expression:

$$\text{Acid} + \text{Base} \rightleftharpoons \text{Conjugate Base} + \text{Conjugate Acid}$$

With an acid, HA, the equation can be written as:

$$HA + B \rightleftharpoons A^- + HB^+$$

In the same year that Brønsted and Lowry published their theory, G. N. Lewis developed another definition of reactions between acids and bases [3]. In this theory, acids are defined as any substance contains an empty orbital that can accept a pair of nonbonding electrons; and Lewis bases are substance that can donate lone pair electrons to Lewis acids.

A catalyst is a substance that is capable of accelerating a chemical reaction or performing such reaction under milder conditions (such as at a lower temperature) than otherwise possible [4]. In general, catalyzed reactions require less activation energy than the corresponding uncatalyzed reaction, thereby increasing the reaction rate under same reaction conditions (Figure 1.1). Catalysts work by enabling an alternative reaction pathway. “Catalyst stabilized” transition states and “catalyst stabilized” intermediates are all lower in relative energy than the energetically highest transition state of an uncatalyzed reaction, and then the temporary intermediate releases the original catalyst in a cyclic process. In asymmetric catalysis, the role of the catalyst is not limited to just accelerating the reaction, it also forms composition of the products, making one of the enantiomers favored. The difference in ability of a single enantiomer of the catalyst to form two different, diastereomeric transition states leads to two enantiomers of desired product. This origin of asymmetric catalysis enantioselectivity is in the fact that a catalytic amount of a pure enantiomer of the catalyst can afford large amounts of enantioenriched product molecules.

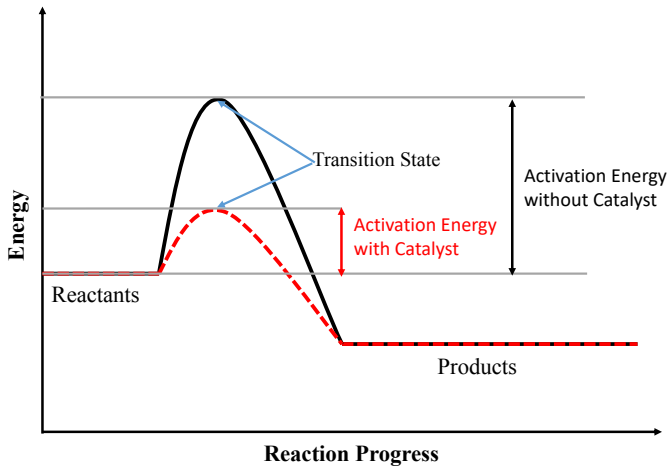

Figure 1.1 Effect of catalysts

Acid catalysis is one of the oldest but the most important and commonly used forms of catalysis in organic synthesis. In most cases, an acid catalyst is employed as a proton source, the proton makes the intermediate charged and more reactive and hence lowers the LUMO energy of the transition state and catalyzes the reaction. Typical reactions that are acid catalyzed include aldol reactions, esterification reactions and ester hydrolysis, etc. For example, the electrophiles in the Mannich reaction are generated from an aldehyde and an amine in the presence of an acid. Many enzymes function through acid-catalysis as well.

Chirality is a property of an object that leading it to be nonsuperimposable on its mirror image [4]. In chemistry and particularly in molecules, there are several elements which would result in this chirality property. Each atom that carries four different substituents in a tetrahedral arrangement is a chirality center. The most common example is a tetrasubstituted carbon atom, but a stererogenic center is not a special characteristic of carbon compounds. Besides point chirality, there are many other molecular substructures that could make molecules chiral (Figure 1.2). Axial chirality is another case of molecular chirality when a molecule does not possess a stereogenic center but has an axis about which a set of substituents is held in a spatial arrangement that is not superimposable on its mirror image. This type of chirality is commonly observed in certain molecules with cumulated double bonds or atropisomeric substituted biaryl compounds. A chirality axis also appears in molecules with a helical shape. Chirality does not result only from a chirality center or chirality axis, but may also arise from another chirality element, namely a chirality plane. A chirality plane is the plane of a

structural fragment in a chiral molecule that cannot lie in a symmetry plane because of restricted rotation or structural requirements. Planar chirality is the special case of chirality for two dimensions. The enantiomers of such a chiral molecule differ in the spatial arrangement of the remaining atoms of the molecule with respect to the chirality plane.

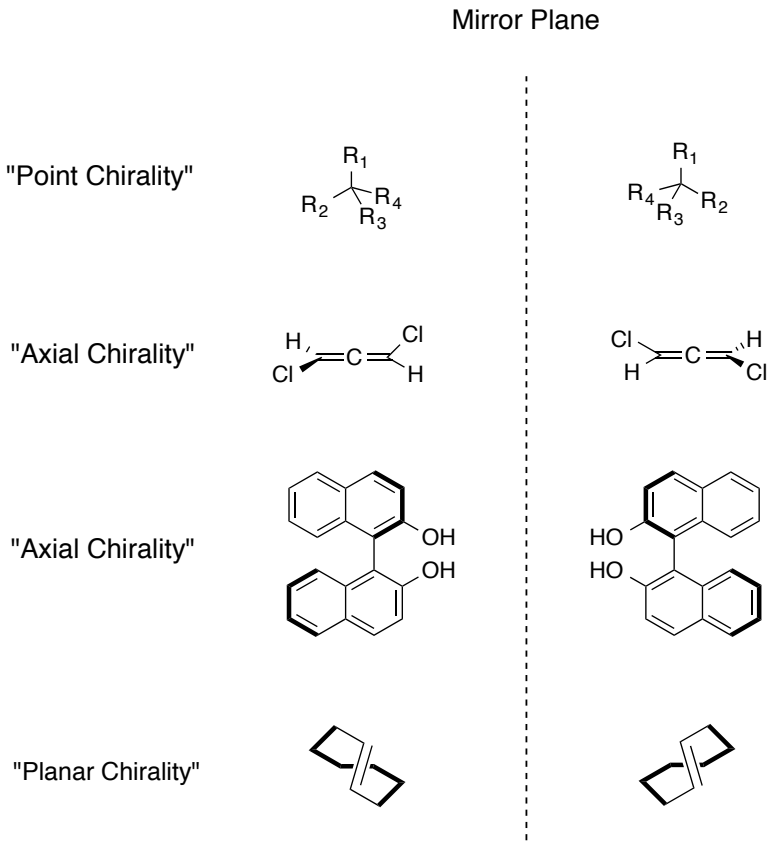

Figure 1.2 Examples of chiral elements

Besides obtaining chiral compounds commercially from the "chiral pool" of existing compounds like amino acids and sugars, there are basically two options to access single enantiomers, either the racemic mixture of a molecule is resolved into separate enantiomers, or the enantioenriched compound is produced by asymmetric synthesis. The

second choice is a more attractive strategy, as it minimizes the site of the undesired enantiomer, which is a general drawback of resolution approaches. In asymmetric synthesis, utilizing starting materials from the chiral pool or of chiral auxiliaries are basic approaches which are well established in industrial processes. External chiral auxiliaries that induce the asymmetry in the target molecule are normally recoverable and recyclable. Natural products often are the source of chirality in these auxiliaries [5].

The stereoselectivity in organic reaction products results from differences in steric effects and electronic effects in the mechanistic pathways and these variances lead to the different stereoisomers. As the differences between activation energy of two mechanistic pathways are limited, stereoselectivity can vary in degree but it cannot be one isomer over the other entirely. Enantiomers are stereoisomers that are mirror images and not identical, an enantioselective reaction is a reaction that one enantiomer is formed in preference to the other, and the degree of selectivity in such reactions is measured by the enantiomeric excess. Diastereomers are stereoisomers that are not mirror images, a diastereoselective reaction is a reaction that one diastereomer is formed in preference to another or one relative stereochemistry dominates the product mixture, the degree of relative selectivity is measured by the diastereomer ratio (dr) [4].

Like other molecular properties that make molecules different, chirality is a distinct geometric characteristic as well. Molecules which are mirror images of one another, like enantiomers, are still different compounds, although they cannot be distinguished from each other in an achiral environment. All living creatures are composed of chiral molecules, and often only one enantiomer or diasteromer is found in

nature. Therefore, when synthesizing a single compound, rather than its racemic mixtures, chirality as well as any other structural property of the molecule must be well controlled.

More than half of the drugs currently in use are chiral compounds and near 90% of them are marketed as racemates consisting of an equimolar mixture of two enantiomers [6]. The effort in realizing pure enantiomers of chiral molecules has significant meanings in organic synthesis. Most importantly, pharmaceutical industry has raised standards in recent years to deal with serious issues resulting from using more easily available racemic or mixtures of enantiomers. Although they have the same chemical structure, most enantiomers of chiral drugs present noticeable differences in biological activities such as pharmacology, toxicology etc. As single enantiomers of chiral compounds like proteins and DNA are parts of our body, and our body provides a chiral environment for any external chiral molecule, the enantiomers of that molecule are expected to have different interaction with our organism. Sometimes these effects between these enantiomers are minor, for example, with enantiomers of the drug molecule having different degrees of activity at target locations. However, the effects can also be profoundly different and lead to serious consequences [4].

Early on 1985, catalysts that rely on hydrogen bond interactions to activate C=X (X = O, NR, CR2) bonds were studied [7], thereby helps to lower LUMO energy and promoting nucleophilic addition to the C=X (X = O, NR, CR2) bonds. These hydrogen bond donating catalysts usually are classified as “organocatalysis”. In organocatalysis, simple organic molecules are used as catalysts instead of metals or enzymes. As non-

metal elements are beneficial to green environment and cutting the cost of expensive metals as well as related toxic impurities, they are also applicable to large-scale synthesis. Chiral organocatalysts enable rapid access to pharmaceutical related compounds and the possibility of their versatile structural modification in mild reaction conditions. Organocatalysis has received increased interest in realizing enantioselective carbon-carbon forming reactions [8].

According to the report by Seayad and List in 2004, most organocatalysts can be classified as Lewis bases, Lewis acids, Brønsted bases and Brønsted acids [9]. They introduced a classification system for organocatalysts based on Brønsted acid/base and Lewis acid/base theories (Figure 1.3). Based on their interaction with substrates, organocatalysts can be classified as proton donors (Brønsted acid), proton acceptors (Brønsted base), electron acceptor (Lewis acid), and electron donors (Lewis base). In Brønsted acid catalysis, the catalyst initiates the catalytic cycle by protonation of nucleophilic substrates. The resulting complex proceeds to undergo a reaction, then product and the catalyst are liberated to enable repetition of the catalytic cycle. Brønsted base catalysis cycles are initiated through a (partial) deprotonation. Lewis acid catalysis and Lewis base catalysis involve catalysts that accept or donate electrons to activate the substrate. Organocatalysts could also facilitate these modes concurrently in the reactions.

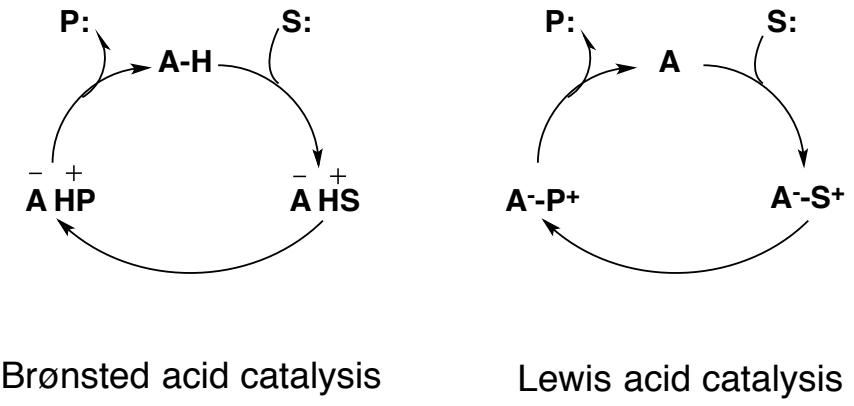

Figure 1.3 Schematic organocatalytic cycles (A = acid, S = substrate, P = product)

Brønsted acid catalysts can generally be divided into two categories, hydrogen bonding catalysts and stronger (or strong) Brønsted acids (Figure 1.4). Hydrogen bonding acts as a ubiquitous glue to support the intricate architecture and functionality of proteins, nucleic acids and many supramolecular components; however, this weak interaction is seldom used as a force for promoting chemical reactions in the past. Hydrogen bonding catalysts are weak Brønsted acids which act by hydrogen bonding to the substrate, rather than fully transferring the proton to it. In other words, hydrogen bonding catalysts are incapable of protonating the substrate. The proton transfer occurs to the transition state in the rate determining step.

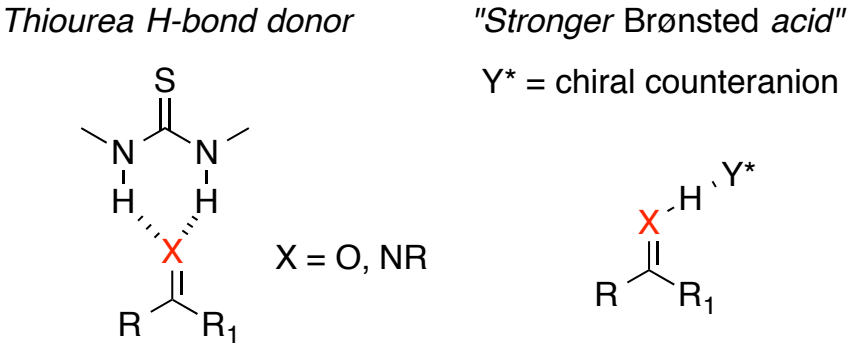

Figure 1.4 Mechanistically activation modes of H-bond donor vs. Brønsted acid catalysis

The most remarkable examples of hydrogen bonding catalysts are chiral thioureas and diols (Figure 1.5). Chiral thioureas as catalysts were accidentally discovered by Sigman and Jacobsen in 1998 for the Strecker reaction [10]. However, the recognition of the general hydrogen bonding activation mode of these catalysts is inspired by the development of organocatalysis years later. Since that initial report, Jacobsen's group has developed a range of chiral thioureas that are versatile, effective organocatalysts. A range of latent nucleophiles can be added to mostly imine-type electrophiles in excellent enantioselectivity with a broad substrate scope. Based on the known fact that polar protic solvents accelerate certain Diels-Alder reactions the group of Rawal developed an asymmetric version of this reaction using a chiral diol TADDOL as the catalyst (Figure 1.5) in toluene [11].

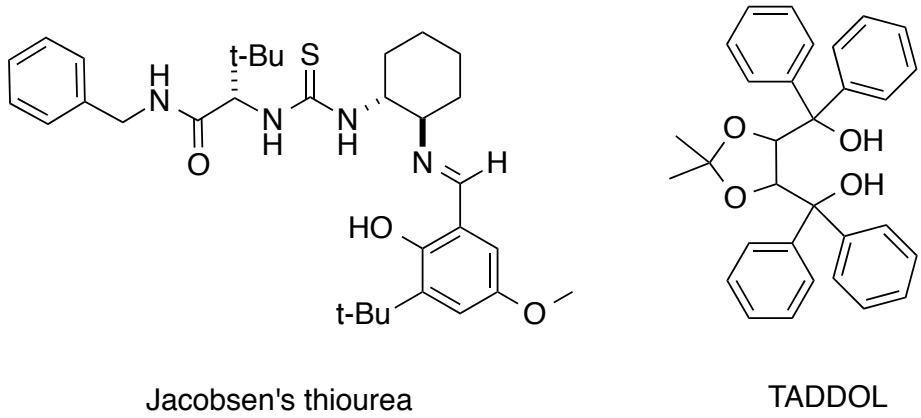

Jacobsen's thiourea TADDOL

Figure 1.5 Chiral hydrogen bonding catalysts

Unlike H- bond donors which activate substrates through generally weaker, less-defined electrostatic interactions, strong Brønsted acid catalysts likely function through discrete proton transfer mechanisms. Following proton transfer, the resulting conjugate base of the catalyst may now associate with the newly protonated heteroatom on the

activated substrate (Figure 1.4). Stronger Brønsted acids can function as specific acid catalysts that would fully protonate the substrate prior to the subsequent transformation. Although in general, acidity of proton donor sites correlates well with the strength of the donor, it is still unclear how donor strength correlates with desired reactivity. However, through careful design, the close association of the catalyst molecule with substrate would make Brønsted acid catalysis a powerful method of inducing stereo selectivity in carbon−carbon bond forming reactions.

As mentioned previously Brønsted acids are proton donors and Brønsted bases are proton accepters. The proton can be thought of as a Lewis acid, although the term Lewis acid usually refers to molecules of heavier elements. As the proton does not have substituents, which could be presented chiral, asymmetric Brønsted acid catalysis has remained undeveloped until 2004. Only recently with the advent and development of organocatalysis, it is recognized that a protonated substrate can be closely associated with its anion, which can influence stereoselectivity of the reaction.

1.2 Strong Brønsted Acids for Stereoselective Reactions

Brønsted acid catalysis has emerged as a relatively new range of catalysis in modern organic synthesis and these organocatalysts are capable of activating the widest range of functional groups. Brønsted acid catalysts are relatively easy to store and generally stable toward oxygen and water. Their metal-free nature also makes them an attractive alternative to metal catalyst routes in the pharmaceutical industry, as traces of toxic metal impurities are sometimes very hard to remove from the desired products.

Brønsted acid catalysis may realize the formation and cleavage of C-O bonds, such as hydrolysis and formation of esters and acetals, or work as effective catalyst for a variety of carbon-carbon bond forming reactions. In order to make the application of the Brønsted acid catalysis as extensive as the well-developed Lewis acid catalysis, it is desirable to evolve Brønsted acids exhibiting both fulfilling reactivities and stereoselectivities.

Recently, the use of chiral Brønsted acid catalysts has become a growing area of investigation. Among all the asymmetric Brønsted acid catalysts, chiral phosphoric acids are one of the earliest and best studied subfields of organocatalysis [12]. Chiral phosphoric acid catalysts based on the axially chiral 1,1′-Bi-2-naphthol (BINOL) framework were first reported independently by the research groups of Terada and Akiyama for enantioselective Mannich reactions [13] [14] (Figure 1.6). However, it was later shown that in Terada's case the phosphoric acid is not the true catalyst, but rather the calcium salt [15], although Brønsted acid catalysis mechanisms were proposed. Substituted chemical groups at 3,3'-position were key for achieving high enantioselectivity. BINOL phosphoric acids were chosen as chiral catalysts due to their low pKa to promote the reaction, cyclic structure to attain high asymmetric induction, and availability as the chiral source. Since then, catalysts in this class have been developed extensively inducing high levels of enantioselective control in carbon−carbon bond forming reactions [16].

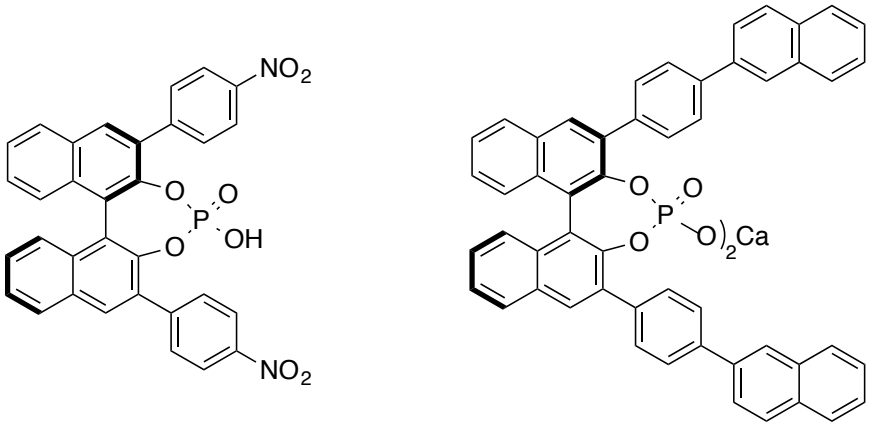

Akiyama et al. 2004 **Uraguchi & Terada. 2004**

Figure 1.6 BINOL phosphoric acid catalysts from initial reports

Chiral phosphoric acid catalysts have become one of the most popular subfields in asymmetric catalysis, and many reactions using this scaffold have been reported [8] [9]. The readily modified 3,3'-substituents are key to most of these successful cases which make it possible to associate bulky groups near the active site. The substitution of a bulky 2,4,6-$iPr_3C_6H_2$-group resulted in one of the most successful phosphoric acid catalysts so far, TRIP acid which is first reported by List et al. to afford asymmetric transfer hydrogenation of imines (Figure 1.7) [17]. And in 2006 Mayer and List chose TRIP anion as a counteranion in their pioneering work in asymmetric-counteranion directed catalysis (ACDC). Exceedingly high enantioselectivity in a catalytic reaction can be realized even when the chirality resides only in the counteranion of the catalyst. In their work a salt composed of an achiral ammonium cation and a chiral phosphate counteranion catalyzed asymmetric transfer hydrogenations of aromatic and aliphatic α, β-unsaturated aldehydes with a Hantzsch ester in excellent enantioselectivities [18].

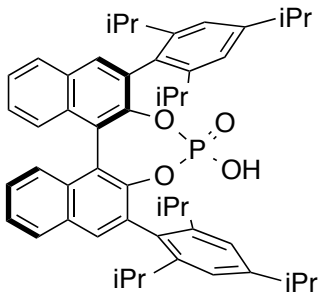

Figure 1.7 (R)-TRIP acid reported by List et al. 2005

The development of catalysts with alternative backbones other than the basic BINOL structure are also prompted by the success of BINOL-derived catalysts, with the purpose of modifying geometrical and chemical parameters of the active site. Akiyama group synthesized a novel cyclic dialkyl phosphate derived from TADDOL and examined its catalytic activity in the Mannich-type reaction of a ketene silyl acetal with aldimines. However, these catalysts failed to promote highly enantioselective transformations (Figure 1.8) [19].

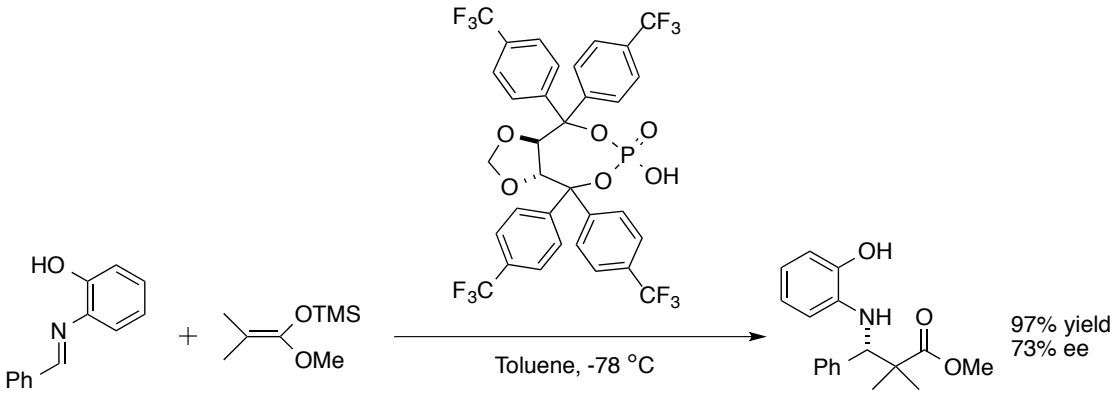

Figure 1.8 Enantioselective Mannish type reaction by TADDOL derived catalysts

Antilla et al. introduced a hindered biaryl phosphoric acid catalyst derived from 2,2‘-diphenyl-[3,3‘-biphenanthrene]-4,4‘-diol (VAPOL) for synthesis of protected aminals using sulfonamides as nucleophiles. The desired aminals were realized with excellent yields and enantioselectivities (Figure 1.9) [20]. Gong and coworkers evaluated a series of BINOL- and H8-BINOL-based phosphoric acids for the first time in Biginelli reactions of aldehydes, thiourea or urea, and β-keto esters. This closely related 3,3‘-diphenyl-H8-BINOL backbone proved to exhibit superior catalytic activity and enantioselectivity compared to its structural analogue BINOL backbone, affording high enantioselectivities with a wide scope of substrates [21]. Du et al. introduced a series of novel double axially chiral phosphoric acid catalysts based on bis-binol scaffold for the asymmetric transfer hydrogenation of 2-aryl- and 2-alkyl-substituted quinolines as well as 2,3-disubstituted quinolines in excellent yields and with excellent diastereoselectivities and high enantioselectivities [22]. Enantiotopic C(sp^3) −hydrogen was selectively activated by biphenol-derived phosphoric acids for asymmetric C–H functionalization to afford tetrahydroquinoline derivatives with good to excellent enantioselectivities via an internal redox process [23].

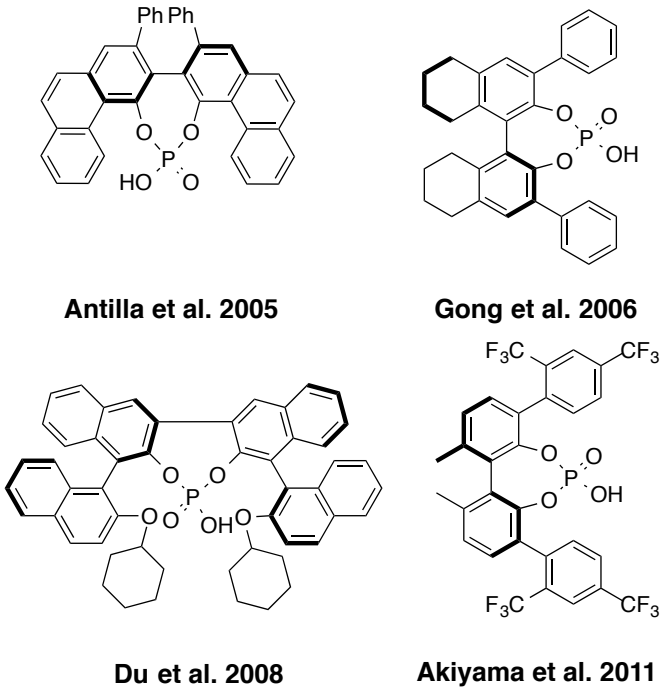

Figure 1.9 Chiral phosphoric acids with alternative backbones

As shown in Scheme 1.4, Lin, Wang and coworkers conveniently synthesized a new class of chiral phosphoric acids **1** with spirobiindane as scaffold from (S)-1,1′-spirobiindane-7,7′-diol ((S)-SPINOL) and **1** was successfully employed in the asymmetric Friedel−Crafts reaction of indoles with imines to afford 3-indolyl methanamines, giving comparable results to BINOL-derived phosphoric acid [24]. In the same year, List et al. independently reported another SPINOL-derived phosphoric acid **2** (Figure 1.10) STRIP, STRIP acid **2** was designed and identified as a superior catalyst to TRIP acid for a kinetic resolution of alcohols via intramolecular transacetalization [25].

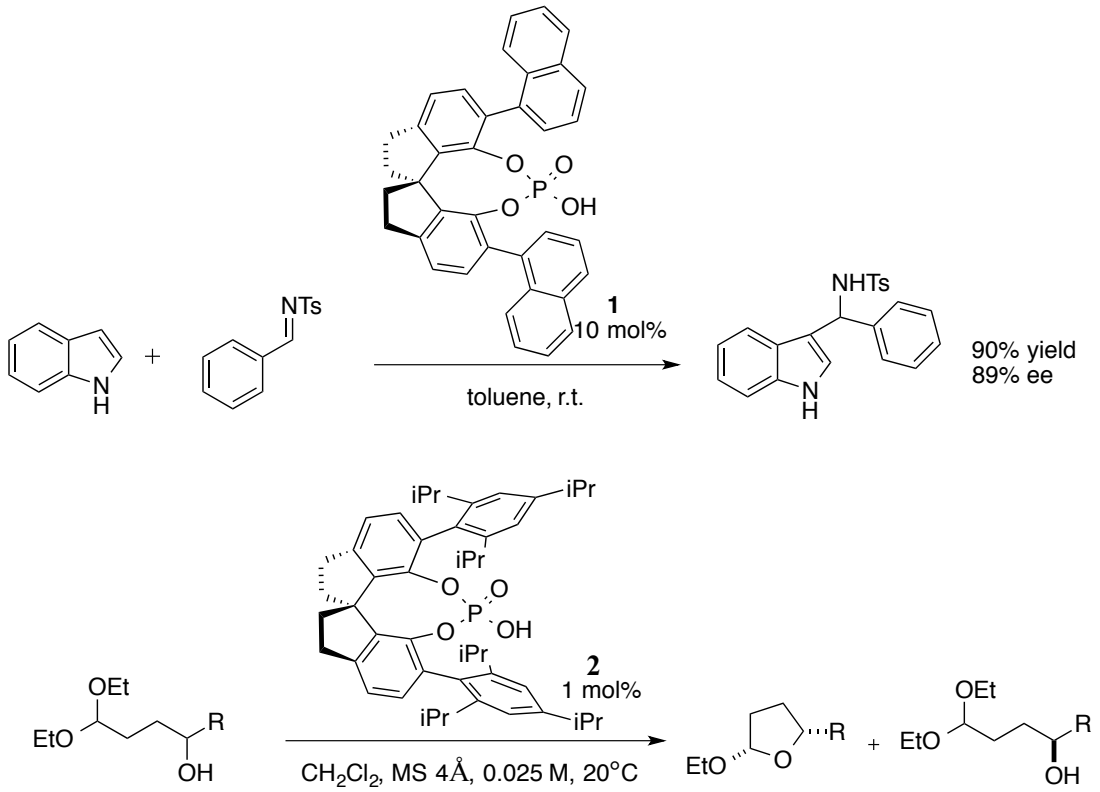

Figure 1.10 SPINOL derived catalysts by Lin, Wang et al. 2010 and List et al. 2010

The success of chiral phosphoric acid catalysts encouraged numerous attempts to prepare chiral catalysts possessing other functional groups. BINOL-derived dicarboxylic acid is introduced by Hashimoto and Maruoka as highly enantioselective catalysts for Mannich reaction of arylaldehyde, N-Boc imines, and diazo compounds [26] (Figure 1.11). In 2008 List et al. used previously known BINOL-derived 2,4-dinitrobenzenesulfonic acid (DNBA) as a chiral catalyst in a three-component Hosomi–Sakurai reaction without realizing enantioselectivity. Aldehydes react with silyl ethers or the corresponding alcohols and allylsilanes to provide a wide range of homoallylic ethers in moderate to high yields [27]. Yet in the same year, Ishihara et al. found DNBA's pyridinium salts pyridinium 1,1′-Binaphthyl-2,2′-disulfonates were able to successfully

realize an Mannich-type reaction of diketones and ketoester equivalents with aldimines with decent enantioselectivity. This chiral Brønsted acid-base combined salt acts as convenient chiral tailor-made organocatalysts in situ [28].

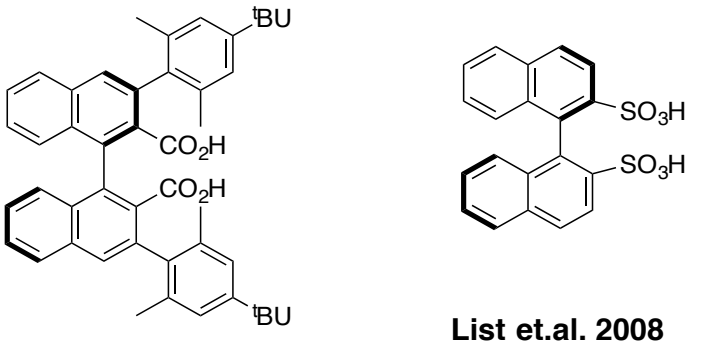

Hashimoto & Maruoka.2007 **List et.al. 2008 & Ishihara et al. 2008**

Figure 1.11 Other chiral stronger Brønsted acids

There are few reports using highly acidic disulfonic acids alone as efficient catalysts for asymmetric coupling reactions so far. Disulfonimides were initially reported by the List group as powerful new precatalysts for silicon Lewis acids in enantioselective Mukaiyama aldol reactions of silyl ketene acetals with aldehydes. The actual catalyst is proposed to be an N-silyl imide which is generated in situ [29] (Figure 1.12). Subsequently, the Lee group used this Binaphthyl-based chiral sulfonamides as productive strong Brønsted acid catalysts for the first time to realize well-established asymmetric Friedel-Crafts alkylation of indoles with imines [30].

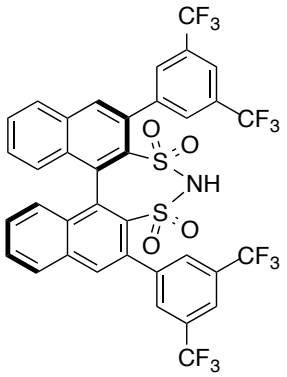

List et.al 2009 & Lee et al. 2011

Figure 1.12 Disulfonimides as Lewis acid and Brønsted acid catalysts

Chiral disulfonic acids and disulfonimides in Figure 1.7 and Figure 1.8 are stronger acids than phosphoric acids and, therefore, can realize reactions inaccessible with chiral phosphoric acid catalysis, but their application as asymmetric Brønsted acid catalysts has proven challenging.

Yamamoto and Ishihara proposed the concept of "Lewis acid-assisted chiral Brønsted acids", a strong Brønsted acid that was generated from combining chiral phenol derivatives with a Lewis acid [31] [32]. The protonation of metal enolates by chiral proton sources [33], [34] and hydrolysis of enol esters promoted by enzymes [35], [36] and antibodies [37] have been reported under basic and neutral conditions. Lewis acid-assisted chiral Brønsted acids catalyzed hydrolysis of enol ethers is an interesting alternative, and Yamamoto and Ishihara successfully accomplished the enantioselective protonation of silyl enol ethers with such an acid catalyst (Figure 1.13) [38].

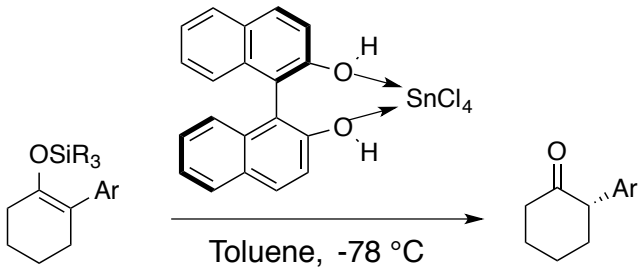

Figure 1.13 Lewis acid-assisted chiral Brønsted acids example

Despite the success of these phosphoric acid catalysts and BINOL-derived catalysts, other acidic moieties capable of asymmetric synthesis are relatively undeveloped, and the second generation of stronger chiral Brønsted acid catalysts has not yet been discovered.

1.3 Latifolian A as Potential Drug Candidate for Neurodegenerative Disorders

Neurodegenerative diseases such as Alzheimer's and Parkinson's disease usually start slowly and worsen over time. Alzheimer's disease is primarily a dementia disease, and Parkinson's disease is a movement disorder. Together, they affect around 50 million people worldwide, and this number is still rapidly growing for the elderly population. Neurodegenerative diseases are often diagnosed in patients of an advanced age. Alzheimer's disease is the cause of 60% to 70% of cases of dementia. The most common early symptom is difficulty in remembering recent events (short-term memory loss) [39]. As the disease advances, symptoms can include problems with language, disorientation, mood swings, loss of motivation, not managing selfcare, and behavioral problems [40]. As a person's condition declines, they often seclude themselves from family and society.

Alzheimer's disease is characterized by damage of neurons and synapses in the cerebral cortex and certain subcortical regions. This loss leads to gross atrophy of the affected regions, involving degeneration in the temporal lobe and parietal lobe, as well as in parts of the frontal cortex and cingulate gyrus [40]. Studies using MRI and PET have demonstrated reductions in size in the specific brain regions in people with Alzheimer's disease as they progressed from mild cognitive impairment to Alzheimer's disease, and in comparison with similar images from healthy older adults [41].

The cause of Alzheimer's disease is poorly understood. About 70% of the risk is believed to be genetic with many genes usually involved [42]. Other risk factors include a history of head injuries, depression, or hypertension. There are no medications or supplements that decrease risk of getting Alzheimer's disease and no treatments could stop or reverse its progression. This means there is no cure for Alzheimer's disease, though some treatment may temporarily alleviate or stabilize symptoms for a limited time and improve patients' life quality to some extent.

The U.S. Food and Drug Administration (FDA) has approved two types of medications: acetylcholinesterase inhibitors (Donepezil, Rivastigmine, Galantamine, Tacrine) and NMDA receptor antagonist that acts on glutamatergic system (Memantine) in order to treat the cognitive symptoms such as memory loss, confusion, and difficulties with thinking and reasoning resulting from Alzheimer's disease (Figure 1.14). Reduction in the activity of the cholinergic neurons is a well-known feature of Alzheimer's disease. The most currently available drug medications called cholinesterase inhibitors are based on the cholinergic hypothesis. The cholinergic hypothesis proposes that Alzheimer's

disease results from reduced synthesis of the neurotransmitter acetylcholine. The cholinergic hypothesis failed to hold widespread support, mainly because drugs intended to treat acetylcholine deficiency have not been very effective [43]. There is also a medication called Namzaric that combine one of the cholinesterase inhibitors (donepezil) with memantine targeting both acetylcholine and NMDA signaling pathway in the brain.

Among all the medications that have been approved by FDA, Donepezil (Aricept) is approved to treat all stages of Alzheimer's. Rivastigmine (Exelon) is approved to treat mild to moderate Alzheimer's. Galantamine (Razadyne) is approved to treat mild to moderate Alzheimer's. Memantine (Namenda) and a combination of memantine and donepezil (Namzaric) are approved by the FDA for treatment of moderate to severe Alzheimer's. However, all of these medications have side effects like nausea, vomiting, loss of appetite and increased frequency of bowel movements.

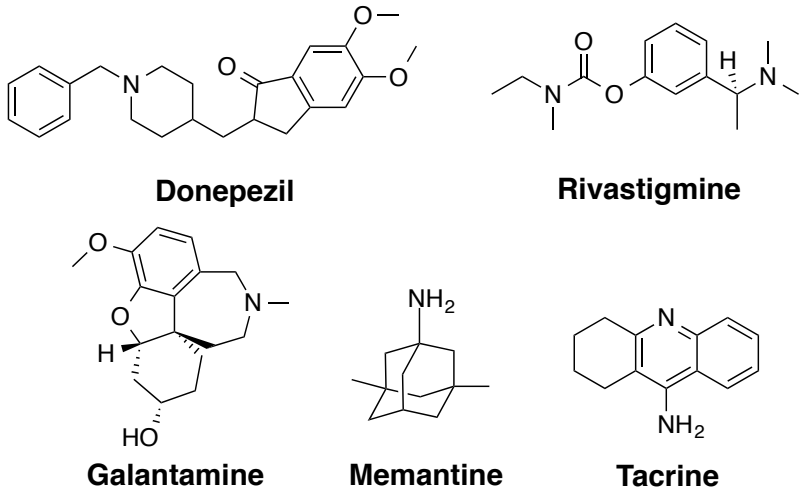

Figure 1.14 Chemical structures of FDA approved medications for Alzheimer's disease

Besides medications, caregiving and psychotherapy are also included in current treatment to Alzheimer's disease. People with Alzheimer's disease gradually unable to

meet their own needs. Caregiving is essential treatment for these patients to live a relatively normal life, and it must be carefully managed during different stages of disease. Caring for people with dementia has become more common as modern medical interventions gradually developed over time. Caregiving may consist of two parts: formal care and informal care. Formal care consists of the professional services of community and medical partners, while informal care consists of the support from family members, close friends, and local communities such as neighbors, but more often from spouses, adult children and other immediate relatives. Psychosocial interventions are used as an adjunct to pharmaceutical treatment and help a person reintegrate into society in a healthy way when they have been disconnected with society during Alzheimer's disease progression. Caregiving and psychosocial interventions are not specifical for treating Alzheimer's disease, and they are involved in treatment to most cases of mental disorders, as well as in the cessation of negative behaviors.

There is no cure for Alzheimer's disease, and drugs currently on the market don't exhibit enough efficacy, in lessening the symptoms or slowing down the disease progression. Identification of the true causes of Alzheimer's disease and discovery of effective therapeutic treatments are urgently needed.

A natural alkaloid latifolian A has been established as a potent c-Jun N-terminal kinase 3 (JNK-3) inhibitor. Recently, such inhibitors have been implicated as potential drug candidates for neurodegenerative disorders such as Alzheimer's and Parkinson's disease. Latifolian A has shown to have activity towards the JNK-3 enzyme that regulates various signal transduction processes in the brain [44]. Blocking expression of JNK-3 in

murine models has been shown to reduce amyloid plaque buildup, implicated in neurodegenerative diseases such as Alzheimer's, by up to 90% [45].

Latifolian A was isolated and characterized in 2005 by Quinn and coworkers [44]. Structurally, the compound features a quaternary ammonium scaffold possessing a rare benzylisoquinoline unit and two tertiary carbon stereogenic centers. It is isolated as its trifluoroacetate salt but the natural counterion is unknown (denoted as X in Figure 1.15). Latifolian A has received little attention from the synthetic community due in part to the lack of interest for JNK-3 inhibitors until very recently.

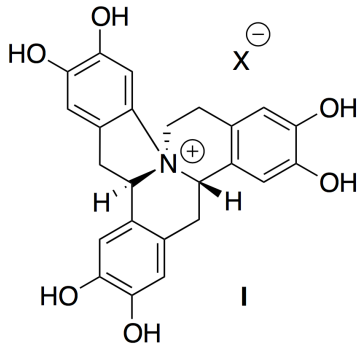

Figure 1.15 Chemical strucutre of the alkaloid natural product latifolian A

Modern organic chemical synthesis has developed into a powerful tool for the construction of complex molecular structures capable of presenting significant biologic effects. The total synthesis of latifolian A functions as a brilliant goal that could help in the understanding of the JNK-3 target through the identification of vital structural features necessary for inhibitor effectiveness. Attempts were made for total synthesis of latifolian A through application of a chiral sulfonic acid catalyzed Pictet–Spengler cyclization reaction as a key synthetic step.

CHAPTER TWO: BRØNSTED ACID CATALYZED AZLACTONE-ACETAL REACTIONS

2.1 Introduction

The modification of reaction conditions for more efficient and environmentally friendly methods to generate medical relevant molecules relies on changing their synthetic pathways. Pharmaceuticals often demand complex synthetic routes and their specific structure is incredibly important for expressing their biological functions to react with their targets. An important structural character in many medical relevant molecules is their chirality. Chirality is a pivotal feature as in most cases one molecule indicates the desired biological functions while its isomer is inactive at the corresponding reactive site. Thus, desirable synthetic pathways with high stereoselectivities involving carbon-carbon bond forming reactions are critical to research and development in the pharmaceutical industry. On the other hand, synthetic pathways with high reactivities is of equal importance to increase the efficiency aiming to cut costs and safer operation in lab and in industry.

As discussed in the first chapter, organocatalysis enables more efficient and greener synthetic pathways to realize a range of pharmaceutical related compounds. In organocatalysis, simple organic molecules are used as catalysts as an alternative to metal salts or enzymes. The aims of this project were to extend the possibility of Brønsted-acid

catalyzed acetal involved carbon-carbon bond formation reactions and optimize reaction conditions. The use of Brønsted acids as catalysts can be an efficient and powerful method of bond forming, especially with the use of weakly basic substrates through the development of stronger chiral Bronsted acids.

Acetals were chosen as starting materials in this project as they are among the most common precursors to stereocenters in nature. Acetals form glycosidic bonds that are essential backbones of carbohydrates, including starch and cellulose, which is the most abundant organic materials on Earth. Stereogenic acetals are ubiquitous in other natural products, ranging from simple insect pheromones to complex spiroketal polyketides [46], [47]. Meanwhile, coupling carbon-carbon bonds and controlling the absolute configuration are crucial to construction of pharmaceuticals and other bioactive compounds with organic backbones.

In organic synthesis, acetals are common functional groups used for the protection of carbonyl groups such as aldehydes and ketones since they are relatively stable with respect to hydrolysis by bases and with respect to many oxidizing and reducing agents. Acetals are also more stable compared to hemiacetals, but their formation is a reversible equilibrium. Formation of an acetal occurs when the hydroxyl group of a hemiacetal becomes protonated and then lost as water. The carbocation that produced is then quickly attacked by a molecule of alcohol. Deprotonation of the attached alcohol then affords the desired acetal (Figure 2.1). The formation of ketal from ketone follows a similar pathway.

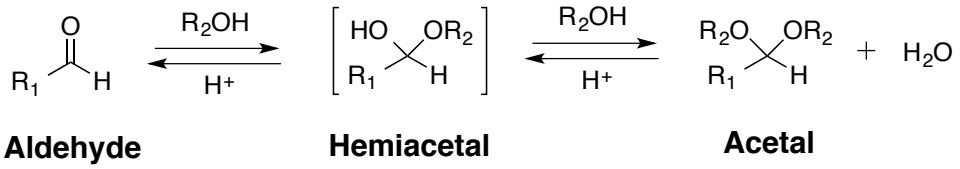

Figure 2.1 Aldehyde to acetal conversion

Processes involving the generation of oxocarbenium ions are foreseen as an area with exciting opportunities. In previous reported examples, electron rich alkenes such as vinyl ethers are protonated by the chiral Brønsted acids. The resulting oxocarbenium ion would serve as an activated electrophile for a range of carbon-based nucleophilic coupling partners. Terada and coworkers reported the first asymmetric Brønsted acid-catalyzed example of such a reaction [48]. It has been established that strong Brønsted acids, such as phosphoric acids, are capable of mediating highly stereoselective transformations of medicinally relevant precursors such as azlactones. They use this BINOL derived phosphoric acid catalyst to realize this enantioselective aldol-type reaction between t-butyl vinyl ether and azlactone to give product in 97% yield with 98% ee following methanolysis (Figure 2.2). Azlactones are five-membered heterocycles formed by the cyclization of N-acyl-α-amino acids and usually employed in the stereoselective synthesis of α-amino acids, heterocycles and natural products. The versatility of the azlactone scaffold arises from the multiple reactive sites, which allowing for its application in a diverse array of transformations [49].

The formation of a chiral ion pair featuring a stabilizing hydrogen bond between a C−H donor from the oxocarbenium ion with the conjugate base of catalyst as the acceptor is proposed as the stereocontrolling element. Also, intermediate oxocarbenium ions

resulting from precursors other than simple vinyl ethers would allow for the preparation of biologically relevant products.

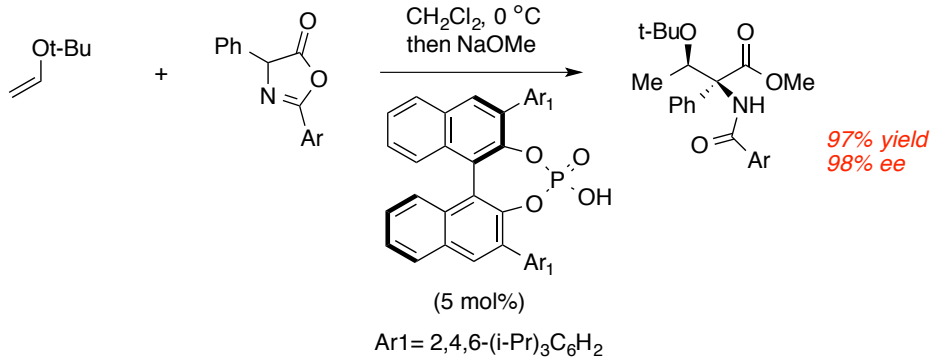

Figure 2.2 Chiral Brønsted acid catalysis involving generation of oxocarbenium ion

The highly electrophilic intermediates oxocarbenium ions generated from acid catalysis are then captured by nucleophiles in carbon-carbon bond forming reactions. This methodology allows for a variety of nucleophiles to get involved in carbon-carbon bond forming reactions thus increasing the versatility of the pathway. Compared to neutral carbonyl compounds like ketones or esters, the charged oxocarbenium ion form would be a larger contributor to the structure. These highly reactive intermediates ions have been proposed in a wide range of chemical transformations since then. This pathway has been studied by Mukaiyama et al. particularly looking at Lewis acids catalysis in 1990 [50], leaving an abundant study area for looking at this coupling reaction using Brønsted Acids instead.

Despite the success of those phosphoric acid catalysts and BINOL-derived catalysts, other acidic moieties capable of realizing asymmetric synthesis are relatively understudied, specifically revolving around sulfur-based mono-protic acids. With pKa

values more acidic than those phosphoric acids, sulfonic acids are promising candidates with growing potential for catalyzing stereoselective carbon-carbon bond forming reactions. The highly acidic nature of the sulfonic acid catalysts may make it possible to activate less basic substrates currently inaccessible with other catalyst systems or optimize reactions that already have been realized with milder conditions and less reaction time.

The Lambert group described a chiral Brønsted acid prepared in one step from naturally occurring (-)-menthol and readily available 1,2,3,4,5-pentacarbomethoxycyclopentadiene. The key contributing factor to the potent acidity of the resulting acid catalyst is aromatic stabilization, which is shown to catalyze both Mukaiyama-Mannich and oxocarbenium aldol reactions with high efficiency and enantioselectivity (Figure 2.3) [51]. Catalyst loadings as low as 1 mol % and alternative

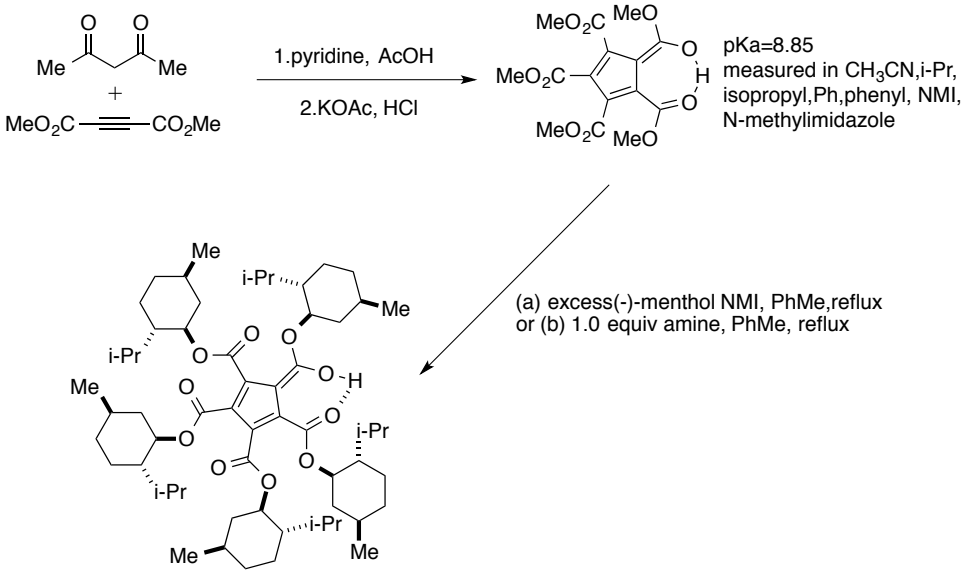

Figure 2.3 One step chiral Brønsted acid preparation

amide catalysts are also shown to be promising platforms. In addition to proton catalysis, a chiral anion pathway is demonstrated to be viable with this catalyst system. This great work supports the idea that catalysts with pKa values similar to sulfonic acids will allow for the discovery of new reactions.

2.2 Preliminary Work of Reaction Design and Optimization of Reaction Conditions

I synthesized a series of azlactones (listed in Figure 2.4) with different substrates attached at the 2- and 4- position on the five-membered heterocycle ring, with overall yields varying from 40% to 88% [48] [52]. The last two azlactones on the row 2,4-diphenyl-4H-1,3-oxazol-5-one and 2-(3,5-Dimethoxybenzyl)-4-phenyl-1,3-oxazol-5(4H)-one are selected for further research owing to their higher yield and relative ease of prepration compared to other azlactones.

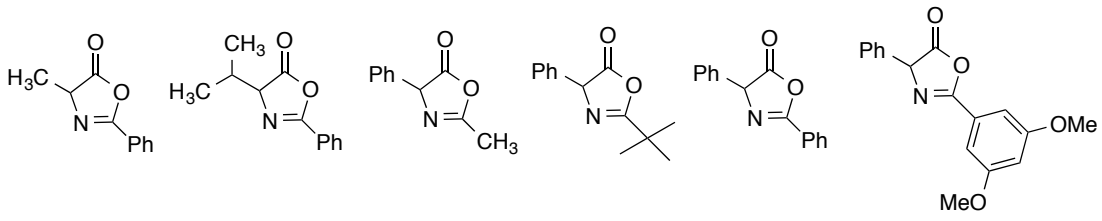

Figure 2.4 List of azlactones

To evaluate this proposal, I began the studies of the coupling reaction between azlactone 2,4-diphenyl-4H-1,3-oxazol-5-one and anisaldehyde dimethyl acetal. CD_3CN was used as solvent to better monitor the reaction by ^1H NMR in initial condition development as we could take one step ^1H NMR immediately in the middle of the reaction without removing the solvent in the system and dissolving the reaction mixture into deuterated solvent. And Na_2SO_4 works as a dehydrating agent in this system since

this coupling reaction is sensitive to water. The reactions are carried out at room temperature for 24 hours in the first place. In these reaction procedures, the generation of reactive oxocarbenium ion intermediates is realized from the treatment of the anisaldehyde dimethyl acetal with a strong Brønsted acid catalyst. This highly electrophilic species is then captured by the nucleophilic azlactones. As shown in Figure 2.5, three different sulfonic acids are utilized to realize this coupling reaction and good yields were achieved with relatively low diastereoselectivities. Among these three sulfonic acids, (R)-1,1'-Binaphthyl-2,2'-disulfonimide didn't afford desired product and *p*-toluenesulfonic acid and (+)-camphorsulfonic acid present similar performance in coupling reactions. The yields are calculated from purified product and diastereoselectivities are calculated from crude ^{1}H NMR. I decided to take both p-toluenesulfonic acid and (+)-camphorsulfonic acid as candidates for coupling reactions of further investigation.

Then coupling reaction between azlactone 2-(3,5-Dimethoxybenzyl)-4-phenyl-1,3-oxazol-5(4H)-one and anisaldehyde dimethyl acetal were performed and other reaction conditions remain the same, similar results were achieved. No product was observed in coupling reaction catalyzed by (R)-1,1'-Binaphthyl-2,2'-disulfonimide. Both *p*-toluenesulfonic acid and (+)-camphorsulfonic successfully promoted the coupling reactions with decent yields.

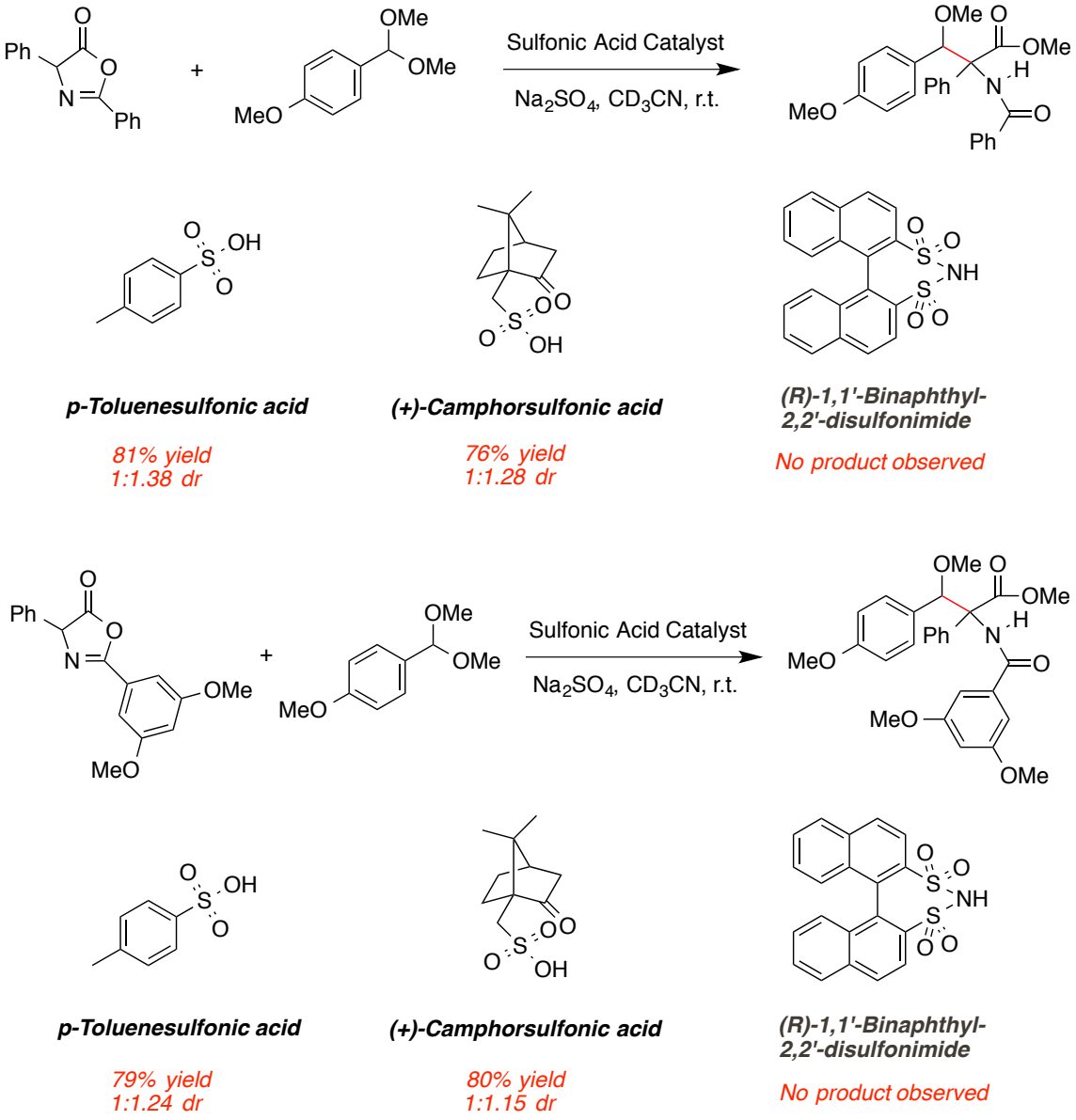

Figure 2.5 Sulfonic acid catalyzed C-C bond coupling reactions with oxocarbenium ions

To evaluate this novel coupling reaction between diphenyl azlactone (**1a**, 2 equiv.) with anisaldehyde dimethyl acetal (**2a**, 1 equiv.) using Brønsted Acid Catalysts, initial optimization studies were carried out and different reaction conditions were tried. As seen in Table 1 entry 1, when utilizing Na_2SO_4 as a dehydrating agent and run the

coupling reaction in CD_3CN at room temperature for 24 hrs, these reaction conditions afforded 81.07% of desired product with 1:1.38 dr. Increase the temperature to 60 ℃ remarkably accelerated the reaction rate. Reaction time was reduced from 24 hrs to 4 hrs but there is not much difference in yield and selectivity. Reactions at the temperature of 4 ℃ in the cold room would significantly slowed the reaction rate (entry 2,3 and entry 14,17). In later optimization studies various acid catalyst were used and studied. I was pleased to see that catalyst (+)-camphorsulfonic acid gives satisfying yield which is comparable to those with *p*-toluenesulfonic acid. Diphenyl phosphate gives relatively good selectivity, but the yield is too low (entry 5). Although TRIP acid is a better candidate for this coupling reaction compared to other phosphoric acid, its performance was not comparable to sulfonic acids and the expensive price and difficulty in preparation limit its usage (entry 6). Other acid catalysts we utilized such as (R)-1,1'-Binaphthyl-2,2'-disulfonimide, CH_3COOH and TFA were not acidic enough to promote this reaction (entry 8-10). Considering that both diphenyl azlactone and anisaldehyde dimethyl acetal display a wide range of solubility in organic solvents, various solvent systems were investigated, and CH_3CN was the most promising one compared to other solvents I used like toluene or DCM. Na_2SO_4 was a better dehydrating agent compared to molecular sieves (5Å and 4Å), the performance of $MgSO_4$ was comparable to Na_2SO_4 in this specific coupling reaction but in coupling reactions with other acetals, the performance of Na_2SO_4 was more stable (entry 15).

Table 2.1. Initial optimization studies

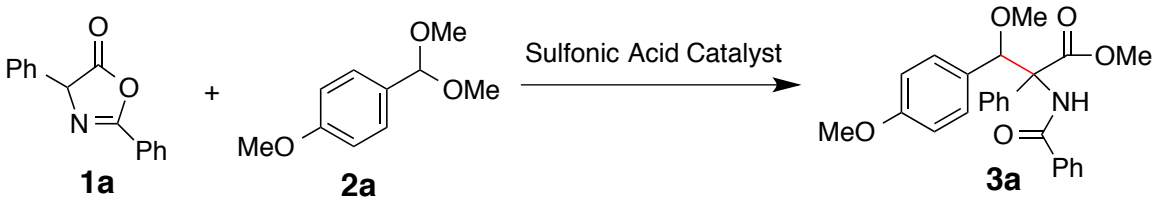

Entry	Dehydrant	Catalyst	Solvent	Temp	Yield%	dr	Time(h)
1	Na_2SO_4	*p*-TsOH	CD_3CN	r.t.	81	1:1.38	24
2	Na_2SO_4	*p*-TsOH	CD_3CN	60 ℃	83	1:1.33	4
3	Na_2SO_4	*P*-TsOH	CD_3CN	4 ℃	75	1:1.14	24
4	Na_2SO_4	CSA	CD_3CN	r.t.	76	1:1.28	24
5	Na_2SO_4	Diphenyl phosphate	CH_3CN	r.t.	26	1:1.84	24
6	Na_2SO_4	(R)-TRIP	CD_3CN	r.t.	40	1:1.15	24
7	Na_2SO_4	(R)-1,1'-Binaphthyl-2,2'-disulfonimide	CH_3CN	r.t.	0		24
8	Na_2SO_4	CH_3COOH	CH_3CN	r.t.	0		24
9	Na_2SO_4	TFA	CH_3CN	r.t.	0		24
10	Na_2SO_4	*p*-TsOH	Toluene	r.t.	31	1:1.8	24
11	Na_2SO_4	*P*-TsOH	DCE	r.t.	38	1:1.56	24
12	Na_2SO_4	*P*-TsOH	DMF	r.t.	30	1:3.43	24
13	Na_2SO_4	*p*-TsOH	CH_3Cl	r.t.	11	1:1.71	24
14	Na_2SO_4	*p*-TsOH	C_6D_6	r.t.	60	1:1.4	24
15	$MgSO_4$	*p*-TsOH	CH_3CN	r.t.	82	1:1.16	24
16	Moleculer sieves	*p*-TsOH	CH_3CN	4 ℃	2	1:1.24	24
17	Moleculer sieves (5Å)	*p*-TsOH	CH_3CN	r.t.	37	1:1.69	24
18	Moleculer sieves(4Å)	*p*-TsOH	CH_3CN	r.t.	35	1:1.33	24
19	Moleculer sieves	*p*-TsOH	CD_3CN	60 ℃	36	1:1.08	4

a. Yield calculated from crude ^1H NMR

With initial optimized conditions in hand, we set out to explore the substrate scope. I tried to couple azlactone with a series of aldehydes and acetals (Figure 2.6) with *p*-TsOH and CSA as catalysts, Na_2SO_4 as dehydrate and CH_3CN as solvent. Reactions are run at room temperature for 24 hrs. Most of the acetals and aldehydes are commercially available and I only synthesized some in our lab [53] [54].

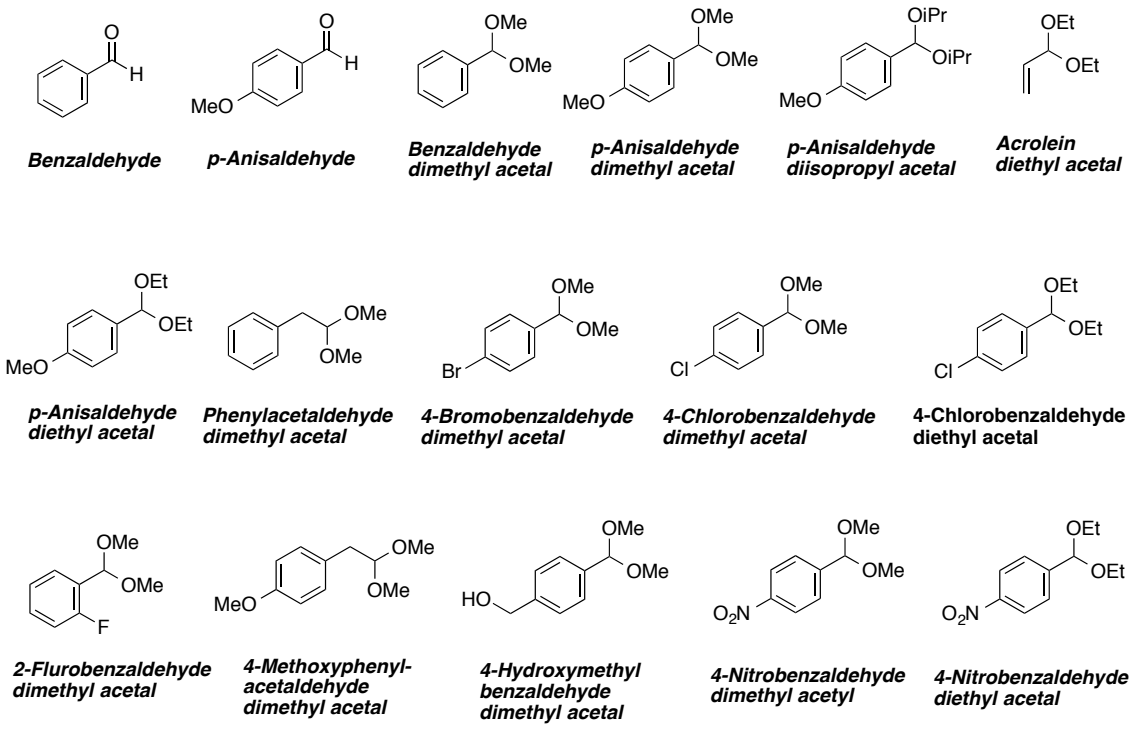

Figure 2.6 List of aldehydes and acetals used in coupling reactions

Most of coupling reactions went smoothly, but there were some acetals that we could not couple with azlatone (listed in Figure 2.7). For coupling partner like p-anisaldehyde diisopropyl acetal, as isopropyl is bulkier than a methoxy group, so it might need stronger acid to hydrolyze acetal to aldehyde for coupling reactions. In previous reports, researchers successfully hydrolyzed acrolein diethyl acetal with acid catalysts

like CSA and HCl, both reactions require heating the mixture up to 65- 70℃ [55] [56], there is no surprise that our attempt at room temperature did not proceed well. Neither phenylacetaldehyde dimethyl acetal nor 4-methoxyphenyl phenylacetaldehyde dimethyl acetal work in coupling reactions with azlactone. This might be due to the fact that the resulting oxocarbenium ion is benzylic in the reactive case and not benzylic in the case where no reaction is seen.

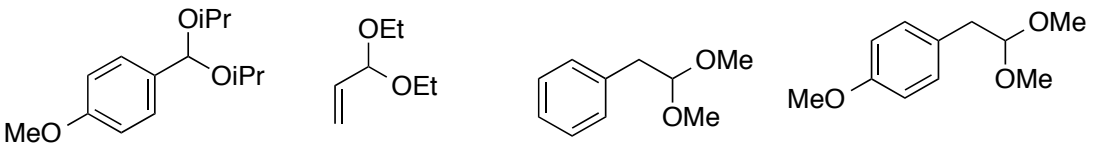

***p*-Anisaldehyde diisopropyl acetal** | ***Acrolein* diethyl acetal** | **Phenylacetaldehyde dimethyl acetal** | ***4*-Methoxyphenyl-acetaldehyde dimethyl acetal**

Figure 2.7 List of acetals in unsuccessful coupling reactions

For those successful cases, the main byproduct of the coupling reaction is an ester resulting from methanolysis and it is difficult to separate from the resulting desired diastereomers through purification procedure such as flash column chromatography due to their similar polarity. The only case that I was able to achieve the pure desired product from one step flash column chromatography purification is the one with *p*-anisaldehyde dimethyl acetal as starting material. In order to gain the pure product from all previous successfully performed coupling reactions with simple and universal modified procedures, in situ reduction of moderately electron poor benzylic alcohols to remove a stereogenic center and facilitate purification, was attempted. There are three general

procedures from previous reports. Unfortunately, none of the three routes was feasible as little desired product was observed based on crude ^{1}H NMR (Figure 2.8) [57] [58] [59].

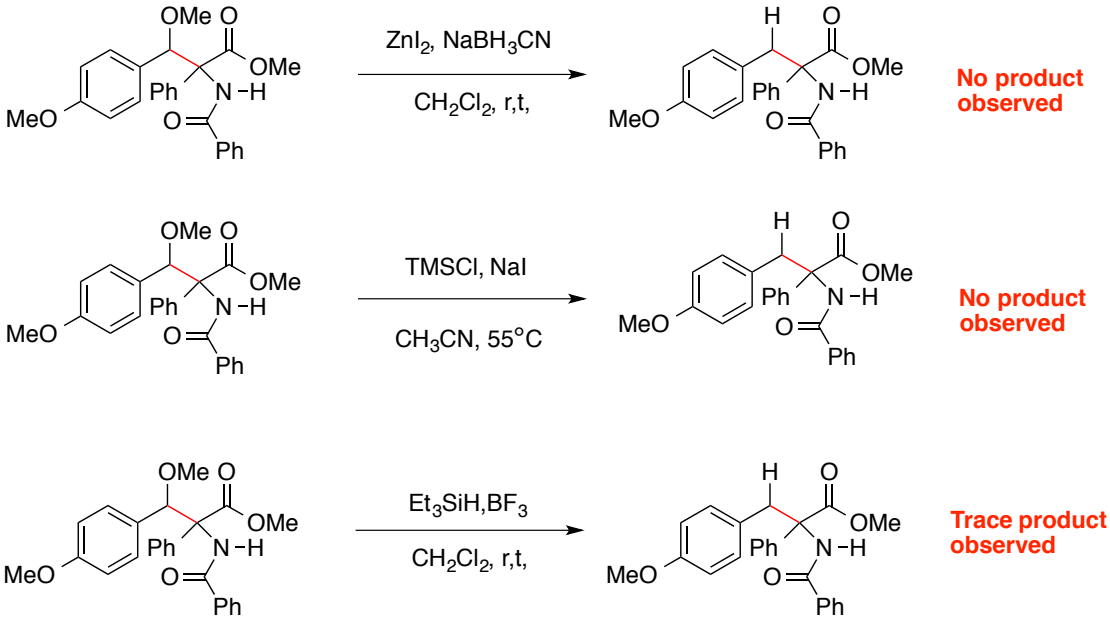

Figure 2.8 Benzylic reduction

Since benzylic reduction failed to work, an alternative approach was explored. Extra work-up steps to remove catalytic acid were added to general experiment procedures (see experimental details). Then crude product mixture was purified through a silica gel column to remove aldehyde from the mixture. In order to gain the pure product, reduction was performed to enlarge the polarity differences between azlactone methanolysis byproduct and resulting diastereomers (Figure 2.9). I was delighted to see that reductant 10 equiv. $NaBH_4$ only reduced the azlactone methanolysis, leaving the diastereomers untouched. Following 2nd column chromatography, the reduced azlactone methanolysis was separated with desired diastereomers. In this way, I am finally able to

gain pure desired product separated from reaction mixture in these simple and universal procedures.

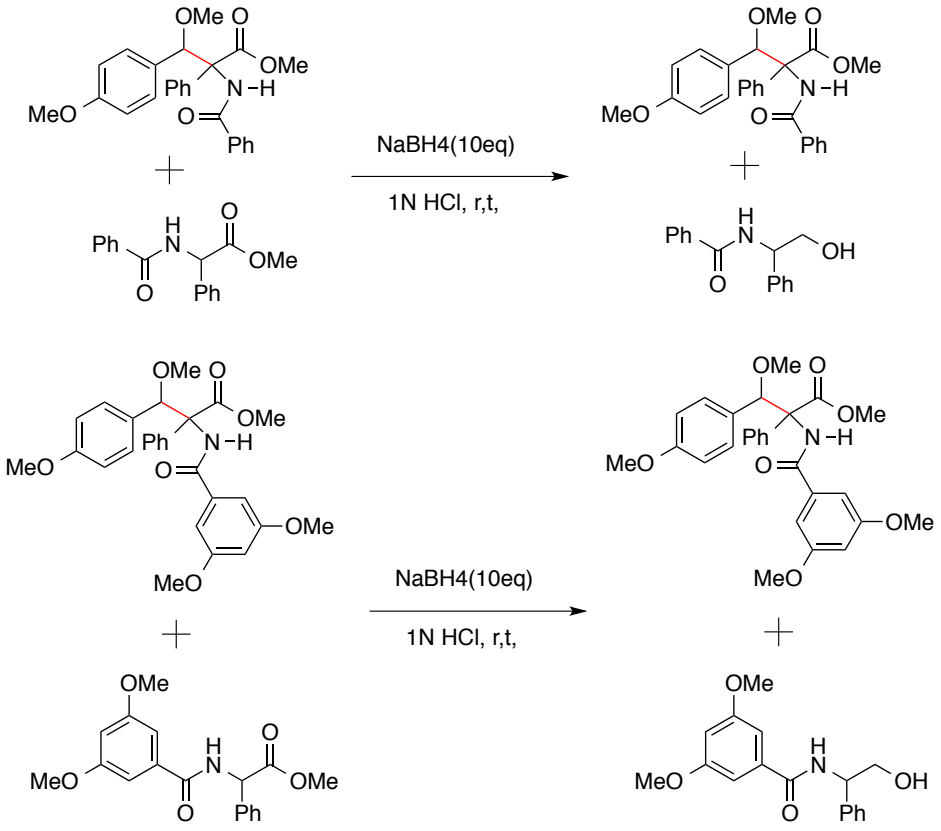

Figure 2.9 Azlactone methanolysis reduction

2.3 Substrate Scope of Coupling Reactions and Ring Open Mechanism

The next step was to evaluate functional group tolerance and its reactivity. I performed these coupling reactions in solvent C_6D_6, model reaction in Figure 2.10 used *p*-TsOH as catalyst, Na_2SO_4 as a dehydrating agent and the reactions were run at room temperature for 24h. Acetals substituted with -OMe, -Br, -F, -Cl and -NO_2 group were all able to afford modest yields varying from trace amounts to 60% and diastereomer ratios

were between 1:1.3 and 1:2.1. Unfortunately, acetals possesseing hydroxymethyl group and 1-(diethoxymethyl)-4-nitrobenzene failed to give desired product. Both the yields and dr are calculated from crude ^{1}H NMR.

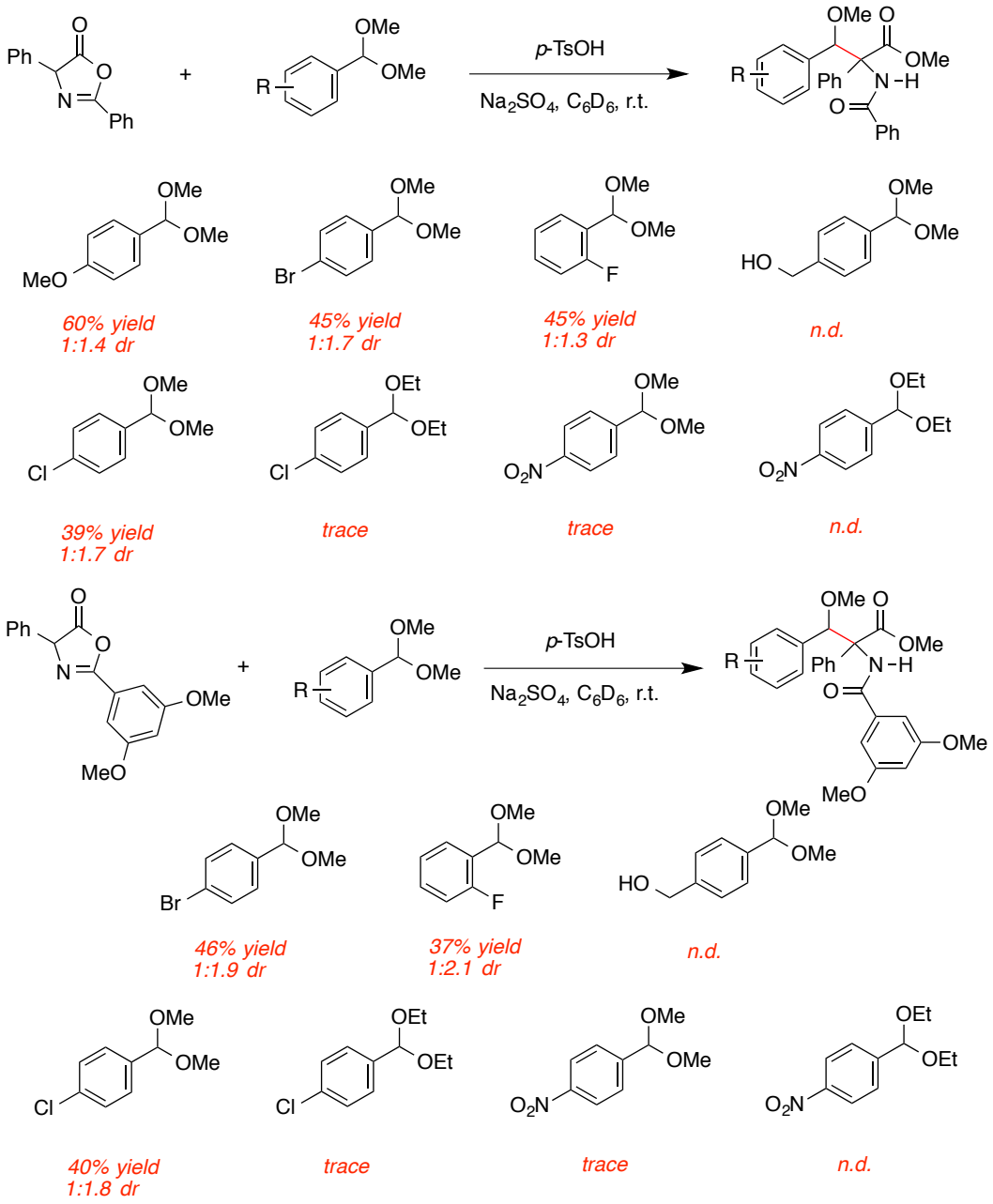

Figure 2.10 Substrate scope for various acetal derivatives in C_6D_6 (*p*-TsOH)

When the catalyst was switched from *p*-TsOH to CSA and other reaction conditions stayed the same as in Figure 2.10, I got the similar results but slightly lower yields (Figure 2.11). Acetals substituted with -OMe, -Br, -F, -Cl and -NO_2 group were all able to afford modest yields varying from trace amounts to 50 %. There was not much change in diastereoselectivity, and dr were between 1:1.2 and 1:2. Both the yields and dr were calculated from crude ^{1}H NMR.

By comparing all the data in Figure 2.10 and Figure 2.11 with data in Table 2.1, C_6D_6 only give fair performance though it was better than toluene, chloroform, DCM or DMF. CH_3CN was the best solvent in coupling cases with various acetals.

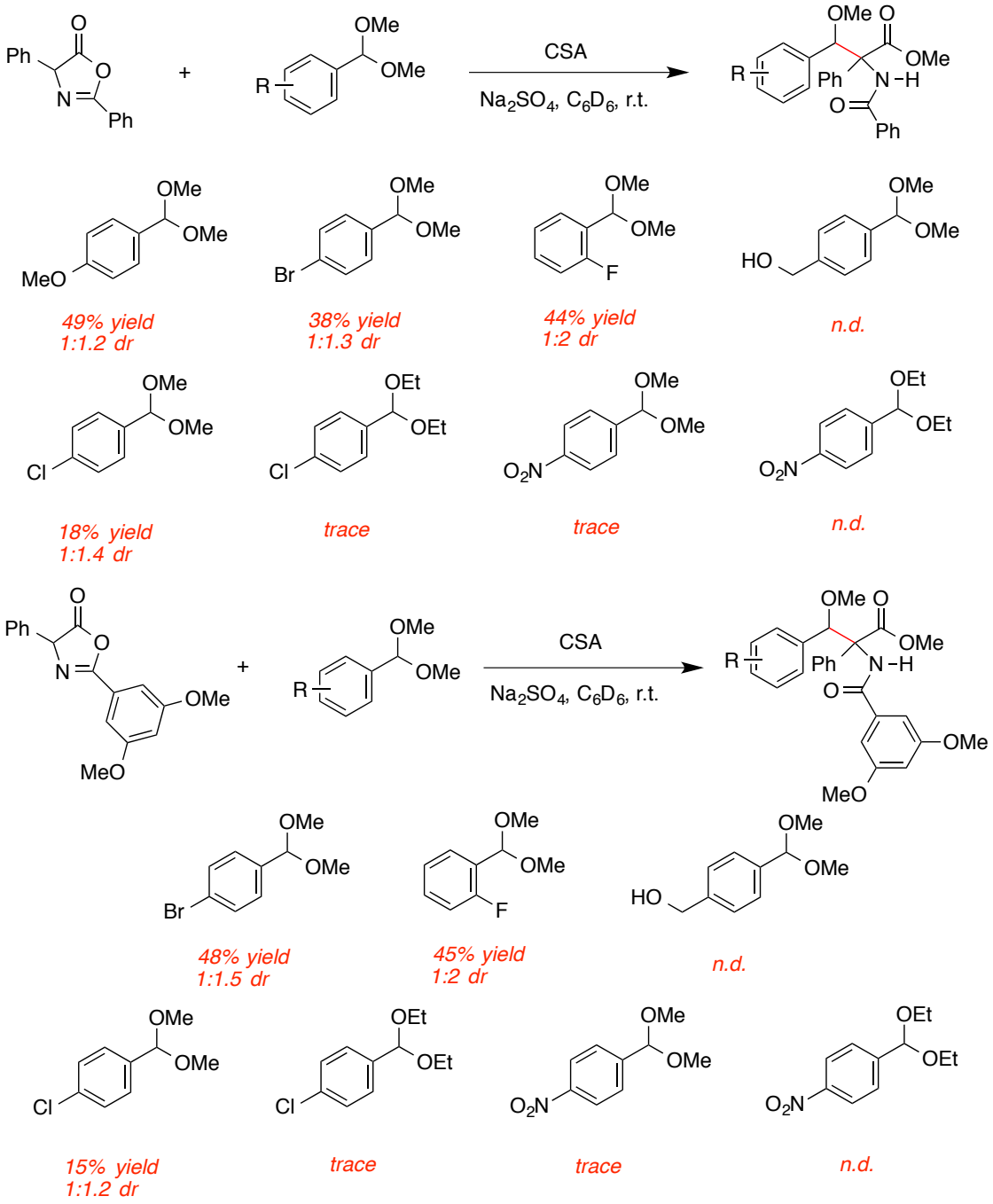

Figure 2.11 Substrate scope for various acetal derivatives in C_6D_6 (CSA)

Once the optimal reaction conditions were determined, the scope of the reactions were then probed with regard to various starting acetals. The results are shown in Figure

2.12 and 2.13 (model reaction in Figure 2.12 used *p*-TsOH as catalyst, CH_3CN as solvent, Na_2SO_4 as dehydrant and the reactions were run in r.t. for 24h). The acetals **2a**,**2b**,**2c**,**2d** and **2f** provided desired products in modest to good yields. Products realized from **2d** gave the lowest yields with both azlactones, due to steric hinderance from -F on ortho position. On the other hand, **2g** and **2h** only afforded trace amounts of products which could not be separated from crude. Unfortunately, acetals **2e** and **2i** did not furnish the desired product, which led us to speculate that strong electron withdrawing groups on acetals would reduce overall efficiency. Notably, yields of these reactions run in CH_3CN were significantly higher compared to those run in C_6D_6. The diastereoselectivities in purified products were between 1:1.04 to 1:67, and these numbers are all lower than those calculated from crude ^1H NMR which led us to speculate that one diastereomer was lost more in purification column chromatography over the other diastereomer. Both the yields and diastereoselectivity listed in Figure 2.12 and Figure 2.13 are calculated from ^1H NMR of pure isolated product after 2 steps of column chromatography.

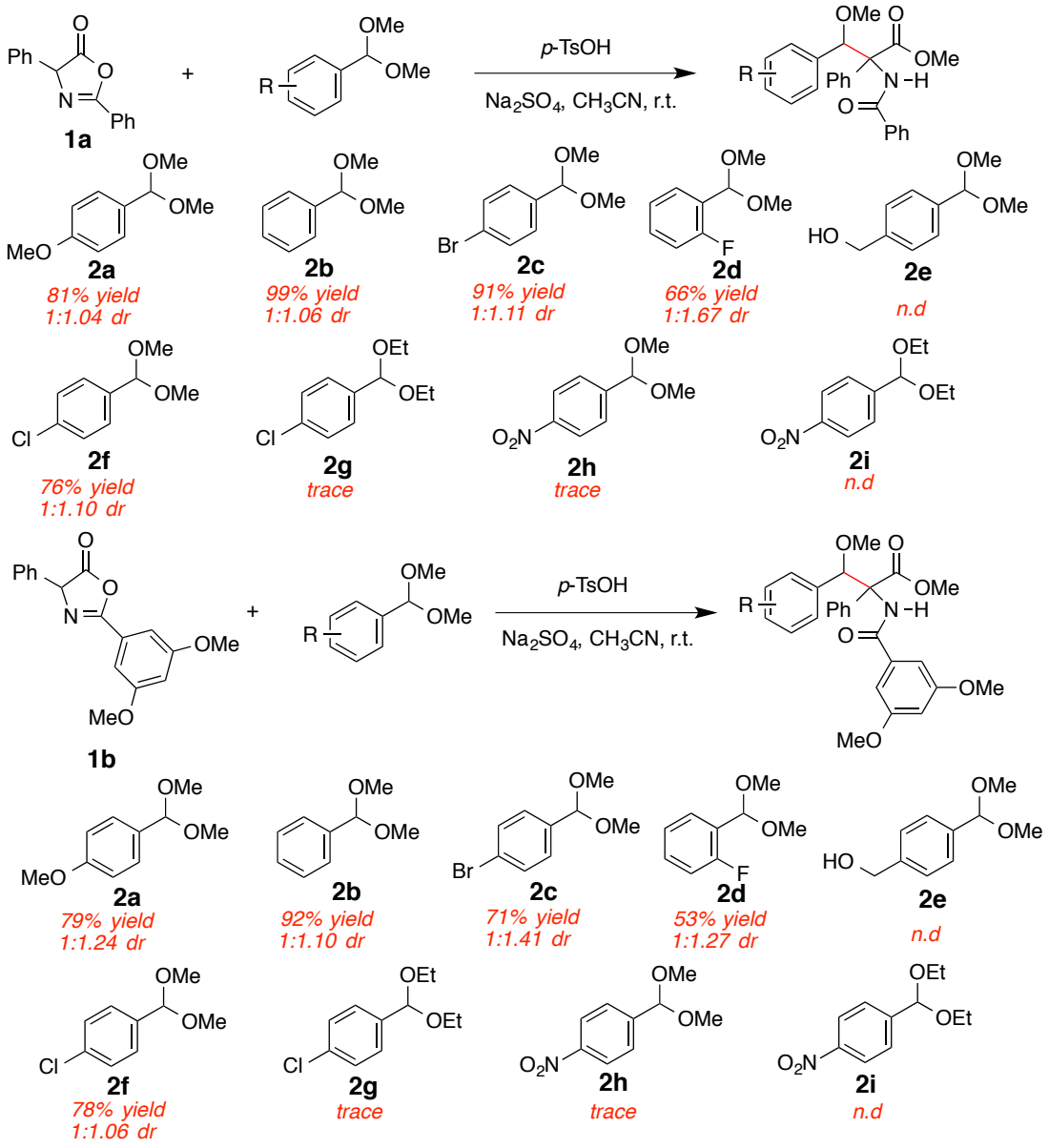

Figure 2.12 Substrate scope for various acetal derivatives in CH_3CN (*p*-TsOH)

When the catalyst was switched from *p*-TsOH to CSA and other reaction conditions stayed the same as in Figure 2.12, I got the similar yield results (Figure 2.13) varying from 60 % to 99 %, and slightly higher diastereoselectivities. The diastereoselevtivities in purified products were between 1:1.03 to 2.24.

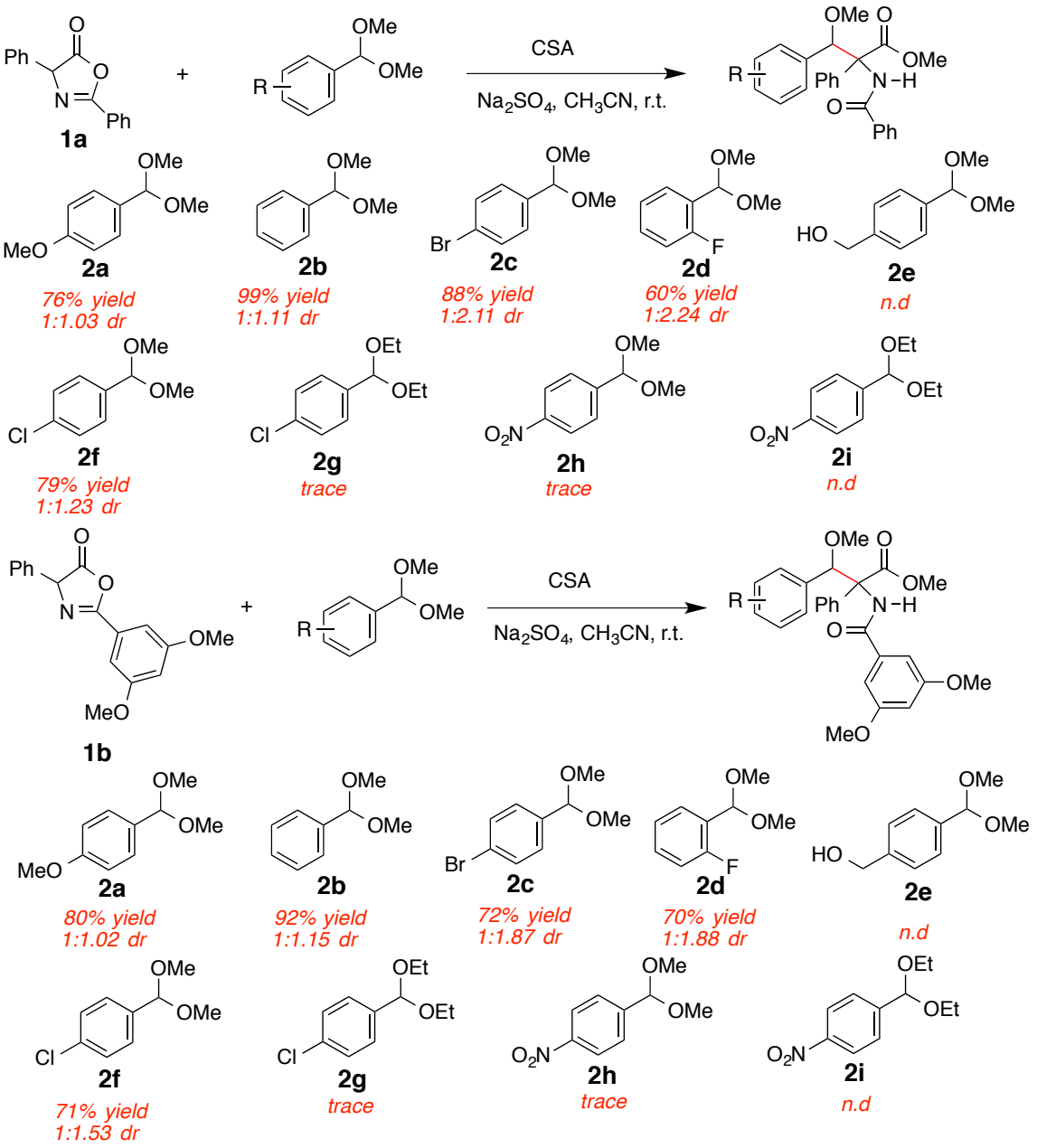

Figure 2.13 Substrate scope for various acetal derivatives in CH_3CN (CSA)

Since coupling reactions between 4-hydroxymethyl benzaldehyde dimethyl acetal with azlactones always failed to afford the desired products regardless of which solvent or catalyst was used. I thought the versatile hydroxyl functional group on acetal **2e** might

get in the way of coupling reactions. Therefore, it is desired to put a protecting group on the hydroxyl to deactivate it from reacting with azlactones. When I tried to protect the hydroxyl group with pivaloyl and tert-butyldiphenylsilyl group [60] [61] (Figure 2.14), I found the H atom on the acetal group was also missing from ^{1}H NMR, this indicates that the hydroxyl group is not the only reactive site in these alcohol protection reactions.

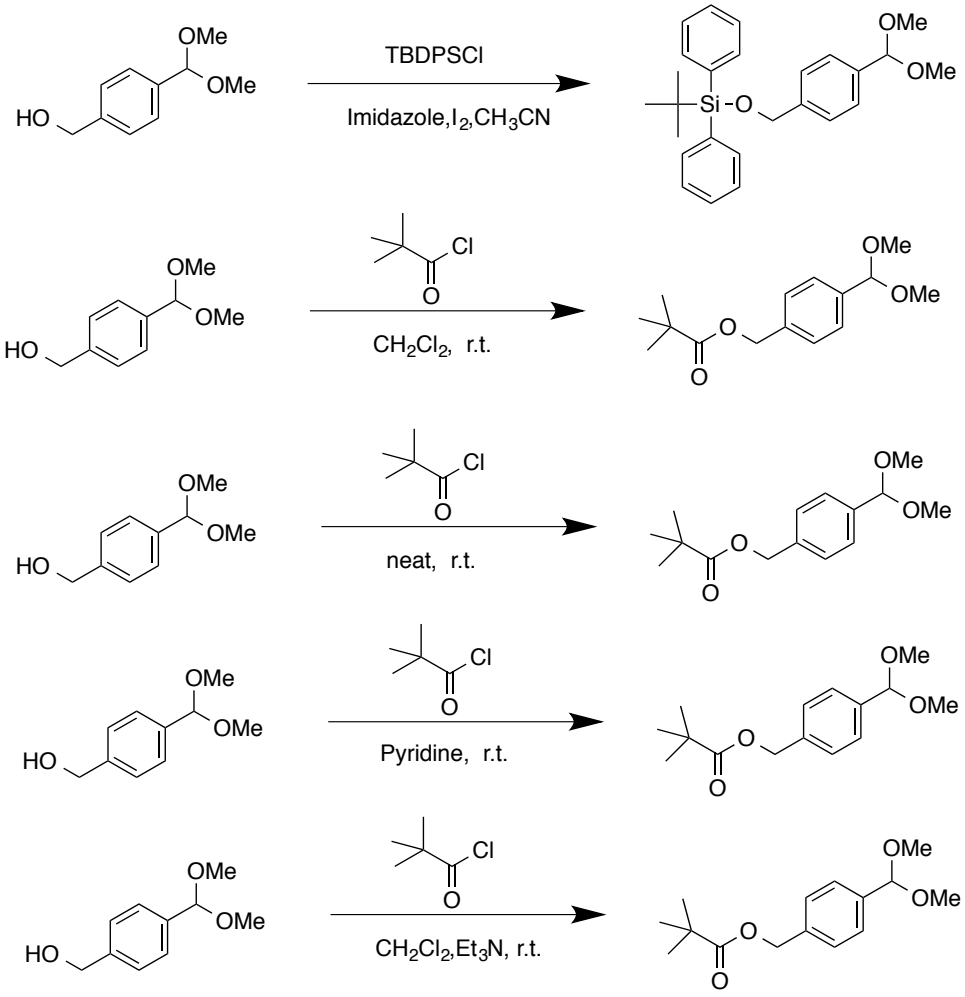

Figure 2.14 Hydroxyl group protection on acetal

In all successfully realized coupling reactions, the generation of reactive oxocarbenium ion intermediates was realized from the treatment of the acetal with a strong Brønsted acid catalyst. This highly electrophilic species is then captured by the nucleophilic azlactones. Interestingly, the desired azlactone tends to ring-open during reaction. Two possible mechanisms are proposed to explain this phenomenon (Figure 2.15). In order to tell which mechanism actually happened, I prepared phenyl glycine methyl ester directly and tried to couple it with benzaldehyde dimethyl acetyl. ^{1}H NMR showed that little open ring product was achieved. Mechanistically, the most likely scenario for this coupling reaction occurred before the ring open stage, which supports path A as the mechanism.

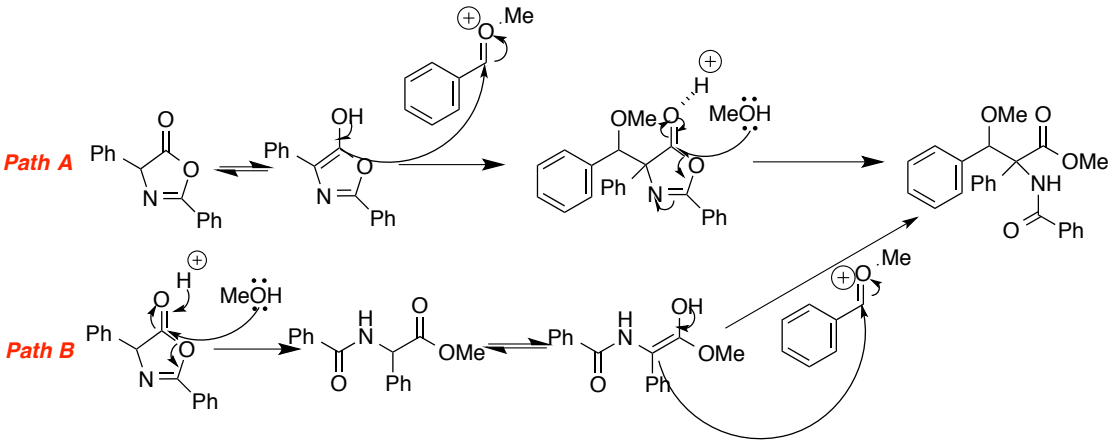

Figure 2.15 Ring open mechanism

In conclusion, we have discovered a novel coupling reaction between azlactones and acetals using Brønsted acid catalysts. Products are isolated in modest to good yields, Reaction condition optimization for better yield and diastereoselectivity is currently underway.

2.4 TRIP Acid Catalyzed Azlactone-Acetal Coupling Reaction

As introduced in previous background information, R-TRIP (3,3′-bis(2,4,6-triisopropylphenyl)-1,1′-binaphthyl-2,2′-diyl hydrogen phosphate) has emerged as one of the most successful and widely used chiral Brønsted acid catalyst for asymmetric transformations. A challenge using TRIP is that it easily becomes contaminated with metal impurities in the form of phosphate salts during synthesis.

TRIP was first introduced for the asymmetric transfer hydrogenation of imines [17] [62], A 1 mol % loading of the TRIP acid catalyst converts aromatic and aliphatic imines into the corresponding amines in high yields and enantioselectivities if treated with Hantzsch dihydropyridine (Figure 2.16). Other remarkable applications in which TRIP gradually became the best asymmetric Brønsted acid catalyst include: the reductive amination of α- branched aldehydes, that treating racemic α- branched aldehydes with p-anisidine and a Hantzsch ester in the presence of TRIP to give β-branched secondary amines [63]; an aldol addition−dehydration−conjugate reduction–reductive amination cascade to provide potential intermediates of pharmaceutically active compounds [64]; Friedel–Crafts and Pictet– Spengler reactions [65]-[67] and cycloadditions [68], [69].

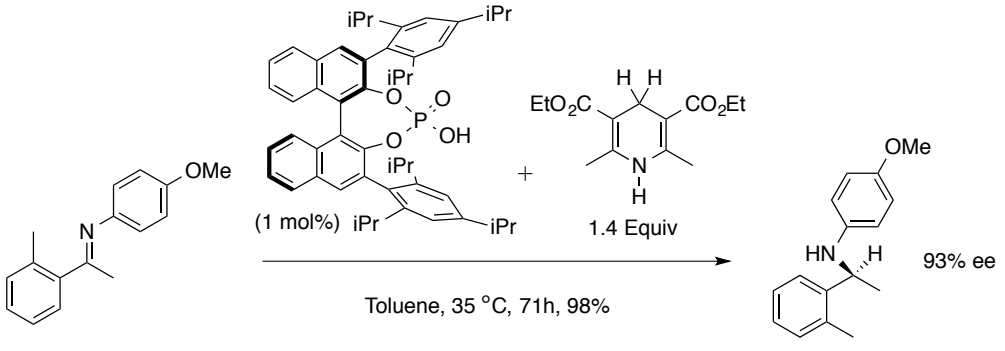

Figure 2.16 TRIP organocatalytic asymmetric transfer hydrogenation of imines

In the aforementioned reactions, asymmetry is controlled by the conjugate base of TRIP. The chiral phosphate can also influence stereoselectivity if employed in the form of salts in reactions with cationic intermediates [70], a strategy also termed asymmetric counteranion directed catalysis (ACDC) [17]. The TRIP anion induces high stereoselectivity in combination with organic counterions, for example, in the transfer hydrogenation and epoxidation of α, β--unsaturated aldehydes [18] [71] and ketones [72], [73], respectively. The use of the TRIP anion in otherwise achiral transition-metal complexes enabled asymmetric gold-catalyzed allene cyclizations [74] and palladium-catalyzed allylic alkylations [75] with ideal high degree of stereoselectivity. In addition, TRIP would work in combinations of Brønsted acid and transition- metal catalysis [76]-[80].

We speculate that TRIP would enable the coupling reaction between azlactone and acetal under our general reacting procedure, TRIP was synthesized following established synthetic procedures from the List group [81]. Detailed synthetic routes are shown in Figure 2.17, which used 1g (R)-BINOL as starting material. After 6 steps I was able to abtain desired (R)-TRIP for using in coupling reactions.

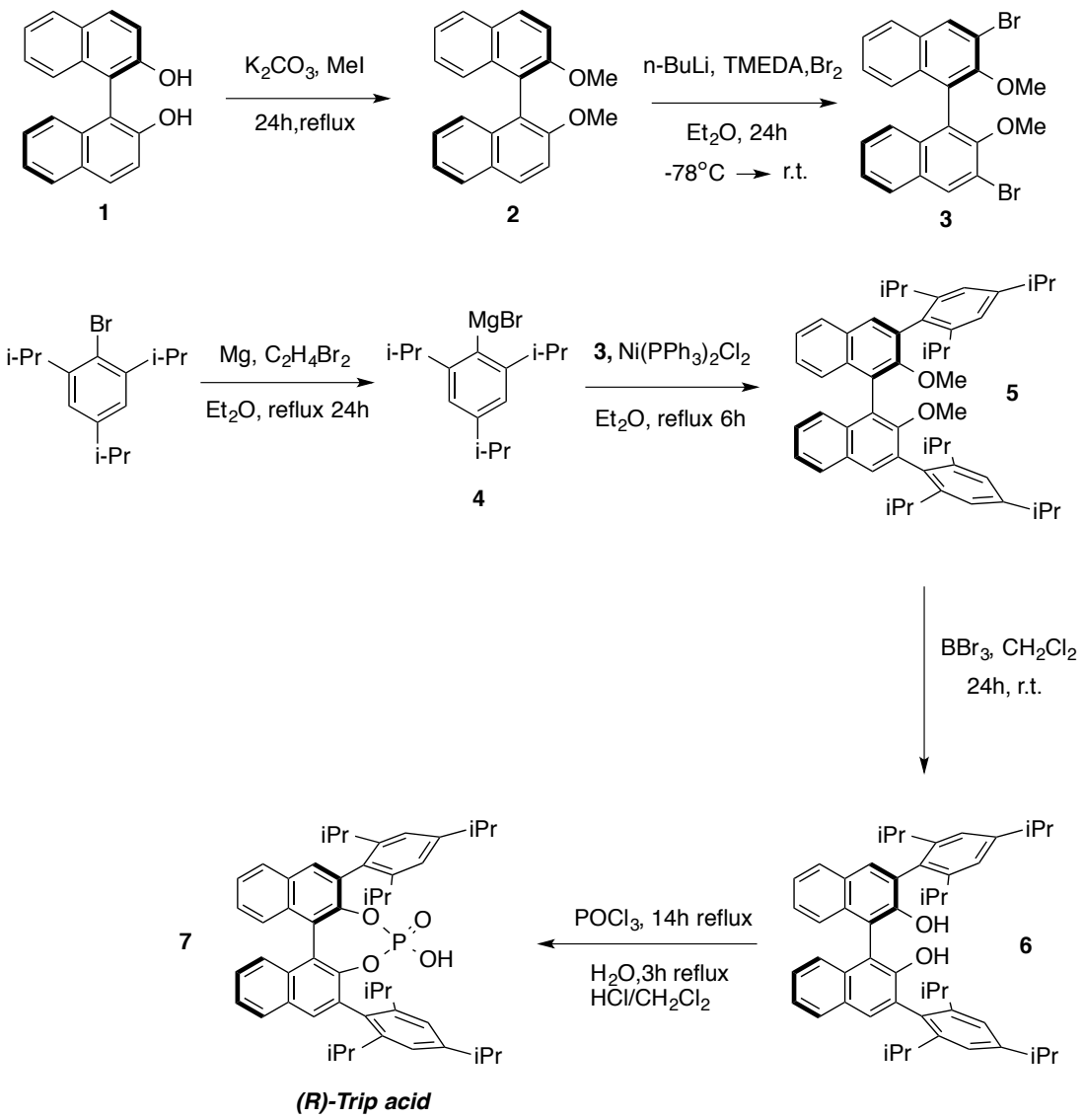

Figure 2.17 (R)- TRIP acid synthesis route

Based on crude ^{1}H NMR of (R)-TRIP, TRIP that was synthesized in our laboratories was of the quality needed to use in the azlactone-acetal coupling reaction. Reactions shown in Figure 2.18 used TRIP as catalyst, Na_2SO_4 as dehydrate and the reactions were run in CD_3CN at r.t. for 24h. TRIP catalyzed coupling reaction of diphenyl azlactone (2 equiv.) with p-anisaldehyde dimethyl acetal (1 equiv.) giving 40 %

yield with 1:1.15 dr. For the coupling reaction between 2-(3,5-dimethoxyphenyl)-4-phenyloxazol-5(4H)-one and p-anisaldehyde dimethyl acetal, TRIP catalysis afforded desired product in 20 % yield with 1:1.44 dr. Both of the yields and dr were calculated based on crude ^{1}H NMR. Although (R)-TRIP was able to promote coupling reactions, the performance was not as good as those sulfonic acids like CSA or p-TsOH, and the expensive price and difficulty in preparation limit its usage.

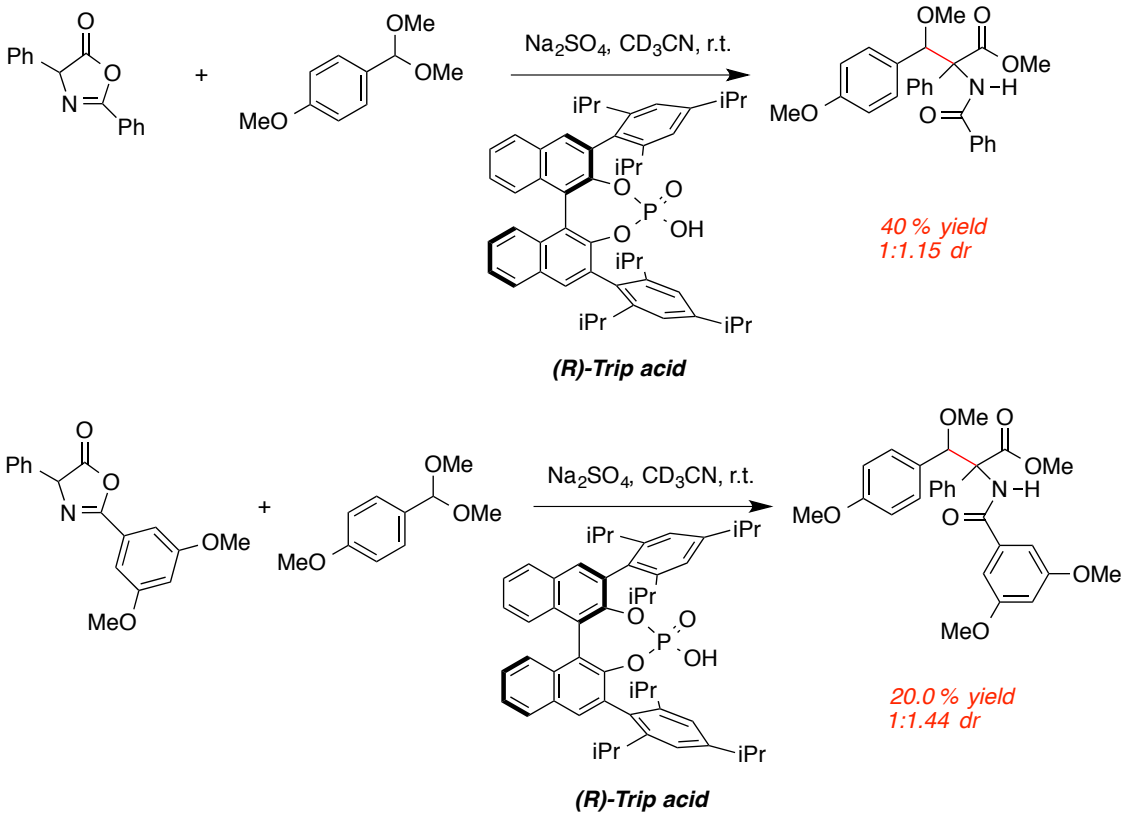

Figure 2.18 Trip acid catalyzed coupling reactions

2.5 Experimental Details

2.5.1 General experimental procedure for azlactone synthesis [48] [52].

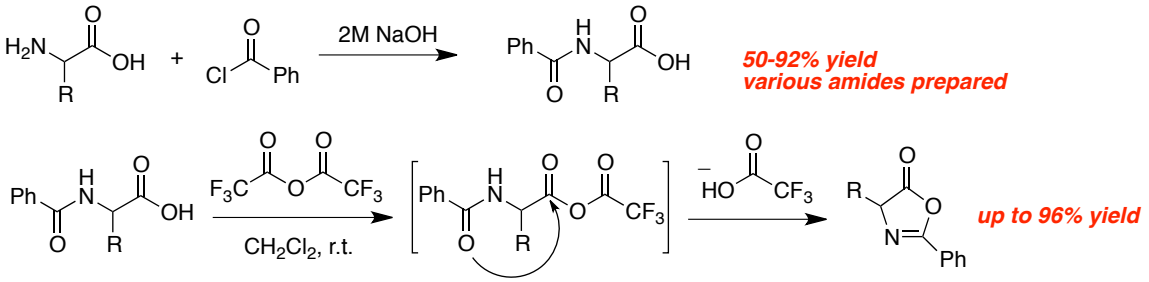

An oven-dried 100 mL round bottom flask was charged with phenyl glycine (13.24 mmol, 1.00 equiv.) and a magnetic stirring bar. To this flask 2M NaOH (0.15M) is added, the mixture is then stirred at room temperature for 5 min. Then the mixture was cooled to 0 °C, benzoyl chloride (1.69 mL, 14.52 mmol, 1.10 equiv.) then added dropwise. The reaction was run at room temperature for 2 hrs, then the reaction was quenched with 2N HCl until pH is 5-6 and the crude mixture was washed with brine and ethyl acetate, dried over Na_2SO_4 and concentrated via rotovap. The resulting phenyl glycine phenyl chloride (3.37 g, 13.20 mmol, 1.00 equiv.) was dissolved in CH_2Cl_2 (0.15M). Then the mixture was cooled to 0 °C, Trifluoroacetic anhydride (1.85 mL, 13.20 mmol, 1equiv.) was then added dropwise. The reaction was run at room temperature for 2 hrs, then the reaction was quenched with saturated $NaHCO_3$ aq. The product was then extracted into dichloromethane (3 x 50.00 mL), and the combined organic layers were dried over Na_2SO_4 and evaporated under reduced pressure via rotatory evaporation.

2.5.2 General experimental procedure for acetal possessing -Cl, -NO_2 synthesis [53].

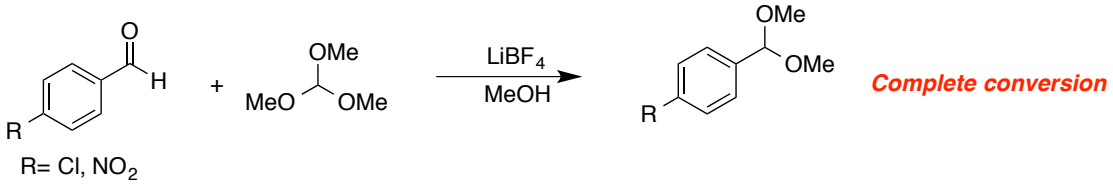

R= Cl, NO_2

To a solution of 4-chlorobenzaldehyde (4.20 g, 29.90 mmol, 1.00 equiv.) and $LiBF_4$ (0.28 g, 2.99 mmol, 0.10equiv.) in MeOH (15.00 mL) was added trimethyl orthoformate (6.95 mL, 41.80 mmol, 1.40 equiv.). The mixture was refluxed overnight and quenched by saturated $NaHCO_3$ aq (30.00 mL) followed by extraction with ethyl acetate (3 x 50.00 mL). The collected organic layer was washed with brine (2 x 30.00 mL). After drying with Na_2SO_4, the solvent was removed, and the product was collected (5.60 g, 99.8%).

Chloro-4-(dimethoxymethyl) benzene: ^{1}H NMR (500 MHz, Chloroform-d) δ 7.43 – 7.29 (m, 4H), 5.38 (s, 1H), 3.31 (s, 6H)

1-(dimethoxymethyl)-4-nitrobenzene: ^{1}H NMR (500 MHz, Chloroform-d) δ 8.27 – 8.16 (m, 2H), 7.68 – 7.59 (m, 2H), 5.48 (s, 1H), 3.34 (s, 6H)

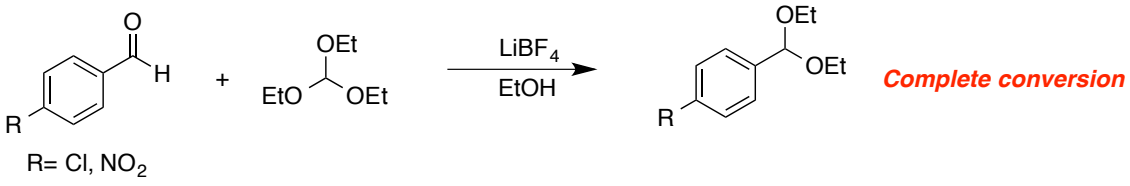

R= Cl, NO_2

To a solution of 4-chlorobenzaldehyde (4.20 g, 29.90 mmol, 1.00 equiv.) and $LiBF_4$ (0.28 g, 2.99 mmol, 0.10 equiv.) in EtOH (15.00 mL) was added triethyl

orthoformate (6.95 mL, 41.80 mmol, 1.40 equiv.). The mixture was refluxed overnight and quenched by saturated $NaHCO_3$ aq (30.00 mL) followed by extraction with ethyl acetate (3 x 50.00 mL). The collected organic layer was washed with brine (2 x 30.00 mL). After drying with Na_2SO_4, the solvent was evaporated, and the product was collected (6.4g, 99%).

1-chloro-4-(diethoxymethyl) benzene: ^{1}H NMR (500 MHz, Chloroform-d) δ 7.45 – 7.25 (m, 4H), 5.48 (s, 1H), 3.65 – 3.45 (m, 4H), 1.23 (t, J = 7.1 Hz, 6H).

1-(diethoxymethyl)-4-nitrobenzene: ^{1}H NMR (500 MHz, Chloroform-d) δ 8.22 (ddt, J = 9.2, 2.4, 1.5 Hz, 2H), 7.70 – 7.61 (m, 2H), 5.58 (s, 1H), 3.66 – 3.51 (m, 3H), 3.41 (s, 1H), 1.30 – 1.16 (m, 6H).

2.5.3 General experimental procedure for acetal possessing isopropyl synthesis [54]

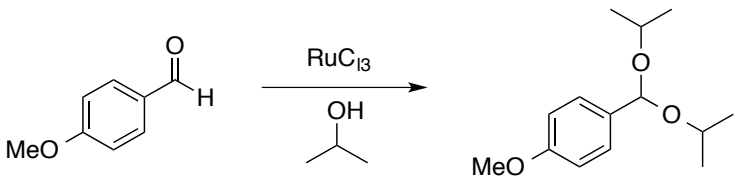

An oven-dried 50 mL round bottom flask was charged with *p*-anisaldehyde (243.12 μL, 2.00 mmol, 1.00 equiv.) and a magnetic stirring bar. To this flask 20mL dry i-PrOH was added and followed by $RuCl_3$ (20.70 mg, 0.10 mmol, 0.05 equiv.). The mixture was heat up to 75°C and refluxed for 12 hrs in oil bath. Once completed, the solvent was removed via rotatory evaporation. Crude product was purified through column chromatography (10% ethyl acetate in hexane).

2.5.4 General experimental procedure for coupling reactions in Table 2.1

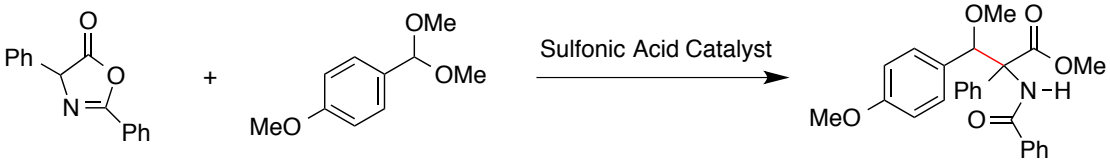

An oven-dried 10 mL round bottom flask was charged with azlactone (94.80 mg, 0.40 mmol, 2.00 equiv.) and a magnetic stirring bar. To this flask dehydrant (0.24 mmol, 1.20 equiv.) and 2.00 mL solvent was added under argon atmosphere, the mixture was then stirred at room temperature for 5 min. To the mixture, anisaldehyde dimethyl acetal (34.08 μL, 0.20 mmol, 1.00 equiv.) and catalyst (0.04 mmol, 0.20 equiv.) were added under argon atmosphere. After 24 h, the reaction was quenched with ethyl acetate (20 mL). The collected organic layer was drying with Na_2SO_4, the solvent was evaporated, and the crude mixture was collected. The crude mixture was directly purified without further work up by SiO_2 column chromatography (elution mixture of hexane with ethyl acetate).

2.5.5 Benzylic reduction [57]-[59]

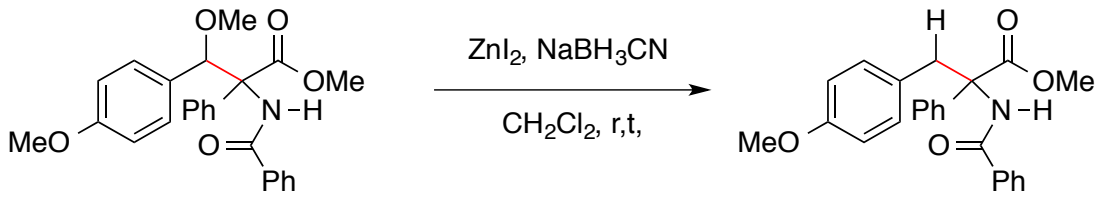

An oven-dried 25mL round bottom flask containing methyl 2-benzamido-3-methoxy-3-(4-methoxyphenyl)-2-phenylpropanoate (42.00 mg, 0.10 mmol, 1.00 equiv.) was equipped with a magnetic stirrer bar. The flask was evacuated and flushed with

argon. Subsequently the flask was charged with 8.80 mL CH_2Cl_2 at room temperature followed by solid zinc iodide (48.00 mg, 0.15 mmol, 1.50 equiv.) and sodium cyanoborohydride (47.00 mg, 0.75 mmol, 7.50 equiv.). The reaction mixture was stirred at room temperature for 20 hrs. It was then filtered through Celite. The Celite was washed with dichloromethane (10.00 mL). The combined filtrate was evaporated to dryness via rotatory evaporation.

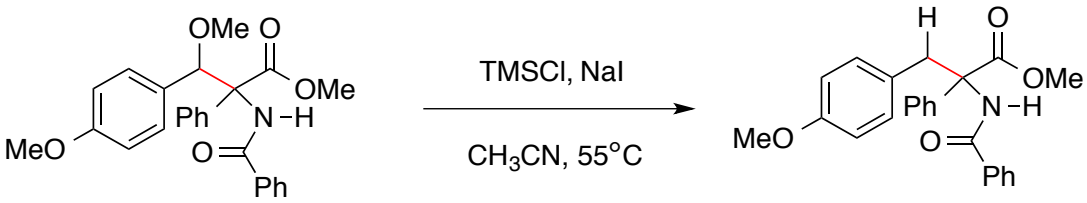

An oven-dried 10mL round bottom flask containing methyl 2-benzamido-3-methoxy-3-(4-methoxyphenyl)-2-phenylpropanoate (42.00 mg, 0.10 mmol, 1.00 equiv.) was equipped with a magnetic stirrer bar. The flask was evacuated and flushed with argon. Subsequently, the flask was charged with 2.00 mL CH_3CN followed by NaI (89.90 mg, 0.60 mol, 6.00 equiv) and trimethylsilyl chloride (76.20 µL, 0.60 mol, 6.00 equiv), heated to 55 °C in oil bath and refluxed for 48 hrs.

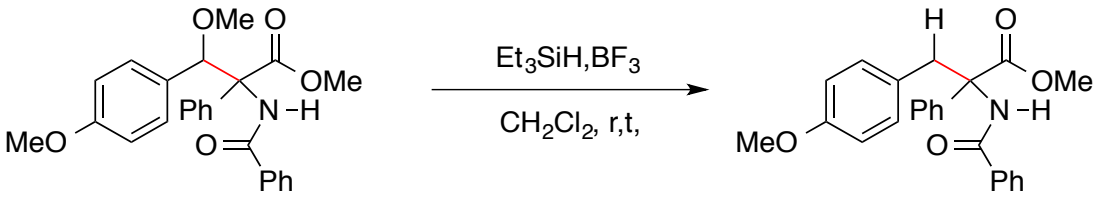

An oven-dried 25mL round bottom flask containing methyl 2-benzamido-3-methoxy-3-(4-methoxyphenyl)-2-phenylpropanoate (42.00 mg, 0.10 mmol, 1.00 equiv.)

was equipped with a magnetic stirrer bar. The flask was evacuated and flushed with argon. Subsequently the flask was charged with 4.80 mL CH_2Cl_2 at room temperature followed by triethylsilane (79.90 µL, 0.50 mmol, 5.00 equiv.) and boron trifluoride (185.10 µL, 1.50 mmol, 15.00 equiv.). The reaction mixture was stirred at room temperature for 15 min and monitored by SiO_2 preparative TLC. The reaction was quenched carefully by addition of saturated $NaHCO_3$ solution. The product was extracted with CH_2Cl_2 (3 x 10.00 mL) and the organic layer was washed with brine. The organic phase was dried over Na_2SO_4, and after filtration the solvent was removed via rotatory evaporation.

2.5.6 General experimental procedure for coupling reactions in Scheme 2.7&2.8

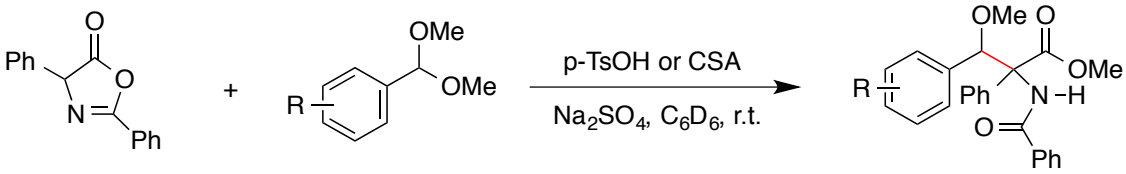

An oven-dried 10 mL round bottom flask was charged with azlactone (94.80 mg, 2.00 equiv., 0.40 mmol) and a magnetic stirring bar. To this flask dehydrant (0.24 mmol, 1.20 equiv.) and 2.00 mL C_6D_6 were added under argon atmosphere, the mixture was then stirred at room temperature for 5 min. To the mixture, acetal (0.20 mmol, 1.00 equiv.) and catalyst (0.04 mmol, 0.20 equiv.) were added under argon atmosphere. After 24 hrs, the crude ^1H NMR was taken, and reaction mixture was collected. The crude mixture was directly purified without further work up by SiO_2 column chromatography (elution mixture of hexane with ethyl acetate).

2.5.7 General experimental procedure for coupling reactions in Scheme 2.9&2.10

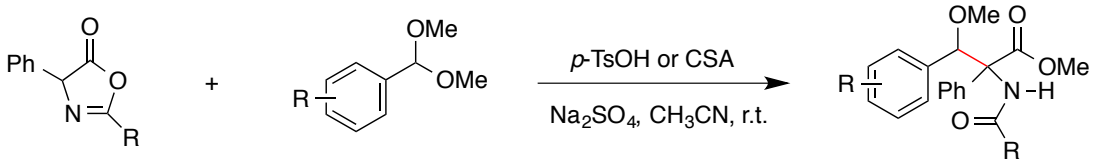

An oven-dried 10 mL round bottom flask was charged with azlactone (2.00 equiv., 0.4 mmol) and a magnetic stirring bar. To this flask Na_2SO_4 (0.24 mmol, 1.20 equiv.) and 2.00 mL CH_3CN were added under argon atmosphere, the mixture is then stirred at room temperature for 5 min. To the mixture, acetals (0.20 mmol, 1.00 equiv.) and catalyst (0.04 mmol, 0.20 equiv.) were added under argon atmosphere. After 24 hrs, the reaction was quenched with ethyl acetate (20.00 mL), the resulting mixture was washed with saturated $NaHCO_3$ solution and brine, the collected organic layer was drying with Na_2SO_4, the solvent was evaporated, and the crude mixture was collected. The crude mixture was purified by column chromatography (elution mixture of hexane with ethyl acetate), mixture of desired diastereomers and azlactone methanolysis were obtained.

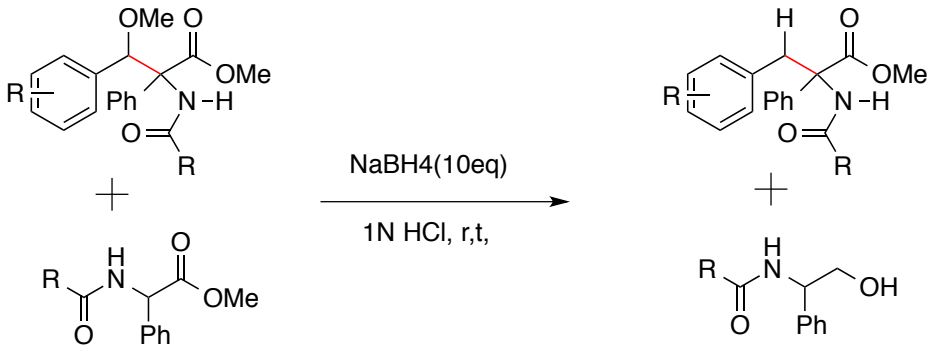

An oven-dried round bottom flask was charged with mixture of desired diastereomers and azlactone methanolysis and a magnetic stirring bar. To this flask MeOH (2.00 mL) was added followed by $NaBH_4$ (10.00 equiv.) The reaction mixture

was stirred at room temperature and monitored by SiO_2 preparative TLC. The reaction was quenched with 1N HCl once completed, the product was then extracted into ethyl acetate (20.00 mL), and the combined organic layers were dried over Na_2SO_4 and evaporated under reduced pressure via rotatory evaporation. The crude residue was then purified by SiO_2 column chromatography (elution mixture of hexane with ethyl acetate) to give the desired diastereomers.

2.5.8 General experimental procedure for hydroxyl group protection [60], [61]

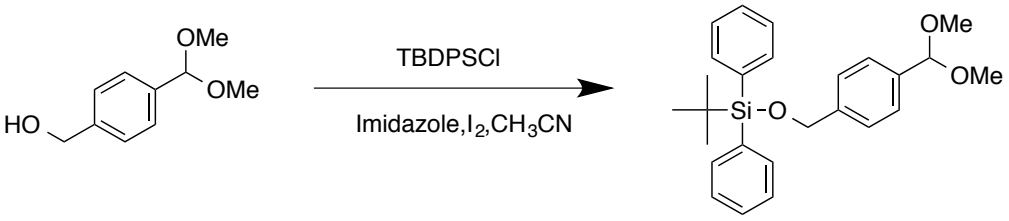

An oven-dried 10mL round bottom flask containing 4-(hydroxymethyl)-benzaldehyde dimethyl acetal (72.80 mg, 0.40 mmol, 1.00 equiv.) was equipped with a magnetic stirrer bar. The flask was evacuated and flushed with argon. Subsequently the flask was charged with 2.00 ml CH_3CN followed by tert-butyldiphenylchlorosilane (114.42 µL, 0.44 mmol, 1.10 equiv.) and iodine (152.28 mg, 1.20 mmol, 3.00 equiv.), the resulting mixture was added imidazole (59.9 mg, 0.88 mmol, 2.20 equiv.) then reaction was left at r.t. and monitored by SiO_2 preparative TLC. Once completed, the solvent was removed via rotovap. The residue was dissolved in EtOAc and washed with saturated $Na_2S_2O_3$ solution. The organic phase was dried over Na_2SO_4, and after filtration the solvent was removed via rotatory evaporation.

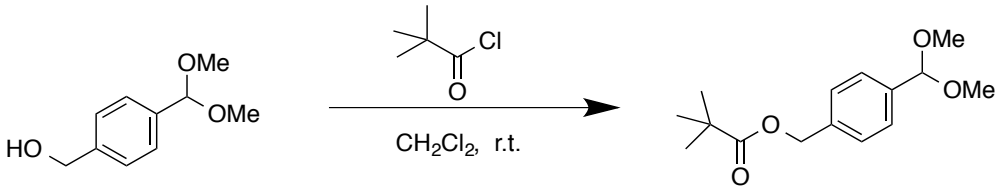

An oven-dried 10mL round bottom flask containing 4-(hydroxymethyl)-benzoaldehyde dimethyl acetal (36.40 mg, 0.20 mmol, 1.00 equiv.) was equipped with a magnetic stirrer bar. The flask was evacuated and flushed with argon. Subsequently the flask was charged with 1.00 mL CH_2Cl_2 followed by pivaloyl chloride (27.1 µL, 0.22 mmol, 1.1 equiv.), the resulting mixture was left at r.t. and monitored by SiO_2 preparative TLC. Once completed, these organic mixtures were washed with distilled water. The organic phase was dried over Na_2SO_4, and after filtration the solvent was removed via rotatory evaporation.

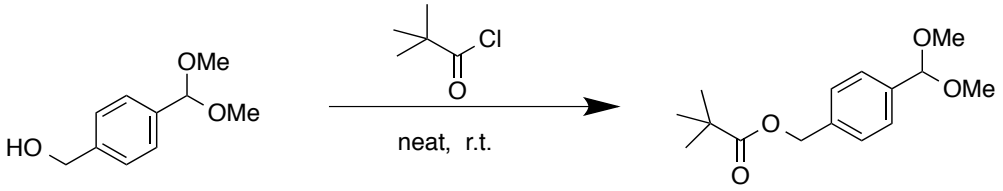

An oven-dried 10mL round bottom flask containing 4-(hydroxymethyl)-benzoaldehyde dimethyl acetal (72.89 mg, 0.40 mmol, 1.00 equiv.) was equipped with a magnetic stirrer bar. The flask was evacuated and flushed with argon. Subsequently the flask was charged with pivaloyl chloride (54.2 µL, 0.44 mmol, 1.10 equiv.), the resulting mixture was left at r.t. and monitored by SiO_2 preparative TLC. Once completed, the mixture was dissolved in 2.00 mL CH_2Cl_2 and washed these organic mixtures with distilled water. The organic phase was dried over Na_2SO_4 and concentrated via rotovap.

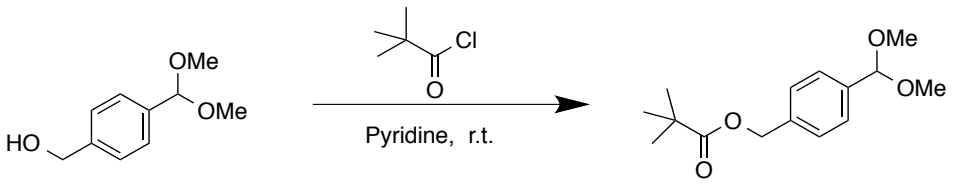

An oven-dried 10mL round bottom flask containing 4-(hydroxymethyl)-benzoaldehyde dimethyl acetal (58.3 mg, 0.32 mmol, 1.00 equiv.) was equipped with a magnetic stirrer bar. The flask was evacuated and flushed with argon. Subsequently the flask was charged with 1mL Pyridine followed by pivaloyl chloride (43.30 µL, 0.352 mmol, 1.10 equiv.), the resulting mixture was left at r.t. and monitored by SiO_2 preparative TLC. Once completed, these organic mixtures were washed with EtOAc and 1M HCl, then resulting mixture was washed with saturated $NaHCO_3$ solution and saturated NaCl solution. The organic phase was dried over Na_2SO_4, and after filtration the solvent was removed via rotatory evaporation.

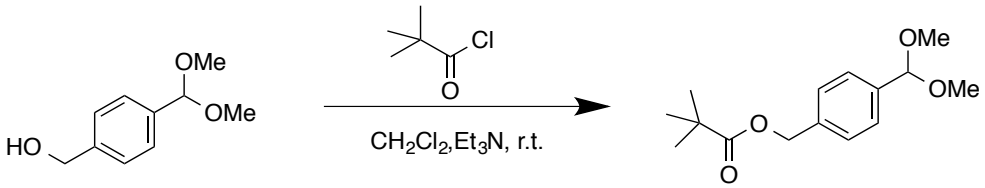

An oven-dried 10mL round bottom flask containing 4-(hydroxymethyl)-benzoaldehyde dimethyl acetal (36.40 mg, 0.20 mmol, 1.00 equiv.) was equipped with a magnetic stirrer bar. The flask was evacuated and flushed with argon. Subsequently the flask was charged with 1.00 mL CH_2Cl_2 followed by pivaloyl chloride (27.00 µL, 0.22 mmol, 1.10 equiv.) and Et_3N (0.488 mL, 3.50 mmol, 17.50 equiv.), the resulting mixture was left at r.t. and monitored by SiO_2 preparative TLC. Once completed, these organic

mixtures were washed with EtoAc and 1M HCl, then the resulting mixture was washed with saturated $NaHCO_3$ solution and saturated NaCl solution. The organic phase was dried over Na_2SO_4, and after filtration the solvent was removed via rotatory evaporation.

2.5.9 Experimental procedure for path B of ring open mechanism

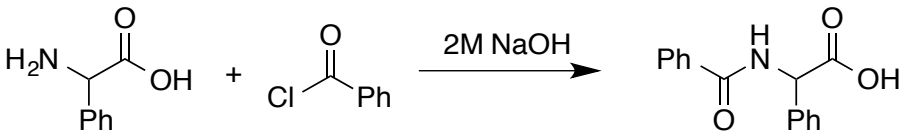

An oven-dried 100 mL round bottom flask was charged with phenyl glycine (2.00 g, 13.24 mmol, 1.00 equiv.) and a magnetic stirring bar. To this flask 2M NaOH (0.15M) was added, the mixture was then stirred at room temperature for 5 mins. Then the mixture was cooled to 0 °C, benzoyl chloride (1.69 mL, 14.52 mmol, 1.10 equiv.) was then added dropwise. The reaction was run at room temperature for 2 hrs, then the reaction was quenched with 2N HCl until pH became 5-6 and the crude mixture was washed with brine and ethyl acetate, dried over Na_2SO_4 and concentrated via rotatory evaporation.

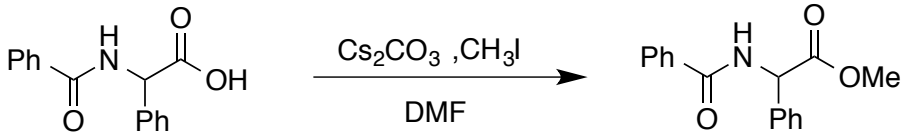

An oven-dried 50 mL round bottom flask was charged with phenyl glycine phenyl chloride (189.00 mg, 0.73 mmol, 1.00 equiv.) and a magnetic stirring bar. To this flask 10.00 mL DMF and Cs_2CO_3 (286.70 mg, 0.88 mmol, 1.20 equiv.) were added, the mixture was cooled to 0 °C and CH_3I was then added dropwise. The reaction was

allowed to warm up to room temperature and reaction was run for 2 hrs. The mixture was diluted with EtOAc and washed with saturated NaCl aq, the crude mixture was dried over Na_2SO_4 and concentrated via rotatory evaporation. The resulting white solid crude was subjected to a column chromatography (hexanes/ethyl acetate 10:1) for the next step.

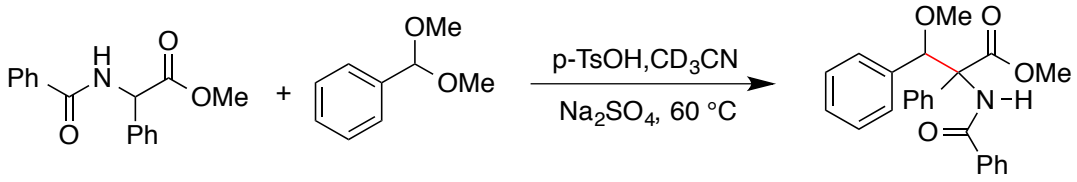

An oven-dried 10 mL round bottom flask was charged with methyl 2-benzamido-2-phenylacetate (122.10 mg, 0.45 mmol, 2.00 equiv.) and a magnetic stirring bar. To this flask Na_2SO_4 (38.35 mg, 0.27 mmol, 1.20 equiv.) and 4.00 mL CD_3CN were added under argon atmosphere, the mixture was then stirred at room temperature for 5 mins. To the mixture, benzaldehyde dimethyl acetal (34.50 μL, 0.23 mmol, 1.00 equiv.) and p-TsOH (8.56 mg, 0.045 mmol, 0.20 equiv.) were added under argon atmosphere. Then the mixture was heated to 60 °C in oil bath and reaction was monitored by SiO_2 preparative TLC and ^1H NMR.

2.5.10 General experimental procedure for TRIP acid synthesis [81]

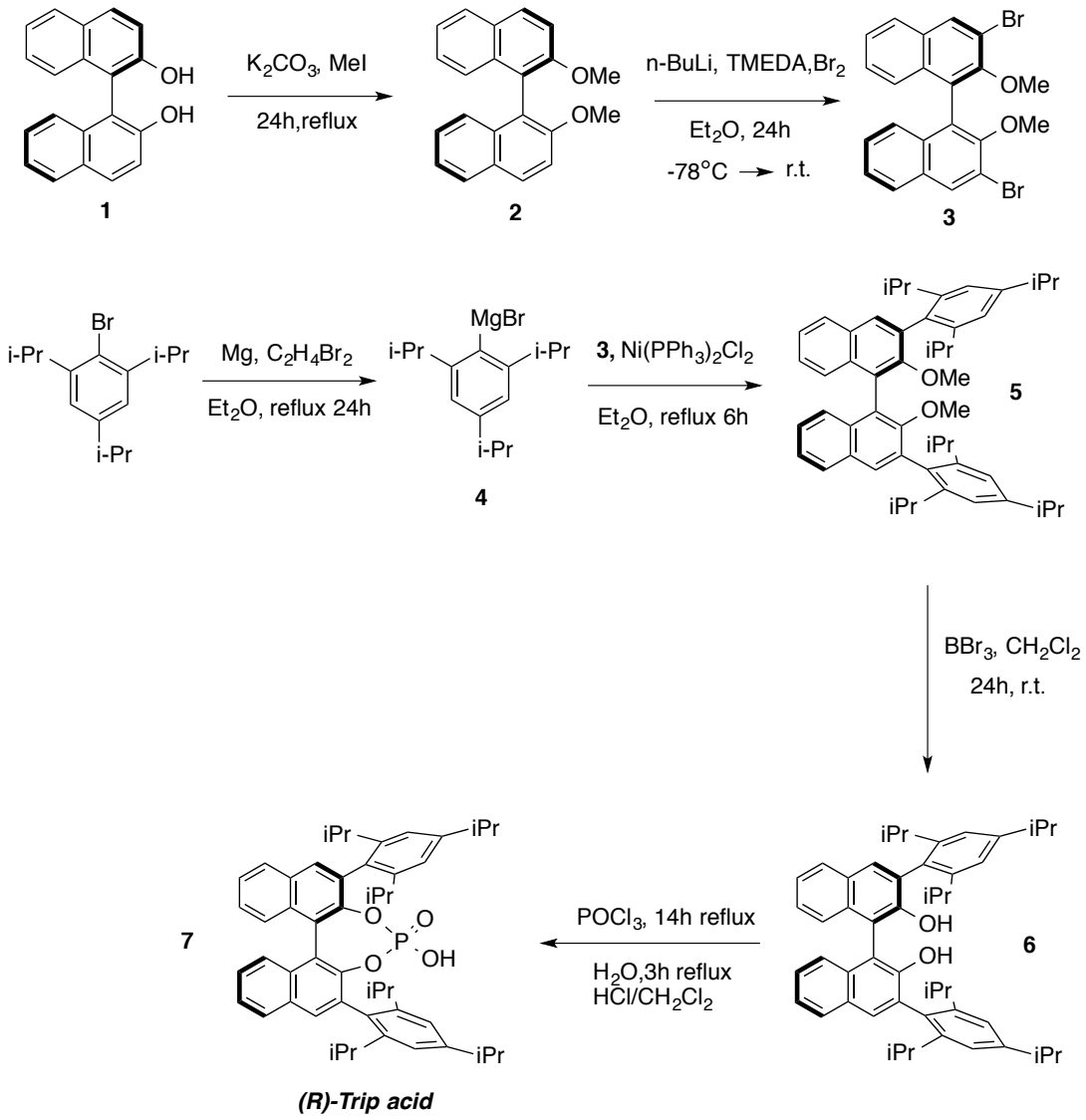

A. (R)-2,2'-dimethoxy-1,1'-binaphthyl (**2**). A 250-mL three-necked round-bottom flask containing (R)-BINOL 1 (1.00 g, 3.458 mmol, 1.00 equiv.) was equipped with a magnetic stirrer bar, an addition funnel, a reflux condenser with argon inlet and a glass stopper. The flask was evacuated and flushed with argon. Subsequently the vessel was charged with 32 mL dried acetone, upon complete solution of the prior compound,

potassium carbonate (1.576 g, 11.42 mmol, 3.30 equiv.) was added followed by methyl iodide (0.87 mL, 1.982 g, 13.84 mmol, 4.00 equiv.). The resulting mixture was heated to reflux in an oil bath (oil temperature ~85°C) for 24 hrs. After that time the volatile compounds were removed under reduced pressure. The resulting slurry was redissolved in 36 mL of water and stirred for 2 hrs. The resulting solid was collected on a funnel, washed with water and dried in oven to furnish 1.00 g (91.7%) of the title compound **2** as a slight yellow solid.

B. (R)-3,3'-dibromo-2,2'-dimethoxy-1,1'-binaphthyl (**3**). A 100-mL three-necked round- bottom flask equipped with a magnetic stirrer bar, an addition funnel, an argon inlet and a glass stopper was evacuated and flushed with argon. Subsequently 50 mL dried diethyl ether were added, followed by tetramethylethylenediamine (0.41 ml, 2.80 mmol, 2.20 equiv.). To the resulting solution n-butyllithium (2.5 M in hexanes, 2.80 mL, 4.42 mmol, 3.5 equiv.) was added slowly at r.t. via syringe, the mixture was allowed to stir for 1 h. Then compound **2** (0.40 g, 1.272 mmol, 1.00 equiv.) was added as a solid at r.t. and the resulting solution was stirred for 3.5 hrs. After this time the reaction was cooled to -78°C (dry ice/acetone bath) and bromine (0.32 mL, 6.40 mmol, 5.0 equiv.) was added dropwise via addition funnel. After complete addition, the cooling was removed, and the yellowish-brown reaction mixture was allowed to stir for 20 hrs at r.t. The reaction was quenched with 8 mL ≈ Na_2SO_3-solution and stirred for 1 h. The mixture was extracted with Et_2O (3 x 10.00 mL), the organic phases were combined, washed with brine (10.00 mL) and dried over Na_2SO_4. After filtration the solvent was removed via rotatory evaporation and the crude mixture was subjected to column chromatography

(hexanes/ethyl acetate 20:1) resulting in a yellowish solid material which is recrystallized from CH_2Cl_2/hexanes. The mother liquor was subjected to a second column chromatography (same conditions as above) and the resulting material was crystallized (same conditions as above). In total 0.40 g (67.2 %) of the title compound **3** were obtained as slight yellow crystals.

C. (2,4,6-triisopropylphenyl) magnesium bromide (**4**). A dried 100 mL two necked flask with Ar-inlet, magnetic stirrer bar, reflux condenser and septum was charged with Mg (0.252 g, 10.4 mmol, 2.00 equiv., activated with a spatula tip of iodine). The Mg was covered with Et_2O (1.00 mL), subsequently 2-bromo-1,3,5-triisopropylbenzene (1.534 g, 5.20 mmol, 1.00 equiv.), the rest of the Et_2O (7.00 mL) and 0.02 mL 1,2-dibromoethane (as activator) were charged in different syringes and added in a manner of maintaining the exothermic Grignard-reaction active. After complete addition of the compounds, the resulting grey solution was placed in a pre-heated oil bath to be refluxed for 24 hrs. The resulting solution was filtered through a short pad of cotton and used in unmodified form in the next step.

D. (1R,3R)-2,2'-dimethoxy-3,3'-bis(2,4,6-triisopropylphenyl)-1,1'-binaphthyl (**5**). An oven dried 15 mL two-necked flask with Ar-inlet, magnetic stirrer and addition funnel was charged with compound **3** (0.40 g, 0.848 mmol, 1.00 equiv.) and $Ni(PPh_3)_2Cl_2$ (55.4 mg, 0.084 mmol, 0.10 equiv.) evacuated and set under Argon. Subsequently Et_2O (5.00 mL) was added and to the resulting suspension the Grignard-solution **4** was added dropwise at r.t. After complete addition the resulting mixture was refluxed for 6 hrs. The resulting brown solution was allowed to reach r.t. and then cooled to 0°C with an ice bath

and quenched with 1 M HCl (6.00 mL). The resulting mixture was extracted with Et_2O (3 x 5.00 mL), the organic phase was dried over Na_2SO_4, filtered and the solvent was removed via rotatory evaporation. The resulting slight yellow solid crude was subjected to a column chromatography (hexanes/ethyl acetate 20:1) resulting compound **5** 308 mg.

E. (1R,3R)-3,3'-bis(2,4,6-triisopropylphenyl)-1,1'-binaphthyl-2,2'-diol (**6**). In a 15-mL three-necked flask with magnetic stirrer, Ar-inlet and addition funnel the crude material 5 was evacuated, set under Argon and dissolved in 10.50 mL dry dichloromethane. Subsequently the solution was cooled with an ice bath followed by slow addition of BBr_3 (1 M in hexanes, 2.97 mL, 2.97 mmol, 7.00 equiv.). After complete addition, the resulting clear solution was allowed to stir for 24 hrs at r.t. Subsequently water (4.00 mL) was added to quench the reaction. The aqueous layer was extracted with CH_2Cl_2 (3 x 2.50 mL), the combined organic layers were dried over Na_2SO_4, filtered and the solvent was reduced via rotatory evaporation. Column chromatography (hexanes/ethyl acetate 99:1) gave a slight yellow material which was triturated with hexanes resulting in 0.15 g (51.13 % over two steps) of the title compound **6**.

F. TRIP-Phosphoric Acid (**7**). A 15 mL three-necked flask with reflux condenser, Ar-inlet and glass stopper was charged with 6 (150 mg, 0.217 mmol, 1.00 equiv.) and set under Argon. Subsequently pyridine (0.45 mL) was added, followed by $POCl_3$ (60 µL, 0.65 mmol, 3.00 equiv.). The resulting mixture was refluxed for 14 h. After this time the reaction was allowed to reach r.t., followed by addition of water (0.45 mL). The resulting

brownish slurry was heated to reflux and hydrolyzed for 3 hrs. After the reaction reached r.t. 1.50 mL CH_2Cl_2 were added. The resulting organic phase was thoroughly washed with 1 M HCl (3 x 1.50 mL). The resulting organic layer could be dried over Na_2SO_4 and recrystallized from acetonitrile. The aqueous medium should be clearly acidic (pH = 1~2) throughout the last workup steps to maintain the product in its free acid form. 147.6 mg (90.7 %) of compound **7** were obtained following this route.

2.6 Product Characterization

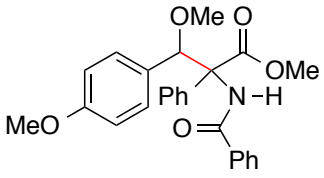

Methyl 2-benzamido-3-methoxy-3-(4-methoxyphenyl)-2-phenylpropanoate(3a)

p-TsOH: dr=1:1.04

^{1}H NMR (500 MHz, Chloroform-d) δ 7.79 – 7.71 (m, 4H), 7.56 – 7.34 (m, 8H), 7.36 – 7.19 (m, 9H), 6.94 – 6.85 (m, 4H), 6.80 – 6.72 (m, 5H), 5.30 (s, 1H), 5.08 (s, 1H), 3.85 (s, 3H), 3.78 (d, J = 1.3 Hz, 6H), 3.75 (s, 3H), 3.33 (s, 3H), 3.23 (s, 3H).

^{13}C NMR (126 MHz, CDCl3) δ 171.65, 170.95, 166.54, 166.52, 159.88, 159.67, 135.82, 135.53, 134.80, 134.05, 131.84, 131.60, 129.73, 129.26, 128.68, 128.62, 128.58, 128.21, 127.77, 127.73, 127.61, 127.43, 127.20, 127.06, 127.04, 113.94, 113.38, 113.31, 86.11, 85.29, 76.77, 70.14, 68.52, 57.40, 57.35, 55.19, 53.17, 52.75.

HRMS (ESI) calcd for $C_{25}H_{25}NO_5$ $[M-H]^+$ 420.1811, found 420.1806

IR(cm^{-1}) 1091,1478,1671,1752, 2835,2949,3062

Rf =0.29 (25:75 EtOAc: Hexane)

CSA: dr=1:1.03

^{1}H NMR (500 MHz, Chloroform-d) δ 7.79 – 7.70 (m, 4H), 7.57 – 7.34 (m, 8H), 7.36 – 7.19 (m, 9H), 6.94 – 6.86 (m, 4H), 6.80 – 6.73 (m, 5H), 5.30 (s, 1H), 5.08 (s, 1H), 3.85 (s, 3H), 3.78 (d, J = 1.5 Hz, 6H), 3.75 (s, 3H), 3.33 (s, 3H), 3.23 (s, 3H).

^{13}C NMR (126 MHz, CDCl3) δ 171.66, 170.96, 166.55, 166.52, 159.88, 159.67, 135.83, 135.54, 134.81, 134.06, 131.84, 131.60, 129.73, 129.26, 128.68, 128.58, 128.21, 127.78, 127.75, 127.62, 127.43, 127.22, 127.06, 127.04, 113.39, 113.31, 86.11, 85.28, 76.76, 70.14, 68.52, 57.41, 57.36, 55.19, 53.17, 52.76.

HRMS (ESI) calcd for $C_{25}H_{25}NO_5$ $[M-H]^+$ 420.1811, found 420.1818

IR(cm^{-1}) 1091,1478,1671,1752, 2835,2949,3060

Rf =0.28 (25:75 EtOAc: Hexane)

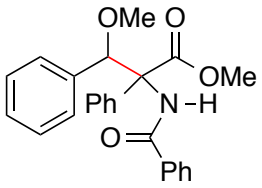

Methyl 2-benzamido-3-methoxy-2,3-diphenylpropanoate(3b)

p-TsOH: dr=1:1.06

^{1}H NMR (500 MHz, Chloroform-d) δ 7.78 – 7.70 (m, 4H), 7.56 – 7.16 (m, 23H), 7.05 – 6.95 (m, 4H), 6.81 (s, 1H), 5.36 (s, 1H), 5.16 (s, 1H), 3.86 (s, 3H), 3.73 (s, 3H), 3.35 (s, 3H), 3.25 (s, 3H).

^{13}C NMR (126 MHz, CDCl3) δ 171.61, 170.86, 166.67, 166.52, 136.04, 135.75, 135.59, 135.40, 134.80, 134.09, 131.85, 131.61, 128.69, 128.68, 128.58, 128.50, 128.11, 128.06,

127.95, 127.90, 127.83, 127.66, 127.64, 127.56, 127.49, 127.05, 127.02, 86.25, 85.57, 70.07, 68.55, 57.58, 57.56, 53.22, 52.73.

HRMS (ESI) calcd for $C_{24}H_{23}NO_4$ $[M-H]^+$ 390.1705, found 390.1713

IR(cm^{-1}) 1097,1478,1671,1751,2827,2949,3061

Rf =0.39 (25:75 EtOAc : Hexane)

CSA: dr=1:1.11

^1H NMR (500 MHz, Chloroform-d) δ 7.78 – 7.70 (m, 4H), 7.57 – 7.18 (m, 23H), 7.00 (ddt, J = 11.1, 7.1, 1.4 Hz, 4H), 6.81 (s, 1H), 5.36 (s, 1H), 5.16 (s, 1H), 3.86 (s, 3H), 3.73 (s, 3H), 3.35 (s, 3H), 3.25 (s, 3H).

^{13}C NMR (126 MHz, CDCl3) δ 171.62, 170.87, 166.68, 166.53, 136.05, 135.76, 135.60, 135.41, 134.81, 134.10, 131.85, 131.61, 128.69, 128.59, 128.51, 128.12, 128.06, 127.96, 127.90, 127.83, 127.67, 127.64, 127.56, 127.50, 127.06, 127.03, 86.25, 85.57, 70.08, 68.57, 57.59, 57.57, 53.23, 52.74.

HRMS (ESI) calcd for $C_{24}H_{23}NO_4$ $[M-H]^+$ 390.1705, found 390.1706

IR(cm^{-1}) 1100,1483,1675,1757, 2849,2949,3053

Rf =0.38 (25:75 EtOAc : Hexane)

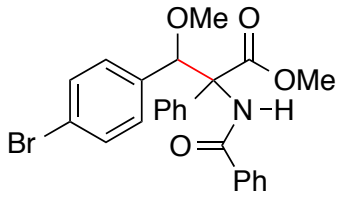

Methyl 2-benzamido-3-(4-bromophenyl)-3-methoxy-2-phenylpropanoate(3c)

p-TsOH: dr=1:1.11

^{1}H NMR (500 MHz, Chloroform-d) δ 7.77 – 7.68 (m, 4H), 7.53 (q, J = 7.8 Hz, 2H), 7.49 – 7.41 (m, 5H), 7.39 – 7.23 (m, 14H), 6.88 (t, J = 9.1 Hz, 4H), 6.74 (s, 1H), 5.39 (s, 1H), 5.26 (s, 1H), 3.84 (s, 3H), 3.75 (s, 3H), 3.32 (s, 3H), 3.25 (s, 3H).

^{13}C NMR (126 MHz, CDCl3) δ 171.49, 170.81, 167.10, 166.57, 135.64, 135.49, 134.84, 134.59, 133.96, 132.00, 131.76, 131.03, 130.94, 130.29, 129.87, 128.76, 128.66, 128.11, 127.89, 127.83, 127.74, 127.67, 127.43, 127.01, 127.00, 122.56, 84.54,76.76, 69.88, 68.56, 57.64, 57.61, 53.29, 52.78.

HRMS (ESI) calcd for $C_{24}H_{22}BrNO_4$ $[M-H]^+$ 470.0793, found 470.0795

IR(cm^{-1}) 1090,1478,1669,1732,2825,2949,3061

Rf =0.34 (25:75 EtOAc : Hexane)

CSA: dr=1:2.11

^{1}H NMR (500 MHz, Chloroform-d) δ 7.78 – 7.68 (m, 6H), 7.58 – 7.41 (m, 9H), 7.41 – 7.21 (m, 22H), 6.93 – 6.84 (m, 6H), 6.74 (s, 2H), 5.39 (s, 1H), 5.26 (s, 2H), 3.84 (s, 3H), 3.75 (s, 6H), 3.32 (s, 3H), 3.25 (s, 6H)

^{13}C NMR (126 MHz, CDCl3) δ 171.49, 170.82, 167.11, 166.58, 135.64, 135.49, 134.84, 134.59, 133.96, 132.00, 131.76, 131.03, 130.94, 130.29, 129.87, 128.77, 128.66, 128.11, 127.89, 127.83, 127.74, 127.67, 127.43, 127.01, 127.00, 122.60, 122.56, 84.54,76.76, 69.88, 68.57, 57.65, 57.61, 53.29, 52.78.

HRMS (ESI) calcd for C24H22BrNO4 $[M-H]^+$ 470.0793, found 470.0791

IR(cm^{-1}) 1102,1496,1646,1735,2849,2921,3040

Rf =0.36 (25:75 EtOAc: Hexane)

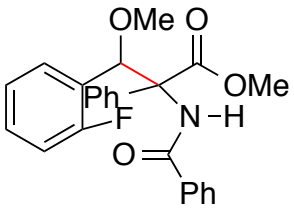

Methyl 2-benzamido-3-(2-fluorophenyl)-3-methoxy-2-phenylpropanoate(3d)

p-TsOH: dr=1:1.67

^{1}H NMR (500 MHz, Chloroform-d) δ 7.89 – 7.76 (m, 6H), 7.60 – 7.14 (m, 30H), 7.12 – 6.86 (m, 6H), 6.66 (td, J = 7.6, 1.8 Hz, 2H), 5.51 (s, 1H), 5.41 (s, 2H), 3.86 (s, 3H), 3.77 (s, 5H), 3.33 (s, 3H), 3.25 (s, 5H).

^{13}C NMR (126 MHz, CDCl3) δ 171.23, 170.38, 166.72, 166.49, 162.47, 162.00, 160.50, 160.07, 135.08, 134.81, 134.67, 133.77, 133.77, 131.89, 131.58, 130.30, 130.23, 130.14, 130.07, 129.98, 129.95, 128.69, 128.57, 128.32, 127.66, 127.63, 127.54, 127.28, 127.26, 127.16, 127.08, 124.11, 124.09, 123.72, 123.05, 122.95, 115.61, 115.43, 115.02, 114.84, 80.57, 76.76, 70.16, 69.10, 57.80, 57.63, 53.21, 52.79.

HRMS (ESI) calcd for $C_{24}H_{22}FNO_4$ $[M-H]^+$ 408.1611, found 408.1612

IR(cm^{-1}) 1085,1485,1656,1726,2850,2923,3062

Rf =0.29 (25:75 EtOAc: Hexane)

CSA: dr=1:2.24

^{1}H NMR (500 MHz, Chloroform-d) δ 7.83 (dd, J = 11.3, 7.6 Hz, 7H), 7.59 – 7.30 (m, 22H), 7.29 – 6.86 (m, 31H), 6.66 (t, J = 7.7 Hz, 2H), 5.51 (s, 1H), 5.42 (s, 2H), 3.86 (s, 3H), 3.77 (s, 6H), 3.33 (s, 3H), 3.25 (s, 6H).

^{13}C NMR (126 MHz, CDCl3) δ 171.24, 170.39, 166.49, 165.00, 135.09, 134.82, 134.69, 133.78, 131.89, 131.57, 130.30, 130.23, 130.14, 130.07, 129.99, 129.96, 128.70, 128.70,

128.57, 128.32, 127.66, 127.55, 127.28, 127.17, 127.09, 124.11, 123.72, 123.07, 115.02, 114.84, 80.58, 76.76, 70.16, 69.11, 57.81, 57.63, 53.21, 52.80.

HRMS (ESI) calcd for $C_{24}H_{22}FNO_4$ $[M-H]^+$ 408.1611, found 408.1613

IR(cm^{-1}) 1086,1484,1678,1750, 2849,2923,3061

Rf =0.30 (25:75 EtOAc: Hexane)

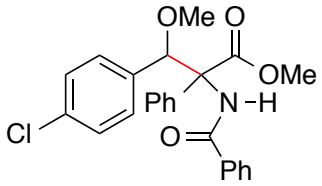

Methyl 2-benzamido-3-(4-chlorophenyl)-3-methoxy-2-phenylpropanoate (3f)

p-TsOH: dr=1:1.10

^{1}H NMR (500 MHz, Chloroform-d) δ 7.77 – 7.69 (m, 4H), 7.53 (q, J = 7.7 Hz, 2H), 7.45 (td, J = 7.5, 3.6 Hz, 5H), 7.39 – 7.17 (m, 14H), 6.99 – 6.91 (m, 4H), 6.75 (s, 1H), 5.40 (s, 1H), 5.27 (s, 1H), 3.84 (d, J = 1.5 Hz, 3H), 3.75 (d, J = 1.5 Hz, 3H), 3.33 (d, J = 1.5 Hz, 3H), 3.25 (d, J = 1.5 Hz, 3H).

^{13}C NMR (126 MHz, CDCl3) δ 171.50, 170.81, 167.07, 166.57, 135.65, 135.50, 134.93, 134.60, 134.35, 134.31, 134.28, 133.96, 131.99, 131.75, 129.94, 129.53, 128.76, 128.66, 128.09, 128.00, 127.87, 127.81, 127.73, 127.68, 127.44, 127.01, 126.99, 84.57, 84.53, 76.77, 69.93, 68.61, 57.62, 57.59, 53.28, 52.77.

HRMS (ESI) calcd for $C_{24}H_{22}ClNO_4$ $[M-H]^+$ 424.1316, found 424.1315

IR(cm^{-1}) 1100,1433,1653,1758,2826,2949,3016

Rf =0.43 (25:75 EtOAc: Hexane)

CSA: dr=1:1.23

^{1}H NMR (500 MHz, Chloroform-d) δ 7.78 – 7.68 (m, 4H), 7.58 – 7.41 (m, 6H), 7.38 – 7.16 (m, 16H), 6.99 – 6.90 (m, 4H), 6.75 (s, 1H), 5.40 (s, 1H), 5.27 (s, 1H), 3.85 (s, 3H), 3.75 (s, 4H), 3.33 (s, 3H), 3.25 (s, 4H).

^{13}C NMR (126 MHz, CDCl3) δ 171.51, 170.82, 167.07, 166.58, 135.66, 135.50, 134.94, 134.61, 134.35, 134.32, 134.29, 133.98, 131.99, 131.75, 129.95, 129.53, 128.76, 128.66, 128.09, 128.00, 127.88, 127.82, 127.73, 127.68, 127.44, 127.01, 127.00, 84.56, 76.75, 69.94, 68.61, 57.63, 57.59, 53.29, 52.77.

HRMS (ESI) calcd for $C_{24}H_{22}ClNO_4$ $[M-H]^+$ 424.1316, found 424.1317

IR(cm^{-1}) 1102,1432,1623,1764, 2827,2922,3018

Rf =0.42 (25:75 EtOAc: Hexane)

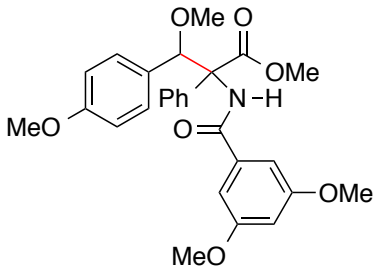

Methyl 2-(3,5-dimethoxybenzamido)-3-methoxy-3-(4-methoxyphenyl)-2-phenylpropanoate(4a)

p-TsOH: dr=1:1.24

^{1}H NMR (500 MHz, Chloroform-d) δ 7.44 – 7.37 (m, 3H), 7.37 – 7.21 (m, 10H), 6.96 – 6.86 (m, 10H), 6.83 – 6.74 (m, 6H), 6.62 (dt, J = 5.6, 2.3 Hz, 2H), 5.27 (s, 1H), 5.07 (s, 1H), 3.88 (s, 3H), 3.84 (d, J = 2.4 Hz, 14H), 3.80 (s, 7H), 3.77 (s, 4H), 3.34 (s, 3H), 3.25 (s, 4H).

^{13}C NMR (126 MHz, CDCl3) δ 171.52, 170.83, 166.33, 166.27, 160.92, 160.86, 159.92, 159.70, 137.00, 136.19, 135.73, 135.51, 129.70, 129.27, 128.19, 127.76, 127.67, 127.62, 127.57, 127.43, 127.12, 113.41, 113.32, 104.99, 104.97, 103.91, 103.79, 86.22, 85.46, 76.76, 70.16, 68.51, 57.42, 57.36, 55.58, 55.57, 55.19, 53.17, 52.76.

HRMS (ESI) calcd for $C_{27}H_{29}NO_7$ $[M-H]^+$ 480.2022, found 480.2028

IR(cm^{-1}) 1156,1456,1593,1674,1753, 2837,2949,3003

Rf =0.15 (25:75 EtOAc: Hexane)

CSA: dr=1:1.02

^{1}H NMR (500 MHz, Chloroform-d) δ 7.42 – 7.34 (m, 2H), 7.34 – 7.19 (m, 9H), 6.93 – 6.82 (m, 8H), 6.80 – 6.71 (m, 5H), 6.59 (dt, J = 5.5, 2.3 Hz, 2H), 5.25 (s, 1H), 5.05 (s, 1H), 3.85 (s, 3H), 3.82 (d, J = 2.4 Hz, 12H), 3.78 (s, 6H), 3.75 (s, 3H), 3.32 (s, 3H), 3.22 (s, 3H).

^{13}C NMR (126 MHz, CDCl3) δ 171.52, 170.83, 166.33, 166.27, 160.92, 160.86, 159.92, 159.70, 137.00, 136.19, 135.73, 135.51, 129.70, 129.27, 128.19, 127.76, 127.62, 127.57, 127.43, 127.12, 113.41, 113.32, 104.99, 104.97, 103.91, 103.79, 86.22, 85.45, 76.76, 70.15, 68.51, 57.42, 57.36, 55.59, 55.57, 55.19, 53.17, 52.76.

HRMS (ESI) calcd for $C_{27}H_{29}NO_7$ $[M-H]^+$ 480.2022, found 480.2030

IR(cm^{-1}) 1155,1456,1593,1674,1753, 2837,2950,3003

Rf =0.16 (25:75 EtOAc: Hexane)

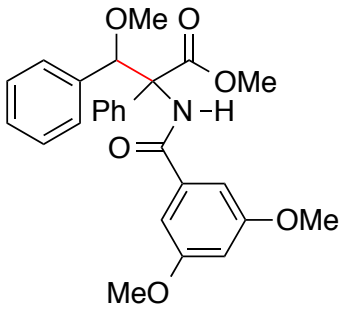

Methyl 2-(3,5-dimethoxybenzamido)-3-methoxy-2,3-diphenylpropanoate(4b)

p-TsOH: dr=1:1.10

^{1}H NMR (500 MHz, Chloroform-d) δ 7.41 – 7.33 (m, 2H), 7.36 – 7.17 (m, 15H), 7.05 – 6.95 (m, 4H), 6.86 (dd, J = 7.7, 2.3 Hz, 4H), 6.77 (s, 1H), 6.59 (dt, J = 6.0, 2.3 Hz, 2H), 5.31 (s, 1H), 5.12 (s, 1H), 3.86 (s, 3H), 3.81 (d, J = 2.9 Hz, 12H), 3.73 (s, 3H), 3.34 (s, 3H), 3.24 (s, 3H).

^{13}C NMR (126 MHz, CDCl3) δ 171.48, 170.75, 166.40, 166.35, 160.92, 160.86, 136.99, 136.21, 135.97, 135.63, 135.53, 135.30, 128.76, 128.54, 128.47, 128.12, 128.05, 127.99, 127.90, 127.82, 127.68, 127.64, 127.52, 127.49, 104.97, 104.94, 103.93, 103.82, 86.36, 85.71, 76.76, 70.09, 68.53, 57.58, 55.58, 55.56, 53.23, 52.74.

HRMS (ESI) calcd for $C_{26}H_{27}NO_6$ $[M-H]^+$ 450.1917, found 450.1928

IR(cm^{-1}) 1163,1505,1606,1674,1747, 2821,2958,3059

Rf =0.235 (25:75 EtOAc: Hexane)

CSA: dr=1:1.15

^{1}H NMR (500 MHz, Chloroform-d) δ 7.41 – 7.34 (m, 2H), 7.35 – 7.18 (m, 15H), 7.04 – 6.95 (m, 4H), 6.86 (dd, J = 7.6, 2.3 Hz, 4H), 6.77 (s, 1H), 6.59 (dt, J = 6.0, 2.3 Hz, 2H), 5.31 (s, 1H), 5.12 (s, 1H), 3.86 (s, 3H), 3.82 (d, J = 3.0 Hz, 12H), 3.73 (s, 3H), 3.34 (s, 3H), 3.24 (s, 3H).

^{13}C NMR (126 MHz, CDCl3) δ 171.48, 170.75, 166.40, 166.36, 160.93, 160.87, 137.00, 136.22, 135.98, 135.64, 135.55, 135.31, 128.75, 128.54, 128.48, 128.13, 128.06, 127.99, 127.90, 127.82, 127.68, 127.65, 127.52, 127.49, 104.98, 104.94, 103.94, 103.83, 86.36, 85.73, 76.76, 70.10, 68.54, 57.59, 55.59, 55.57, 53.23, 52.74.

HRMS (ESI) calcd for $C_{26}H_{27}NO_6$ $[M-H]^+$ 450.1917, found 450.1918

IR(cm^{-1}) 1163,1495,1607,1675,1747, 2822,2948,3051

Rf =0.22 (25:75 EtOAc: Hexane)

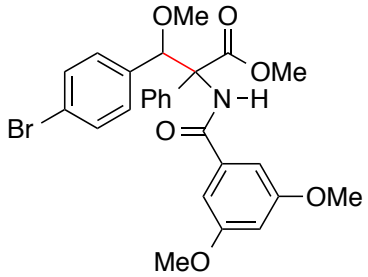

Methyl 3-(4-bromophenyl)-2-(3,5-dimethoxybenzamido)-3-methoxy-2-phenylpropanoate(4c)

p-TsOH: dr=1:1.41

^{1}H NMR (500 MHz, Chloroform-d) δ 7.40 – 7.22 (m, 19H), 6.94 – 6.80 (m, 9H), 6.71 (s, 1H), 6.60 (dt, J = 4.8, 2.3 Hz, 2H), 5.33 (s, 1H), 5.22 (s, 1H), 3.84 (s, 3H), 3.82 (d, J = 3.3 Hz, 15H), 3.74 (s, 4H), 3.32 (s, 3H), 3.24 (s, 4H).

^{13}C NMR (126 MHz, CDCl3) δ 171.36, 170.67, 166.83, 166.39, 160.98, 160.91, 136.77, 136.09, 135.51, 135.43, 134.74, 131.04, 130.97, 130.27, 129.88, 128.09, 127.89, 127.83, 127.77, 127.59, 127.39, 122.63, 122.59, 104.99, 104.95, 103.87, 103.80, 84.71, 84.66, 76.75, 69.89, 68.58, 57.64, 55.61, 55.58, 53.30, 52.77.

HRMS (ESI) calcd for $C_{26}H_{26}BrNO_6$ $[M-H]^+$ 530.1005, found 530.1006

IR(cm^{-1}) 1155,1495,1591,1673,1732, 2837,2937,3005

Rf =0.3 (25:75 EtOAc: Hexane)

CSA: dr=1:1.87

^{1}H NMR (500 MHz, Chloroform-d) δ 7.39 – 7.23 (m, 22H), 6.93 – 6.80 (m, 12H), 6.71 (s, 2H), 6.60 (dt, J = 4.9, 2.1 Hz, 3H), 5.34 (s, 1H), 5.22 (s, 2H), 3.84 (s, 3H), 3.82 (d, J = 3.3 Hz, 17H), 3.74 (s, 5H), 3.32 (s, 3H), 3.24 (s, 5H).

^{13}C NMR (126 MHz, CDCl3) δ 171.36, 170.67, 166.83, 166.41, 160.97, 160.91, 136.76, 136.08, 135.50, 135.43, 134.73, 131.04, 130.97, 130.27, 129.88, 128.09, 127.90, 127.83, 127.78, 127.59, 127.39, 122.63, 122.59, 104.99, 104.95, 103.87, 84.66, 76.76, 69.89, 68.58, 57.64, 57.62, 55.61, 55.58, 53.30, 52.77.

HRMS (ESI) calcd for $C_{26}H_{26}BrNO_6$ $[M-H]^+$ 530.1005, found 530.1003

IR(cm^{-1}) 1156,1495,1592,1674,1734, 2838,2933,3004

Rf =0.29 (25:75 EtOAc: Hexane)

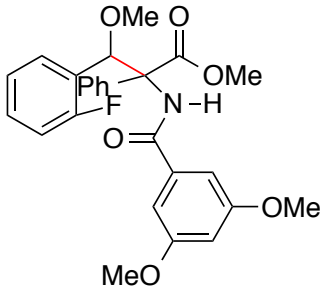

Methyl 2-(3,5-dimethoxybenzamido)-3-(2-fluorophenyl)-3-methoxy-2-phenylpropanoate(4d)

p-TsOH: dr=1:1.27

^{1}H NMR (500 MHz, Chloroform-d) δ 7.48 – 7.39 (m, 4H), 7.34 – 7.12 (m, 12H), 7.11 – 6.86 (m, 10H), 6.70 – 6.58 (m, 4H), 5.46 (s, 1H), 5.40 (s, 1H), 3.86 (s, 3H), 3.84 (d, J = 6.6 Hz, 13H), 3.77 (s, 4H), 3.32 (s, 3H), 3.24 (s, 4H).

^{13}C NMR (126 MHz, CDCl3) δ 171.09, 170.26, 166.52, 166.26, 160.95, 160.86, 136.95, 135.87, 134.99, 134.61, 130.19, 130.12, 129.97, 128.32, 127.67, 127.64, 127.55, 127.28, 127.19, 124.15, 124.12, 123.70, 115.61, 115.01, 105.00, 104.93, 104.35, 103.83, 80.61, 76.76, 70.22, 69.08, 57.80, 57.64, 55.57, 55.57, 53.22, 52.80.

HRMS (ESI) calcd for $C_{26}H_{26}FNO_6$ $[M-H]^+$ 468.1823, found 468.1823

IR(cm^{-1}) 1156,1496,1594,1679,1754, 2837,2947,3004

Rf =0.23 (25:75 EtOAc: Hexane)

CSA:

Dr=1:1.88

^{1}H NMR (500 MHz, Chloroform-d) δ 7.48 – 7.11 (m, 23H), 7.12 – 6.86 (m, 14H), 6.69 – 6.58 (m, 5H), 5.46 (s, 1H), 5.40 (s, 2H), 3.87 (s, 3H), 3.84 (d, J = 6.6 Hz, 17H), 3.77 (s, 6H), 3.32 (s, 3H), 3.24 (s, 5H).

^{13}C NMR (126 MHz, CDCl3) δ 171.15, 170.27, 166.53, 166.26, 160.95, 160.86, 135.87, 134.61, 130.33, 130.19, 130.12, 129.97, 128.32, 128.21, 127.67, 127.55, 127.28, 127.19, 126.77, 124.12, 123.73, 122.91, 115.43, 115.01, 114.83, 105.00, 104.94, 104.35, 103.83, 80.61, 76.75, 70.22, 69.08, 57.81, 57.64, 55.57, 53.22, 52.81.

HRMS (ESI) calcd for $C_{26}H_{26}FNO_6$ $[M-H]^+$ 468.1823, found 468.1828

IR(cm^{-1}) 1156,1496,1593,1678,1753, 2838,2933,3006

Rf =0.23 (25:75 EtOAc: Hexane)

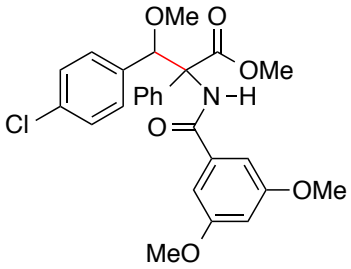

Methyl 3-(4-chlorophenyl)-2-(3,5-dimethoxybenzamido)-3-methoxy-2-phenylpropanoate(4f)

p-TsOH: dr=1:1.06

^{1}H NMR (500 MHz, Chloroform-d) δ 7.36 – 7.16 (m, 15H), 7.00 – 6.88 (m, 4H), 6.84 (dd, J = 17.7, 2.3 Hz, 4H), 6.72 (s, 1H), 6.60 (dt, J = 4.6, 2.3 Hz, 2H), 5.35 (s, 1H), 5.23 (s, 1H), 3.85 (s, 3H), 3.82 (d, J = 2.9 Hz, 12H), 3.74 (s, 3H), 3.32 (s, 3H), 3.24 (s, 3H).

^{13}C NMR (126 MHz, CDCl3) δ 171.37, 170.67, 166.79, 166.39, 160.98, 160.92, 136.79, 136.10, 135.53, 134.87, 134.38, 134.35, 134.19, 129.92, 129.55, 128.09, 128.07, 128.04, 127.88, 127.82, 127.76, 127.62, 127.40, 104.99, 104.96, 103.85, 103.78, 84.69, 76.76, 69.95, 68.62, 57.62, 57.60, 55.60, 55.58, 53.29, 52.76.

HRMS (ESI) calcd for $C_{26}H_{26}ClNO_6$ $[M-H]^+$ 484.1527, found 484.1527

IR(cm^{-1}) 1156,1491,1593,1674,1732, 2838,2946,3007

Rf =0.27 (25:75 EtOAc: Hexane)

CSA: dr=1:1.53

^{1}H NMR (500 MHz, Chloroform-d) δ 7.36 – 7.17 (m, 19H), 7.00 – 6.89 (m, 5H), 6.84 (dd, J = 17.7, 2.3 Hz, 5H), 6.71 (s, 1H), 6.60 (dt, J = 4.7, 2.3 Hz, 2H), 5.35 (s, 1H), 5.23 (s, 2H), 3.85 (s, 3H), 3.82 (d, J = 3.0 Hz, 15H), 3.74 (s, 5H), 3.32 (s, 3H), 3.24 (s, 5H).

^{13}C NMR (126 MHz, CDCl3) δ 171.37, 170.67, 166.79, 166.39, 160.98, 160.92, 136.79, 136.11, 135.53, 134.88, 134.39, 134.19, 129.93, 129.55, 128.09, 128.08, 128.04, 127.88, 127.82, 127.76, 127.62, 127.40, 105.00, 104.96, 103.85, 103.78, 84.69, 76.76, 69.95, 68.62, 57.62, 57.60, 55.61, 55.58, 53.29, 52.76.

HRMS (ESI) calcd for $C_{26}H_{26}ClNO_6$ $[M-H]^+$ 484.1527, found 484.1523

IR(cm^{-1}) 1156,1491,1594,1674,1733, 2838,2937,3004

Rf =0.27 (25:75 EtOAc: Hexane)

CHAPTER THREE: BINOL DERIVED CATALYSTS SYNTHESIS

3.1 BINOL Derived Catalysts Background

The area of asymmetric catalysis with strong Brønsted acids flourished after 2004 when reports were published by Akiyama and Terada groups (briefly discussed in section 1.2) [12]-[14]. Compared to general Brønsted acid catalysts, relatively stronger Brønsted acid catalysts that activate the substrate by fully protonating it can be classified as specific Brønsted acid catalysts. The specific acid is the protonated form of the solvent in which the reaction is being performed. The reaction rate for reactants R depends on the pH of the system but not on the concentrations of different acids, and the acid is not involved in the rate determining step.

The Akiyama group reported the first example of highly enantioselective Mannich reaction using a chiral BINOL-derived phosphoric acid as a catalyst (Figure 3.1)[14]. In the reaction, the carbon–nitrogen double bond is activated by a strong, metal-free chiral Brønsted acid that is based on BINOL framework. Although the detailed mechanism was not explained, in their report, it appears that 3,3'-diaryl groups, which are not coplanar with the naphthyl groups on BINOL framework, would effectively shield the phosphate moiety and bring about efficient asymmetric induction.

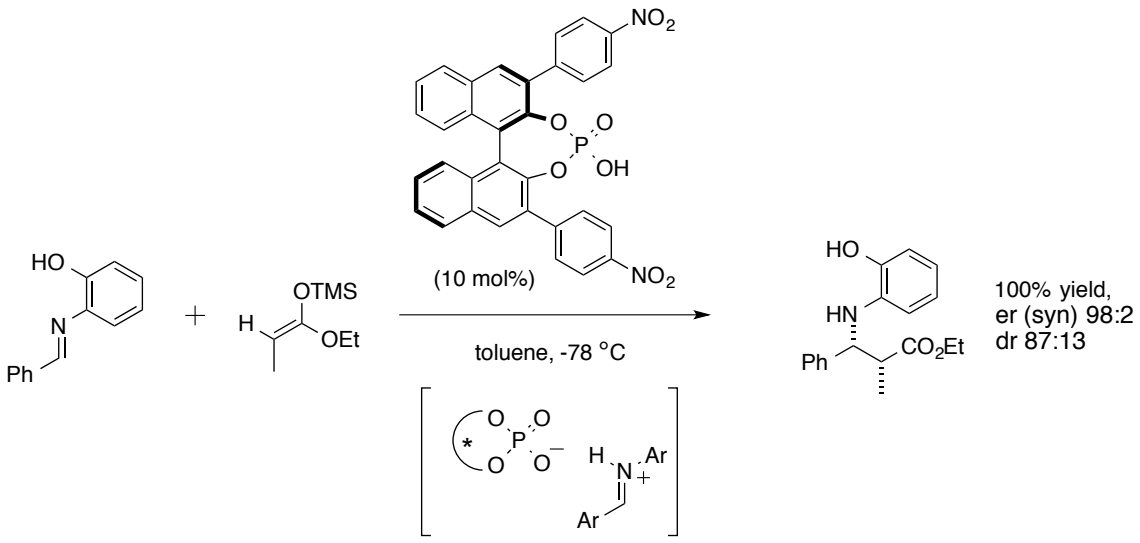

Figure 3.1 BINOL-derived phosphoric acid catalyzed Mannich reaction by Akiyama.

The Terada group independently reported another asymmetric direct Mannich type example catalyzed by a similar chiral BINOL-derived phosphoric acid [13]. The bulky 4-(β-Naph)-C_6H_4 group substituted on 3,3'- position further increased the enantioselectivity to 95% ee with 99% yield compared to other substituted group that they utilized in catalyst scope such as phenel group and 4-biphenyl group. The activation of a carbon nucleophile by the formation of an enamine intermediate via the nucleophilic attack of a secondary amine to a carbonyl compound is one of the most straightforward strategies to realize carbon-carbon bond forming reactions. Years later, however, the Ishihara group discovered that the actual catalyst in this reaction was not the BINOL-derived phosphoric acid, but rather its calcium salt that was formed during purification on silica gel [15].

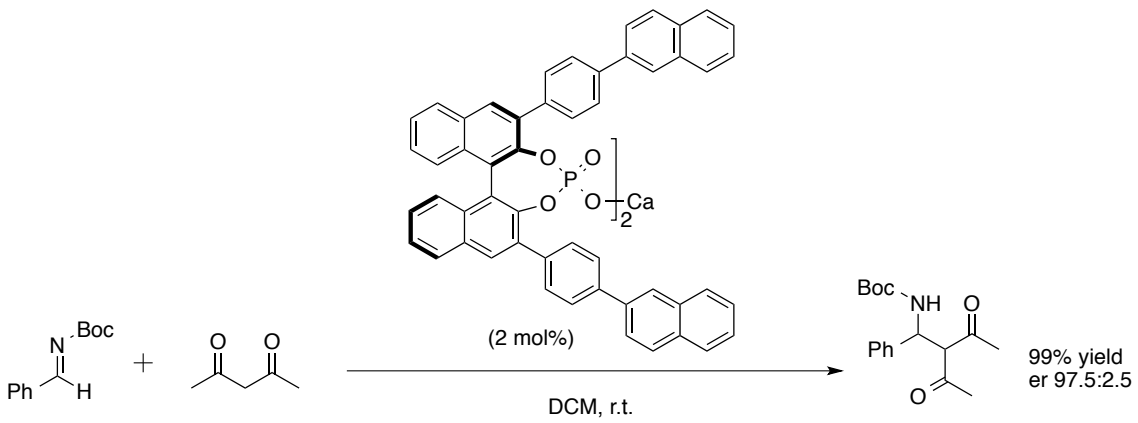

Figure 3.2 BINOL-derived phosphoric acid catalyzed Mannich reaction by Terada et al.

After these reports, BINOL derived chiral phosphoric acid catalysis attracted much more attention of synthetic organic chemists and have been successfully applied to numerous asymmetric reactions [8], [9]. The readily modified 3,3'-substituents are key to most of these successful cases which make it possible to associate bulky groups near the active site to realize stereoselectivity control. It is quite common that the transition states of successful asymmetric reactions are well organized with covalent or hydrogen bonding interactions between the catalyst and the substrates. Furthermore, BINOL derived chiral phosphoric acids enable dual functional activation modes by mono functional catalyst in which a Brønsted acidic site and a Brønsted or Lewis basic site simultaneously activate the electrophile and the nucleophile, respectively (Figure 3.3) [11].

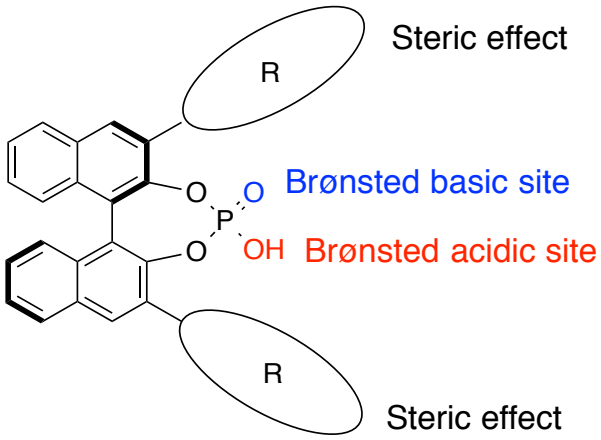

Figure 3.3 Bifunctionality in BINOL derived chiral phosphoric acids.

Although BINOL derived chiral phosphoric acids are highly potent catalysts for development of novel asymmetric transformations, their application has been limited to the processes which involve more basic nitrogen-based electrophiles, attributed to their relatively low acidity [11]. In order to make the utility of the Brønsted acid catalysis as broad as the well-developed Lewis acid catalysis, efforts were made to develop Brønsted acids demonstrating both high reactivities and selectivities. Replacing oxygen atoms of the phosphoric acid diester moiety with other atoms or groups leads to various derivatives. Terada's group developed a phosphorodiamidic acid that was shown to be highly efficient strong chiral Brønsted acids. Phosphorodiamidic acids were proposed as a novel structural motif of enantioselective Brønsted acid catalysts because they possess unique features, and they are capable for the direct Mannich reaction of N-acyl imines with 1,3-dicarbonyl compounds (Figure 3.4) [82]. Unfortunately, only low enantioselectivity was obtained.

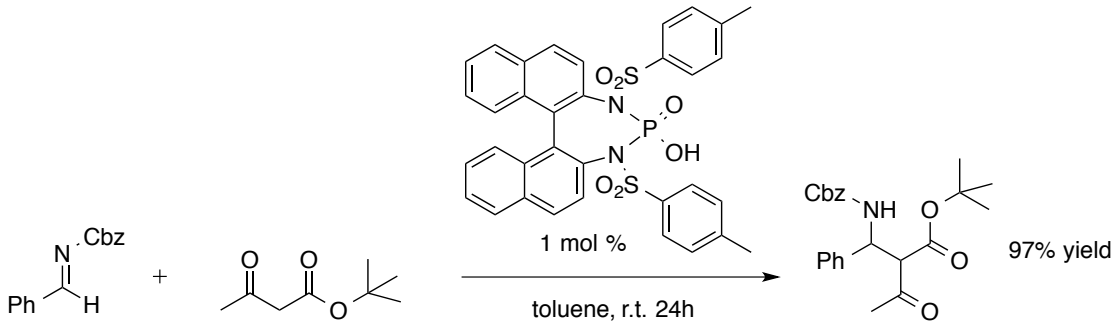

Figure 3.4 Phosphordiamidic acid for direct Mannich reaction by Terada et al.

In order to discover better alternatives for phosphoric acids, development of stronger Brønsted acids that are more reactive and acidic is in urgent need. Various derivatives have been studied by the Yamamoto group. A major breakthrough in Brønsted acid catalysis was the discovery of chiral N-triflyl phosphoramides as strong chiral Brønsted acids by Nakashima and Yamamoto in 2006 [83], and highly enantioselective Diels−Alder reaction of α,β-unsaturated ketone with silyloxydiene was demonstrated with this chiral Brønsted acid catalyst, for which the corresponding phosphoric acids are unable to promote the reactions because of their insufficient acidity. Chiral N-triflyl phosphoramides were demonstrated to promote a number of enantioselective C-C and C-X bond-forming reactions. Their strong acidity enable them as valuable tools for the activation of imines, carbonyl compounds, and other weakly basic substrates. These catalysts are often referred to as Yamamoto's catalysts [84], [85]. Normally, higher acidity of the chiral N-triflyl phosphoramides was crucial for the successful catalysis of the reaction. In 2008, Cheon and Yamamoto also introduced N-triflyl thiophosphoramides and N-triflyl selenophosphoramide derivatives for the first metal-free Brønsted acid catalyzed enantioselective protonation reaction of silyl enol

ethers [86]. The catalyst loading could be reduced to 0.05 mol % without any unfavorable effect on the enantioselectivity.

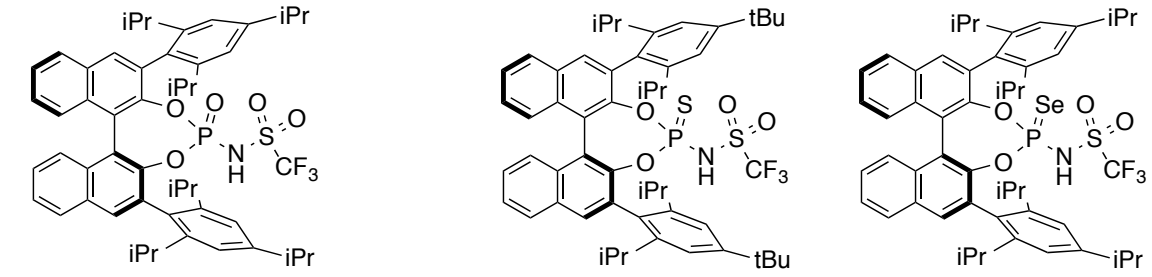

Nakashima and Yamamoto 2006

Cheon and Yamamoto 2008

Figure 3.5 N-triflyl phosphoramides and derivatives

In 2010, List et al. reported the direct asymmetric N, O-acetalization of aldehydes catalyzed by N-phosphinyl phosphoramides. This is a novel class of stronger Brønsted acids that replaces the triflyl group of Yamamoto's catalyst with a phosphinyl electron-withdrawing moiety (Figure 3.6). The use of a phosphinyl moiety resulted in chiral N-phosphinyl phosphoramides which could be furthermore optimized structurally by modifying the structure of the achiral phosphinyl group [87]. This readily accessible N-phosphinyl phosphoramide proved to be highly efficient and enantioselective in catalyzing direct asymmetric N, O-acetalization of aldehydes. The synthetic utility of this methodology was demonstrated with the first catalytic asymmetric synthesis of the analgesic pharmaceutical (R)-chlorothenoxazine.

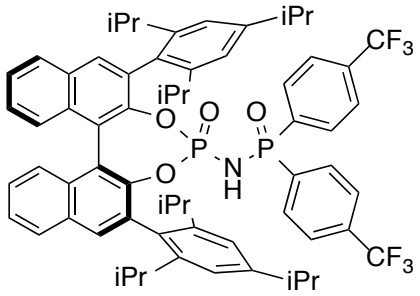

List et al. 2010

Figure 3.6 N-phosphinyl phosphoramides

Phosphoric acid catalysts derived BINOL or other backbones (discussed in section 1.2), although followed by several different acidic motives, are by far the most successful catalysts. Unfortunately, with exception of Yamamoto's catalyst, all other moderately strong and strong Brønsted acid motives are very reaction specific.

Other than phosphoric acids, binaphthyl derived dicarboxylic acid used by the Maruoka group [26] for Mannish reaction and disulfonic acid used by the List group for Hosomi–Sakurai reaction and Ishihara group for Mannich type reaction [27], [28](details in section 1.2) all afford desired products with decent enantioselectivity. These BINOL derived carboxlic acids and sulfonic acids remain relatively undeveloped compared to those phosphoric acids based on the BINOL framework.

3.2 Newman-Kwart Rearrangement Thermal Pathway

Besides exploring the applicability of commercially available sulfonic acids to azlactone- acetal coupling reaction, we also look forward to finding novel and efficient ways to synthesize sulfonic acid catalysts themselves. Developing chiral sulfonic acids

and applying them in previous successful realized carbon-carbon bond forming reactions would allow for potential with greater stereoselectivity, and there is also a possibility to increase the efficiency towards coupling reactions with milder conditions. In order to evaluate the mono protic chiral sulfonic acid's catalytic efficiencies towards asymmetric coupling reactions, our first attempt was trying to synthesize this acid starting from compound BINOL.

Chiral thiols have found some successful applications as anionic ligands in different catalytic enantioselective reactions. These include Cu- catalyzed Grignard reagents such as Michael addition to α, β-unsaturated enones [88], [89]; SN2-substitution on allylic substrates [90] and Rh-catalyzed hydroformylation of styrene [91]. Gladiali and his coworker proposed a useful synthetic procedure for conversion of C2 symmetric 1,1'-binaphthalene-2,2'-dithiol (BINAS) and BINOL into heterotopic S, S'- and heterodonor O, S-chelating atropisomeric ligands [92]. The Newman−Kwart rearrangement is perhaps the quintessential method for the synthesis of thiophenols from the corresponding phenol. This procedure allows for flexible preparation in an environmental friendly way.

As differentiation of diol can be more readily achieved by selective monoacylation, and monoacylated BINOL is a valuable starting material for thermal Newman-Kwart rearrangement to afford desired 2,2'-monothiobinaphthtol or methoxy thiol. Gladiali and his coworker treated BINOL dithiocarbamate with equimolar amount of N, N-dimethylthiocarbamoyl chloride in the presence of NaH as base to afford monoacylated BINOL. They later protected the hydroxyl group before the Newman-Kwart rearrangement to prevent byproduct from thermolysis. Then methoxy carbamate could be

converted into the transposed carbamate after heating the mixture neat to 275 °C for 20 hrs. Simply treating the methoxy carbamate with $LiAlH_4$ in THF would result in desired product methoxy thiol (Figure 3.7), and subsequent removals of the methyl protection could be realized with the treatment of BBr_3 in CH_2Cl_2 at -78 °C then warming up to 25°C and stirring for 12 hrs and treating with $LiAlH_4$ in THF to remove carbamate group.

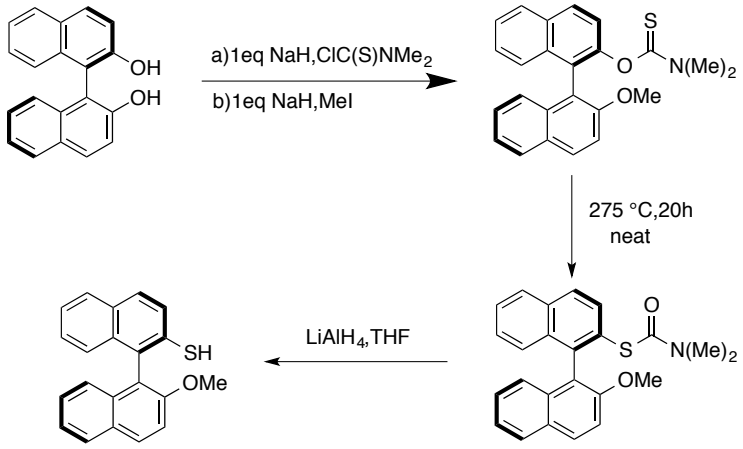

Figure 3.7 Methoxy thiol synthesis route

An efficient monoalkylation of the dithiol was successfully accomplished by differentiation of the corresponding dicarbamate through selective removal of one S-carbamonyl group by treatment of $LiAlH_4$ was a stepwise process. The intermediate monocarbamate was less prone to hydride attack than the relevant dicarbamate (Figure 3.8). Thus, the reaction could be efficiently driven towards selective monodeacylation simply by adjusting the substrate/reactant molar ratio close to optimal limiting value of 1:1. Under these conditions, desired S-monosubstituted dithiol was readily isolated. The thiol group was alkylated with suitable alkyl halide then treating with $LiAlH_4$ in THF to remove the 2nd carbamate group. In this way, S, S'-heterotopic ligands were obtained.

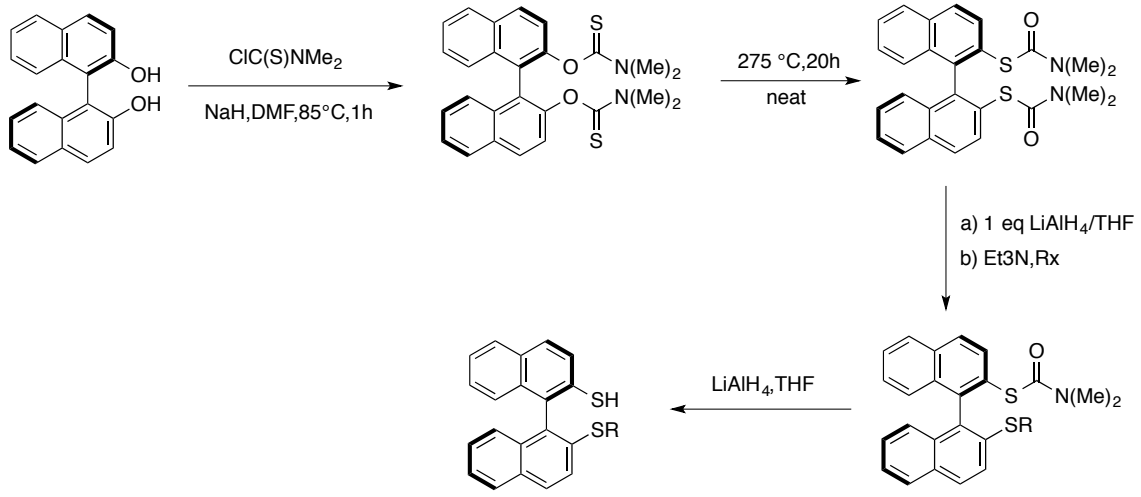

Scheme 3.8 S, S'-heterotopic ligands synthesis route

I followed Gladiali group's synthetic procedure in preparing both methoxy thiol and S, S'-heterotopic ligands in our laboratory. As it is not safe to heat mixture in oil bath to 275 °C, I only tried the Newman-Kwart rearrangement at 160 °C and 200 °C. It is not surprising that reactions failed to work. Based on ^{1}H NMR, starting materials remain unreacted after 20 hrs of heating.

Although the harsh reaction conditions for Newman-Kwart rearrangement limited practical operation of synthetic route of this BINOL derived sulfonic acid, Gladiali group's design in selective monoalkylation of the dithiol and selective monodeacylation of BINAS dicarbamate are quite useful in our BINOL derived construction of sulfonic acid catalysts. Meanwhile, exploring alternative pathway with milder reaction conditions for the Newman-Kwart rearrangement is in urgent need.

3.3 Photocatalytic Newman-Kwart Rearrangement

The Newman−Kwart rearrangement is generally the first choice for the synthesis of thiophenols from the corresponding phenol. However, the harsh thermal conditions required for thermally induced O_{Ar} to S_{Ar} migration in aryl thiocarbamates often leads to decomposition of desired thiophenol products that results in diminished yields, and presents great safety risks in performing such reactions with temperature up to 275 °C.

A more general method was proposed by the Lloyd-Jones group in 2009, wherein catalytic loadings of palladium bis(tri-tert-butylphosphine) enabled successful Newman−Kwart rearrangement of a couple of O- para-substituted dimethylcarbamothioates in toluene at 100 °C (Figure 3.9) [93]. This palladium-catalyzed method demonstrates a similar substrates tendency to the thermal Newman−Kwart rearrangement with shorter reaction times observed for substrates bearing electron-withdrawing functionality, increased reaction times and catalyst loadings necessary for substrates bearing electron-donating groups because of the intrinsically higher barrier to nucleophilic attack of sulfur on the aromatic ring.

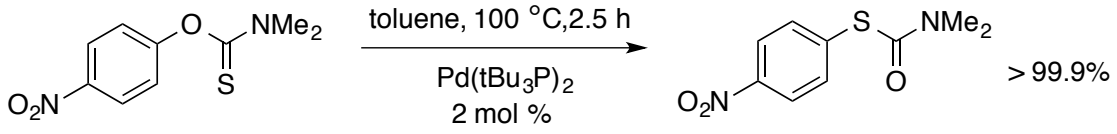

Figure 3.9 Pd- catalyzed Newman−Kwart rearrangement by Lloyd-Jones et al.

In 2015, Nicewicz and his coworker presented a general strategy for catalysis of O-aryl carbamothioates to S-aryl carbamothioates using catalytic quantities of a

commercially available organic single-electron photooxidant 2,4,6-tri(p-tolyl) pyrylium tetrafluoroborate. And most importantly, this Newman−Kwart rearrangement is facilitated at room temperature (Figure 3.10) [94]. The Nicewicz group hypothesized that single electron oxidation of the O-aryl carbamothioate substrate should lower the barrier to nucleophilic attack of sulfur upon the aryl ring and thus accelerate rearrangement procedure. To prove their points, they screened a set of O-substituted dimethylcarbamothioates by irradiating solutions of starting materials with 1.0 mol % of photocatalyst using blue light emitting diodes (LEDs). After 24 hours, rearrangement products were achieved in good to nearly quantitative yields.

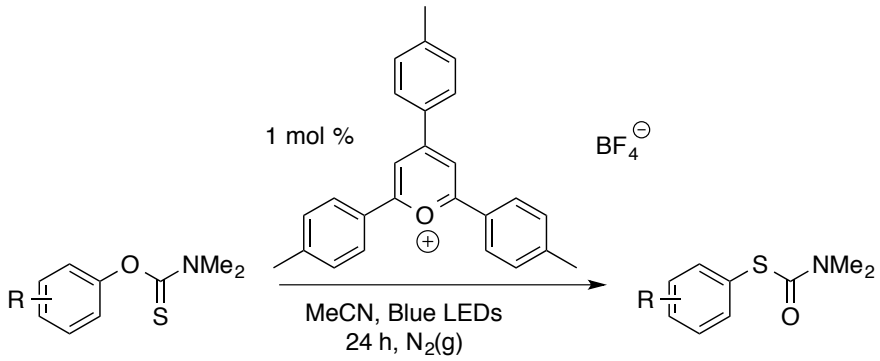

Figure 3.10 Ambient-temperature photocatalytic NKR reaction by Nicewicz et al.

This Ambient-Temperature photocatalytic Newman-Kwart rearrangement pathway has distinctive advantages over other thermal or Pd- catalyzed rearrangement pathways. To figure out if LEDs with specific wavelength are required for this photocatalysis Newman-Kwart rearrangement, attempts were made to synthesize both O, O'-([1,1'-binaphthalene]-2,2'-diyl) bis(dimethylcarbamothioate), and O-(2'-methoxy-[1,1'-binaphthalen]-2-yl) dimethylcarbamothioate utilizing Gladiali group's procedure and

irradiating the mixture with yellow LEDs. Neither of mono- and bis- rearrangement reaction went smoothly, and little product was observed based on crude ^{1}H NMR (Figure 3.11) [95]. This indicates that light with specific wavelength range is necessary to trigger these rearrangements to occur.

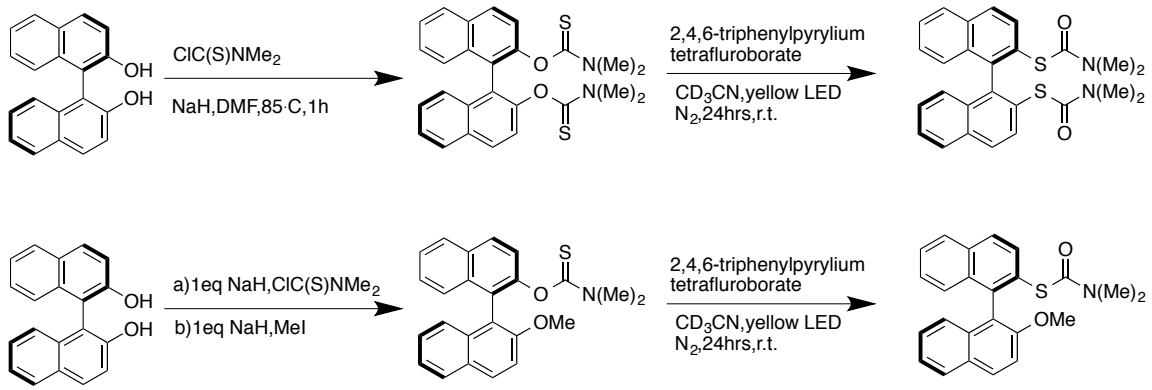

Figure 3.11 Ambient-temperature photocatalytic NKR reaction with yellow LEDs

Next attempt was to run Newman-Kwart rearrangement under UV lights. We set small scale reactions in a steel electrical junction box equipped with two 2.9 W LED Engin LZ4-44UV00 LED Emitters from Kutateladze group (Figure 3.12). These irradiators have a combined 5.8 W of power with $\lambda > 350$ nm. There are also a ring stand and a magnetic stirrer in the steel box for proper mixing during irradiation with extra stability.

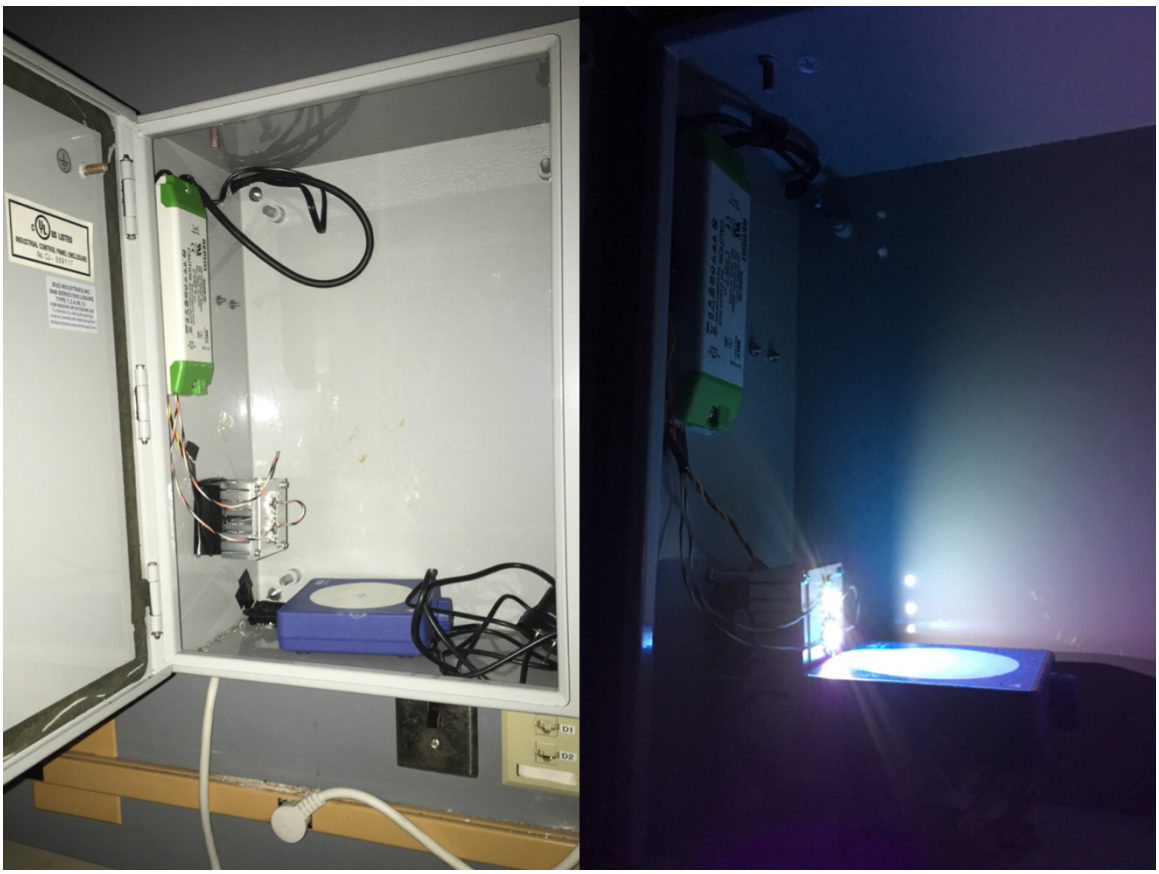

Figure 3.12 Steel electrical junction box equipped with UV LED irradiators

As O-(2'-methoxy-[1,1'-binaphthalen]-2-yl) dimethylcarbamothioate failed to afford the desired rearrangement product under UV lights, 2'-((dimethylcarbamothioyl)oxy)-[1,1'-binaphthalen]-2-yl acetate was synthesized, the carbamoylation of BINOL was followed by protecting of the -OH group which replaced the acidic proton with an acetyl group. I was delighted to see that 2'-((dimethylcarbamothioyl)oxy)-[1,1'-binaphthalen]-2-yl acetate was able to go through the Newman-Kwart rearrangement process and converted into its rearranged product 2'-((dimethylcarbamoyl)thio)-[1,1'-binaphthalen]-2-yl acetate (Figure 3.13).

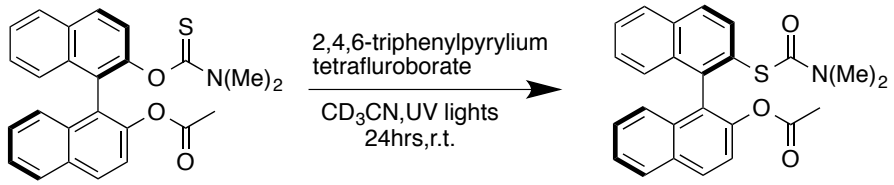

Figure 3.13 Ambient-temperature photocatalytic NKR reaction with UV LEDs

The resulting phenol could be chlorinated with N-chlorosuccinimide. This process is one step closer toward the desired sulfonic acid [96]. However, conversion of the chlorinated product to the acid leads to removal of the acetyl group instead of acid forming from hydrolysis (Figure 3.14). Unfortunately, bromination of 2'-((dimethylcarbamoyl)thio)-[1,1'-binaphthalen]-2-yl acetate with N-bromosuccinimide following a similar procedure failed to give desired product.

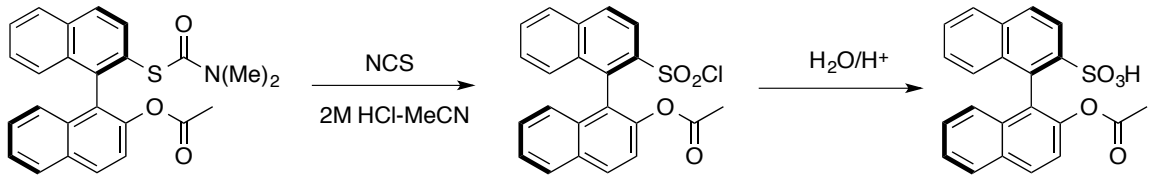

Figure 3.14 Chlorination and hydrolysis to afford BINOL based mono sulfonic acid

In conclusion, we have successfully performed Newman-Kwart rearrangement on BINOL based compounds and we have a better understanding of the properties and functions of BINOL scaffolds. More acidification processes converting sulfonyl chloride to sulfonic acid are still under investigation.

3.4 Experimental Details

3.4.1 General procedure for alkylation of BINOL [92]

A: O, O'-([1,1'-binaphthalene]-2,2'-diyl) bis(dimethylcarbamothioate)

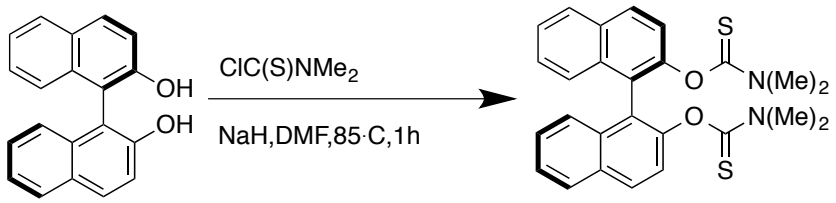

An oven-dried 10 mL round bottom flask containing BINOL (100.00 mg, 0.35 mmol, 1.00 equiv.) was equipped with a magnetic stirrer bar. The flask was evacuated and flushed with argon. Subsequently the flask was charged with 0.78 mL dry DMF and was allowed to cool on ice to 0°C. Followed by sodium hydride in 60% oil dispersion (18.30 mg, 0.76 mmol, 2.20 equiv.) and then N, N-dimethylthiocarbomoyl chloride (95.00 mg, 0.76 mmol, 2.20 equiv.) was added to the reaction mixture. The flask was then refluxed at 85°C in oil bath for 1hr. The mixture was then cooled to room temperature and 2.60 mL 1N KOH aq was added. The white precipitate was filtered, washed with water and dissolved in DCM. The organic phase was washed with brine 3 times and dried over Na_2SO_4, and after filtration the solvent was removed via rotatory evaporation. ^{1}H NMR (500 MHz, Chloroform-d) δ 8.01 (d, J = 8.9 Hz, 2H), 7.96 – 7.92 (m, 2H), 7.69 – 7.46 (m, 6H), 7.37 – 7.31 (m, 2H), 3.11 (s, 6H), 2.56 (s, 6H).

B: O-(2'-methoxy-[1,1'-binaphthalen]-2-yl) dimethylcarbamothioate

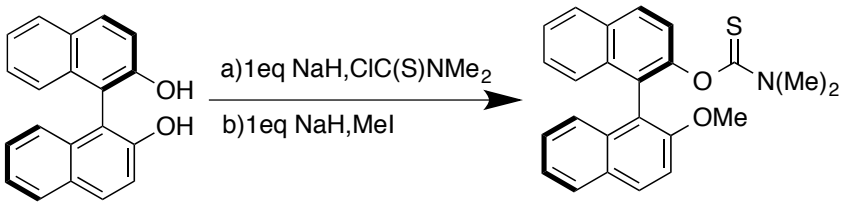

An oven-dried 15 mL round bottom flask containing BINOL (500.00 mg, 1.75 mmol, 1.00 equiv.) was equipped with a magnetic stirrer bar. The flask was evacuated and flushed with argon. Subsequently the flask was charged with 3.50 mL dry DMF and allowed to cool on ice to 0°C. Followed by Sodium hydride in 60% oil dispersion (41.90 mg, 1.75 mmol,1.00 equiv.) and resulting mixture was stirred at room temperature for 1 hour. Then N, N-dimethylthiocarbomoyl chloride (215.47 mg, 1.75 mmol, 1.00 equiv.) was added to the reaction mixture. The flask was then refluxed at 85°C in oil bath for 1hr. Then reaction was allowed to cool to 0°C and additional Sodium hydride (41.90 mg, 1.75 mmol,1.00 equiv.) was added, after 1h stirring, a solution of CH_3I (108.9 µL,1.75 mmol, 1.00 equiv.) in 0.35 mL DMF was slowly added and resulting mixture was heated to 85°C in oil bath for 2 hrs. The mixture was then cooled to room temperature and 9mL 1N KOH aq was added. The colorless precipitate was filtered, washed with water and dissolved in DCM. The organic phase was dried over Na_2SO_4, and after filtration the solvent was removed via rotatory evaporation. Recrystallized crude from DCM/petroleum. The resulting white solid crude was subjected to a column chromatography (hexanes/ethyl acetate 10:2) for next step. ^{1}H NMR (500 MHz, Chloroform-d) δ 8.07 – 8.03 (m, 1H), 8.03 – 7.99 (m, 2H), 7.92 – 7.86 (m, 1H), 7.68 –

7.31 (m, 7H), 7.31 – 7.24 (m, 1H), 7.16 (dd, J = 31.0, 8.4 Hz, 1H), 3.83 – 3.73 (m, 3H), 3.12 (s, 3H), 2.55 (s, 3H).

C: 2'-((dimethylcarbamothioyl)oxy)-[1,1'-binaphthalen]-2-yl acetate

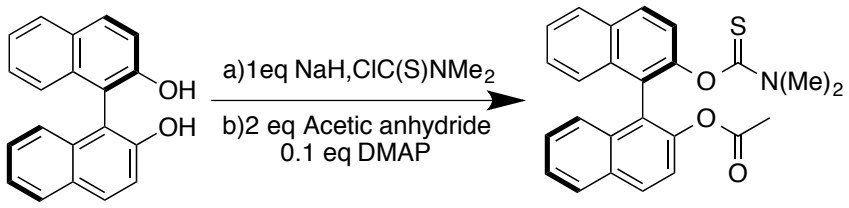

a) An oven-dried 15 mL round bottom flask containing BINOL (500.00 mg, 1.75 mmol, 1.00 equiv.) was equipped with a magnetic stirrer bar. The flask was evacuated and flushed with argon. Subsequently the flask was charged with 3.50 mL dry DMF and allowed to cool on ice to 0°C. Followed by sodium hydride in 60% oil dispersion (41.90 mg, 1.75 mmol,1.00 equiv.) and resulting mixture was stirred at room temperature for 1 hour. Then N, N-dimethylthiocarbomoyl chloride (215.47 mg, 1.75 mmol, 1.00 equiv.) was added to the reaction mixture. The flask was then refluxed at 85°C in oil bath for 1hr. Reaction was allowed to cool to room temperature and 5.00 mL deionized water (DI H_2O) added to reaction mixture, forming white precipitate. Crude mixture was washed with DCM to extract organic product. The organic phase was dried over Na_2SO_4, and after filtration the solvent was removed via rotatory evaporation.

b) An oven-dried 15 mL round bottom flask containing crude carbamoylated product from last step was equipped with a magnetic stirrer bar. The flask was evacuated and flushed with argon. Subsequently the flask was charged with 2.50 mL of DCM. Followed by acetic anhydride (0.34 mL, 3.50 mmol, 2.00 equiv.) and DMAP (22.40 mg,

0.175 mmol, 0.10 equiv.). The reaction mixture was allowed to stir for 24hrs then reaction mixture was concentrated via rotatory evaporation. The resulting white solid crude was subjected to a column chromatography (hexanes/ethyl acetate 10:2) for next step. ^{1}H NMR (500 MHz, Chloroform-d) δ 8.02 – 7.97 (m, 2H), 7.94 – 7.90 (m, 2H), 7.67 – 7.32 (m, 4H), 7.30 – 7.26 (m, 2H), 7.21 – 7.16 (m, 2H), 2.05 (d, J = 14.5 Hz, 3H), 1.84 (d, J = 9.3 Hz, 6H).

3.4.2 Photocatalysis Newman-Kwart rearrangement with yellow LEDs

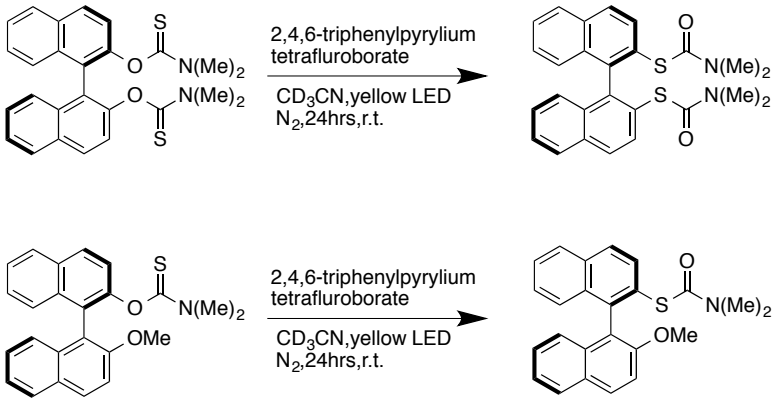

An oven-dried 10 mL round bottom flask containing O, O'-([1,1'-binaphthalene]-2,2'-diyl) bis(dimethylcarbamothioate) or O-(2'-methoxy-[1,1'-binaphthalen]-2-yl) dimethylcarbamothioate (0.375 mmol, 1.00 equiv.) was equipped with a magnetic stirrer bar. The flask was evacuated and flushed with argon. Subsequently the flask was charged with 0.75 mL dry CD_3CN and followed by 2,4,6-triphenylpyrylium tetrafluroborate (3.75 μmol, 0.01 equiv.). The reactions were run under N_2 using yellow LEDs to irradiating solution for 24 hours at room temperature.

3.4.3 Photocatalysis Newman-Kwart rearrangement with UV lights

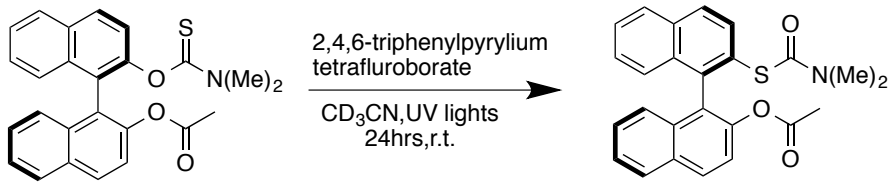

An oven-dried 10 mL Erlenmeyer flask containing 2'-((dimethylcarbamothioyl)oxy) - [1,1'-binaphthalen]-2-yl acetate (0.593 mmol, 1.00 equiv.) was equipped with a magnetic stirrer bar. The flask was evacuated and flushed with argon. Subsequently the flask was charged with 1.18 mL dry CD_3CN and followed by 2,4,6-triphenylpyrylium tetrafluroborate (5.93 μmol, 0.01 equiv.). The cylindrical neck was sealed with grafting tape to prevent solvent evaporation during rearrangement reaction. The reactions were run in junction box that equipped with UV LEDs to irradiating solution for 24 hrs at room temperature. The reaction mixture was concentrated using rotatory evaporation and crude product was purified through column chromatography. ^{1}H NMR (500 MHz, Chloroform-d) δ 7.99 (d, J = 9.3 Hz, 2H), 7.93 (d, J = 8.5 Hz, 2H), 7.61 (d, J = 9.0 Hz, 1H), 7.44 (q, J = 10.1, 8.8 Hz, 3H), 7.27 (q, J = 7.3, 6.6 Hz, 2H), 7.22 (d, J = 9.2 Hz, 1H), 7.18 (d, J = 8.6 Hz, 1H), 2.04 (s, 3H), 1.85 (s, 6H).

3.4.4 Chlorination and hydrolysis to afford BINOL based mono sulfonic acid [96]

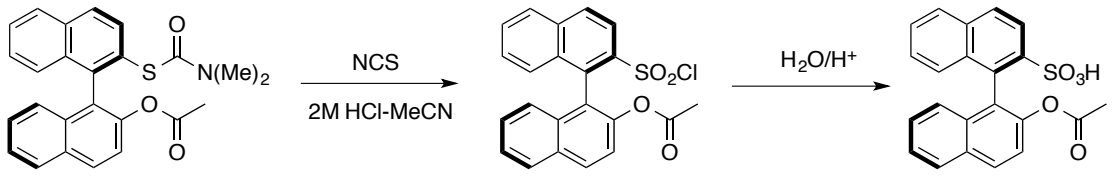

A. Chlorination of 2'-((dimethylcarbamoyl)thio)-[1,1'-binaphthalen]-2-yl acetate

N-chlorosuccinimide (4 equiv) was added to a mixture of 2 M HCl– CH_3CN (1:5; 3 v/w to NCS) and then cooled to 10 °C. A solution of the 2'-((dimethylcarbamoyl)thio)-[1,1'-binaphthalen]-2-yl acetate (1.00 equiv) in CH_3CN (0.5 v/w to NCS) was added dropwise to the mixture, which was kept below 20 °C in water bath. The resulting solution was stirred at <20 °C for 30 min, and then diluted with diethyl ether (3.5 v/w to NCS). The organic layer was washed with saturated aq NaCl (3 × 1.5 v/w to NCS), dried over Na_2SO_4 and concentrated via rotatory evaporation. The resulting yellow oil crude was subjected to column chromatography (toluene/acetone 95:5) for next step.^{1}H NMR (500 MHz, Chloroform-d) δ 8.04 – 7.98 (m, 1H), 7.92 (dd, J = 21.9, 8.4 Hz, 2H), 7.55 (d, J = 9.1 Hz, 1H), 7.47 (d, J = 7.0 Hz, 1H), 7.45 – 7.40 (m, 3H), 7.39 – 7.32 (m, 1H), 7.28 (t, J = 7.7 Hz, 1H), 7.14 (d, J = 8.5 Hz, 1H), 7.09 (d, J = 9.7 Hz, 1H), 1.85 (d, J = 4.4 Hz, 3H).

B. Hydrolysis of sulfonyl chloride to sulfonic acid

Sulfonyl chloride 2'-(chlorosulfonyl)-[1,1'-binaphthalen]-2-yl acetate was dissolved in 2M HCl solvent, added 0.1 M NaCl, the mixture was run at r.t. and procedure was monitored by SiO_2 preparative TLC.

CHAPTER FOUR: PICTET–SPENGLER CYCLIZATION

4.1 Design of Total Synthesis of Latifolian A

We designed the total synthesis of latifolian A through application of a chiral sulfonic acid catalyzed Friedel–Crafts cyclization reaction which is a key synthetic step in the route. Extension of this methodology to the synthesis of latifolian A demands incorporation of nitrogen-containing functionality into substrates suitable for chiral acid catalysis. While Mannich reactions proved a successful test-ground for initial work using phosphoric acid catalysts, incorporation of imine functional groups into advanced synthetic intermediates is challenging due to their relative instability. The generation of transient iminium ions through Brønsted acid catalysis and subsequent trapping by carbon-based nucleophiles could be a more fascinating venture. To this end, a short synthesis allowing for the rapid construction of latifolian A is envisioned.

The proposed synthesis route initiates with monoalkylation of known aniline **1** with primary bromide **2** employing Romera's conditions (Scheme 4.1) [97]. Application of novel sulfonic acid catalysts will then be applied for the subsequent condensation of amine **3** with known aldehyde **4**. This will result in the formation of iminium ion **5** that is poised for enantioselective intramolecular Friedel–Crafts cyclization of the pendant electron rich aryl ring. The use of chiral sulfonic acid catalysts for this transformation

should allow for the control of absolute stereochemistry of the product tetrahydroisoquinoline **6** after some experimentation. Notably, substrate **3** is obtained in one single reaction step from commercially available materials that will stimulate this attempt.

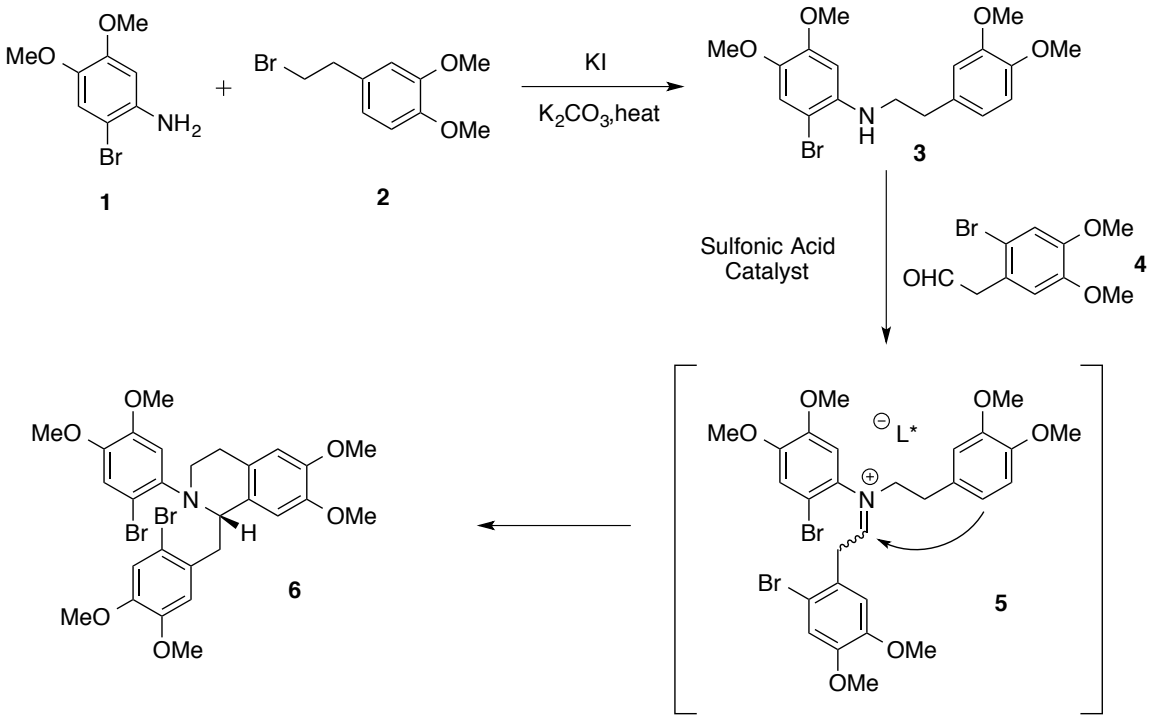

Figure 4.1 Enantioselective sulfonic acid catalysis for the synthesis of latifolian A

After completion of the key asymmetric step in the synthesis route, the bis-aryl bromide **6** would then be cross coupled with tributyl(vinyl) stannane promoted by palladium catalysis to afford bis-styrene product **7** (Scheme 4.2). Ring-closing metathesis using Grubbs' 2nd generation catalyst should provide macrocycle **8** efficiently [98]. Oxidation of this electron-rich alkene with m-CPBA will result in epoxide **9**. Internal tertiary amine under mild heating will give quaternary ammonium salt **10**. The synthesis

is then accomplished through an ionic reduction of the resulting benzylic alcohol concomitant with global demethylation catalyzed by the action of iodotrimethylsilane [58].

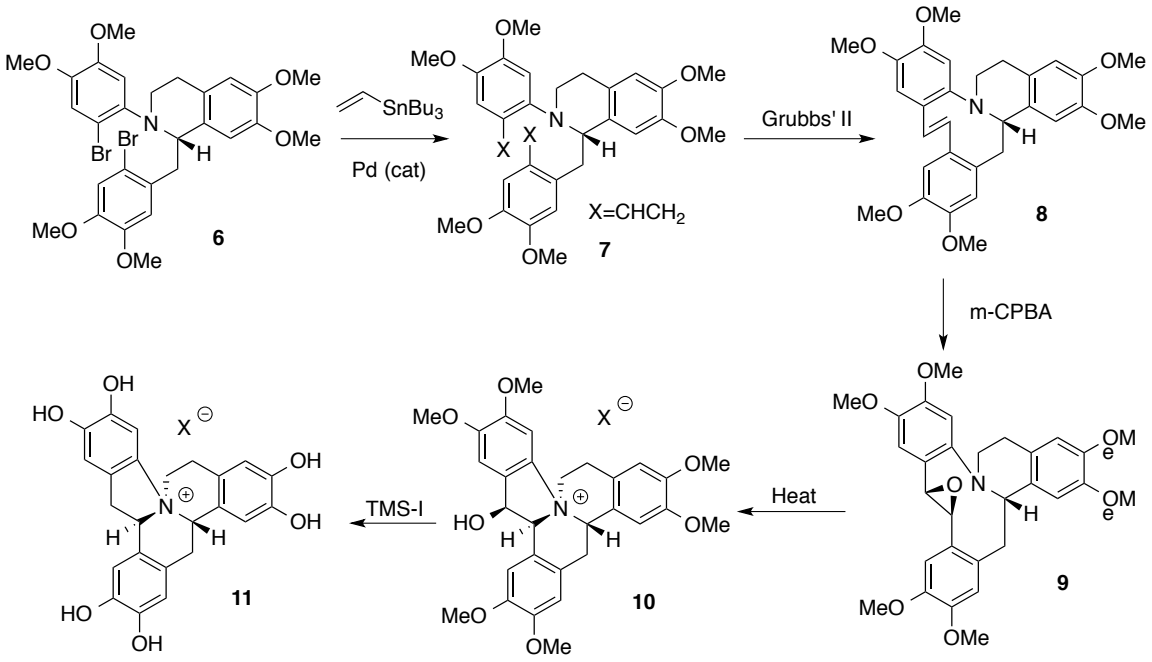

Figure 4.2 The total synthesis of latifolian A

4.2 Pictet–Spengler Cyclization

In order to evaluate the key enantioselective intramolecular cyclization in total synthesis of latifolian A, attampts were made to prepare tetrahydroisoquinolines through Pictet-Spengler cyclization first (Figure 4.1).

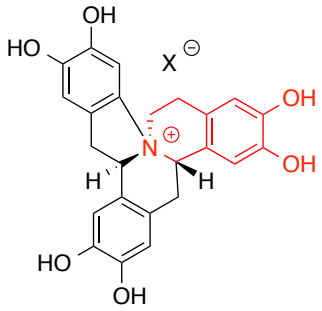

Figure 4.3 Tetrahydroisoquinoline fragment in latifolian A

The historic challenge for this Pictet-Spengler cyclization transformation lies in the relatively low electrophilicity of β-phenylethylamine- or tryptamine-derived imines or iminium ion, and a further challenge is raised by the enhanced basicity of the product amine over the starting materials, leading to issues that product amine tends to inhibit the catalyst cyclization by neutralizing the acid catalyst (Scheme 4.3).

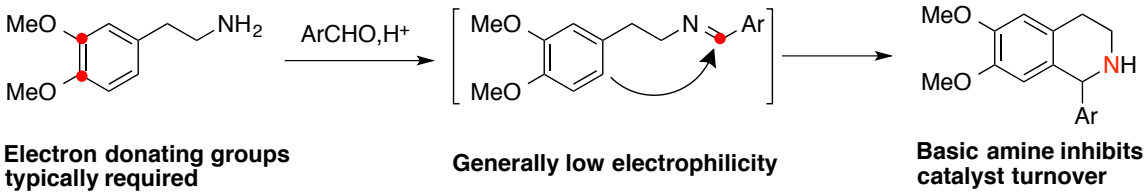

Figure 4.4 Challenges in performing Pictet-Spengler cyclization

Seidel and coworkers established a conjugate-base-stabilized Brønsted acid facilitated catalytic enantioselective Pictet–Spengler reaction with unmodified tryptamine and aldehyde (Scheme 4.4) [99]. They were able to overcome the low reactivity of tryptamine-derived iminium ions by utilizing internally conjugate-base-stabilized Brønsted acid catalysis (Scheme 4.5). Upon substrate protonation, the cooperative action of a catalyst with an acidic functional group and a covalently linked anion-recognition

site ought to result in a rigid substrate/catalyst ion pair. As high catalyst acidity derived from conjugate-base-stabilization via internal anion binding, and the protonated substrate should display enhanced electrophilicity. In order to improve catalyst turnover, the inclusion of $(Boc)_2O$ in such Pictet–Spengler reactions renders the nitrogen in the product less basic, and, hence it no longer can be protonated from the acid. Thus, in situ Boc-protection facilitates catalyst turnover. The chiral carboxylic acid catalyst is readily assembled in just two steps and enables the formation of β-carbolines with up to 92% ee.

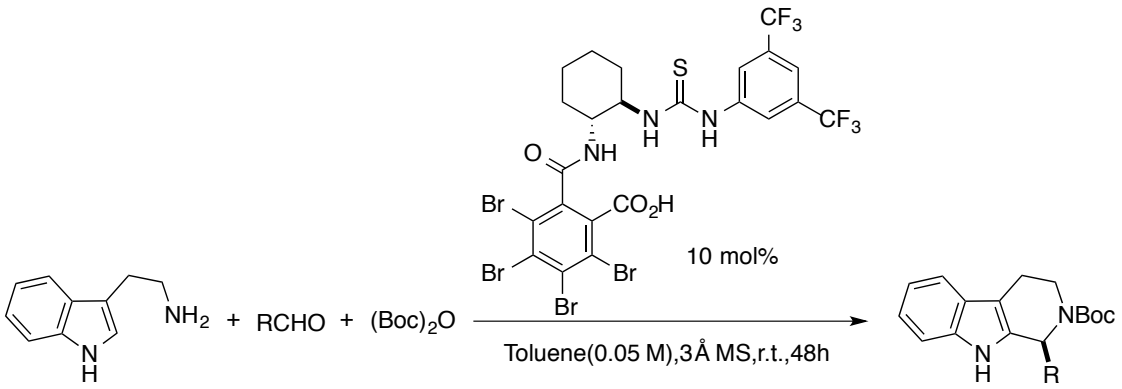

Figure 4.5 Catalytic enantioselective Pictet−Spengler reactions with unmodified tryptamine

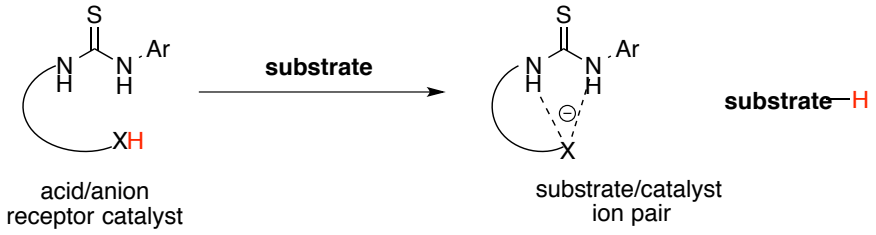

Figure 4.6 Internal anion-binding concept for asymmetric Brønsted acid catalysis

Unlike the Seidel group using tryptamines as amine precursors because of the highly nucleophilic indole system in combination with the hydrogen bonding properties of the indole N−H make this aromatic ring system an ideal reaction partner, in the same year, the Hiemstra group successfully prepared a series of 1-substituted 1,2,3,4-tetrahydroisoquinolines from N-(o-nitrophenylsulfenyl)- phenylethylamines through BINOL-phosphoric acid [(R)-TRIP]-catalyzed asymmetric Pictet−Spengler reactions [100]. In their study, they found 3,4-dimethoxyphenylethylamine is not sufficiently activating the para-position for Pictet–Spengler cyclization, and a 3-hydroxy substituent makes the aromatic ring considerably more reactive. They also introduced a moderately strong electron-withdrawing substituent on the nitrogen atom. The Nps (o-nitrophenylsulfenyl) substituent showed excellent properties with respect to reactivity and stability. Pictet−Spengler products was strongly facilitated by the Nps- group and gave tetrahydroisoquinolines with high enantiopurity (Scheme 4.6).

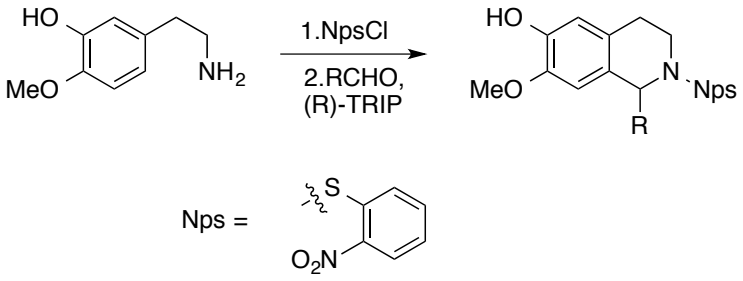

Figure 4.7 Enantioselective Pictet−Spengler reactions catalyzed by (R)-TRIP

To evaluate the key enantioselective intramolecular cyclization in total synthesis of latifolian A, we prepared tetrahydroisoquinolines through Pictet-Spengler Cyclization following the Seidel group's procedure. And we were not surprised to see that following

procedures did not afford desired tetrahydroisoquinoline product in the second step Pictet-Spengler Cyclization (Scheme 4.7). If replacing starting material with isovanillin, the result should be more promising.

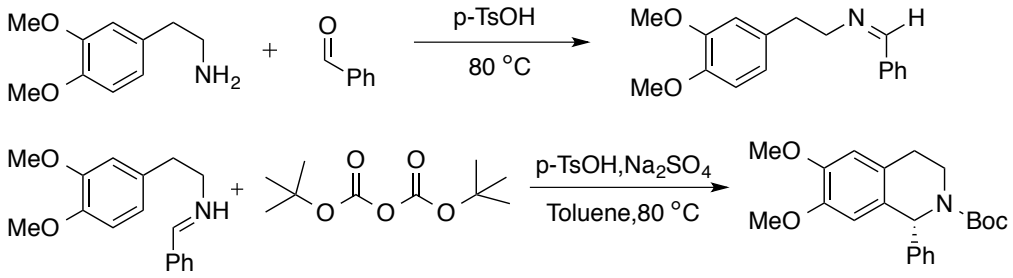

Figure 4.8 Tetrahydroisoquinoline preparation through Pictet-Spengler Cyclization

The next step of this project would be testing how sulfonic acids function with the phenylethylamines containing the free –OH group (isovanillin) with protecting group Boc or Nps substituents.

4.3 Experimental Details

4.3.1 Tetrahydroisoquinolines through Pictet-Spengler cyclization

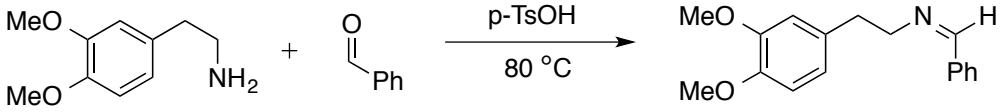

An oven-dried 10 mL round bottom flask containing 3,4-dimethoxy phenethylamine (250.00 mg, 1.48 mmol, 1.00 equiv.) was equipped with a magnetic stirrer bar. The flask was evacuated and flushed with argon. Subsequently the flask was charged with benzaldehyde (158 µL, 1.55 mmol,1.05 equiv.) with p-TsOH (58.00 mg, 0.31 mmol, 0.21 equiv.) and resulting mixture was stirred and refluxed at 85°C in oil bath

for 1 hr. Reaction was allowed to cool to room temperature and washed crude mixture with $NaHCO_3$ (aq) and extracted organic product with DCM. The organic phase was dried over Na_2SO_4, and after filtration the solvent was removed via rotatory evaporation. ^1H NMR (500 MHz, Chloroform-d) δ 8.13 (t, J = 1.3 Hz, 1H), 7.74 – 7.66 (m, 2H), 7.44 – 7.36 (m, 3H), 6.82 – 6.77 (m, 2H), 6.77 – 6.72 (m, 1H), 3.87 – 3.86 (m, 1H), 3.85 (s, 3H), 3.84 (d, J = 1.4 Hz, 1H), 3.79 (s, 3H), 2.96 (t, J = 7.3 Hz, 2H).

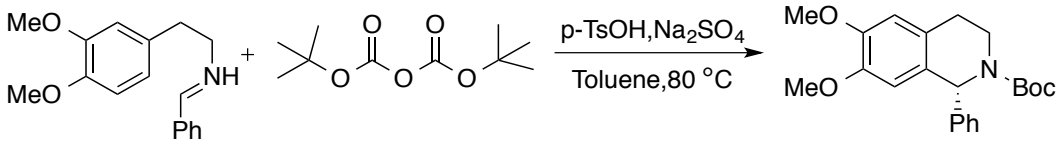

An oven-dried 50 mL round bottom flask containing (E)-N-benzylidene-2-(3,4-dimethoxyphenyl) ethan-1-aminium (1.48 mmol, 1.00 equiv.) was equipped with a magnetic stirrer bar. The flask was evacuated and flushed with argon. Subsequently the flask was charged with 14.80 mL dry toluene and Na_2SO_4 (420.00 mg, 2.96 mmol, 2.00 equiv.), followed by di-tert-butyl dicarbonate (711.00 mg, 3.256 mmol, 2.20 equiv.) with p-TsOH (58.00 mg, 0.31 mmol, 0.21 equiv.) and resulting mixture was stirred and refluxed at 80°C in oil bath for 4 hrs. The reaction was allowed to cool to room temperature and washed crude mixture with $NaHCO_3$ (aq) and extracted organic product with DCM. The organic phase was dried over Na_2SO_4, and after filtration the solvent was removed via rotatory evaporation.

CHAPTER FIVE: FINAL THOUGHTS

All of my three projects focus on the development of new methodology in the field of Brønsted acid catalysis especially sulfonic acids enabling rapid synthesis of medicinally relevant compounds. The use of Brønsted acids as catalysts can be an efficient and powerful method of bond forming, particularly with the use of weakly basic substrates through the development of stronger chiral Bronsted acids.

My initial project has demonstrated the developments of Brønsted acid catalyzed asymmetric transformations of azlactones and acetals. Followed by design and preparation of a novel class of confined Brønsted acid catalysts utilizing photocatalytic Newman-Kwart rearrangement. The total synthesis of latifolian A is currently under investigation. These three projects that I have participated in over the past years are all exciting and meaningful which expanded my knowledge and skills in organic synthesis.

I hope in the future that both the mono-protic sulfonic acid synthesis and total synthesis of latifolian A projects continue to be improved and I hope whoever works on these projects afterwards would find some of the answers that have been elusive so far. I have experienced an incredible journey of great joy and intense frustration, and I am truly grateful.

REFERENCES

[1] J. N. Brönsted, "Einige Bemerkungen über den Begriff der Säuren und Basen," *Recueil des Travaux Chimiques des Pays-Bas*, vol. 42, no. 8, pp. 718–728, 1923.

[2] T. M. Lowry, "The uniqueness of hydrogen," *Journal of the Society of Chemical Industry*, vol. 42, no. 3, pp. 43–47, 1923.

[3] G. N. Lewis, "Valence and the Structure of Atoms and Molecules," 1923.

[4] F. A. Carey, "Organic Chemistry," 2005.

[5] G. M. Coppola and H. F. Schuster, "Asymmetric synthesis: construction of chiral molecules using amino acids," 1987.

[6] L. A. Nguyen, H. He, and C. Pham-Huy, "Chiral drugs: an overview.," *Int J Biomed Sci*, vol. 2, no. 2, pp. 85–100, Jun. 2006.

[7] J. Hine, S. M. Linden, and V. M. Kanagasabapathy, "1,8-biphenylenediol is a double-hydrogen-bonding catalyst for reaction of an epoxide with a nucleophile," *J. Am. Chem. Soc.*, vol. 107, no. 4, pp. 1082–1083, Feb. 1985.

[8] M. Terada, "Chiral Phosphoric Acids as Versatile Catalysts for Enantioselective Transformations," *Synthesis*, vol. 2010, no. 12, pp. 1929–1982, May 2010.

[9] J. Seayad and B. List, "Asymmetric organocatalysis," *Org. Biomol. Chem.*, vol. 3, no. 5, p. 719, 2005.

[10] M. S. Sigman and E. N. Jacobsen, "Schiff Base Catalysts for the Asymmetric Strecker Reaction Identified and Optimized from Parallel Synthetic Libraries," *J. Am. Chem. Soc.*, vol. 120, no. 19, pp. 4901–4902, May 1998.

[11] Y. Huang, A. K. Unni, A. N. Thadani, and V. H. Rawal, "Hydrogen bonding: single enantiomers from a chiral-alcohol catalyst.," *Nature*, vol. 424, no. 6945, p. 146, Jul. 2003.

[12] T. Akiyama, "Stronger Brønsted Acids," *Chem. Rev.*, vol. 107, no. 12, pp. 5744–5758, Dec. 2007.

[13] D. Uraguchi and M. Terada, "Chiral Brønsted Acid-Catalyzed Direct Mannich Reactions via Electrophilic Activation," *J. Am. Chem. Soc.*, vol. 126, no. 17, pp. 5356–5357, May 2004.

[14] T. Akiyama, J. Itoh, K. Yokota, and K. Fuchibe, "Enantioselective Mannich-Type Reaction Catalyzed by a Chiral Brønsted Acid," *Angewandte Chemie International Edition*, vol. 43, no. 12, pp. 1566–1568, Mar. 2004.

[15] M. Hatano, K. Moriyama, T. Maki, and K. Ishihara, "Which Is the Actual Catalyst: Chiral Phosphoric Acid or Chiral Calcium Phosphate?," *Angewandte Chemie International Edition*, vol. 49, no. 22, pp. 3823–3826, Apr. 2010.

[16] T. Akiyama and K. Mori, "Stronger Brønsted Acids: Recent Progress," *Chem. Rev.*, vol. 115, no. 17, pp. 9277–9306, Jul. 2015.

[17] S. Hoffmann, A. M. Seayad, and B. List, "A Powerful Brønsted Acid Catalyst for the Organocatalytic Asymmetric Transfer Hydrogenation of Imines," *Angewandte Chemie International Edition*, vol. 44, no. 45, pp.

7424–7427, Nov. 2005.
[18] S. Mayer and B. List, “Asymmetric Counteranion-Directed Catalysis,” *Angewandte Chemie International Edition*, vol. 45, no. 25, pp. 4193–4195, Jun. 2006.
[19] T. Akiyama, Y. Saitoh, H. Morita, and K. Fuchibe, “Enantioselective Mannich-Type Reaction Catalyzed by a Chiral Brønsted Acid Derived from TADDOL,” *Advanced Synthesis & Catalysis*, vol. 347, no. 11, pp. 1523–1526, Oct. 2005.
[20] G. B. Rowland, H. Zhang, E. B. Rowland, S. Chennamadhavuni, Y. Wang, and J. C. Antilla, “Brønsted Acid-Catalyzed Imine Amidation,” *J. Am. Chem. Soc.*, vol. 127, no. 45, pp. 15696–15697, Nov. 2005.
[21] X.-H. Chen, X.-Y. Xu, H. Liu, L.-F. Cun, and L.-Z. Gong, “Highly Enantioselective Organocatalytic Biginelli Reaction,” *J. Am. Chem. Soc.*, vol. 128, no. 46, pp. 14802–14803, Nov. 2006.
[22] Q.-S. Guo, D.-M. Du, and J. Xu, “The Development of Double Axially Chiral Phosphoric Acids and Their Catalytic Transfer Hydrogenation of Quinolines,” *Angewandte Chemie International Edition*, vol. 47, no. 4, pp. 759–762, Jan. 2008.
[23] K. Mori, K. Ehara, K. Kurihara, and T. Akiyama, “Selective Activation of Enantiotopic C(sp 3)−Hydrogen by Means of Chiral Phosphoric Acid: Asymmetric Synthesis of Tetrahydroquinoline Derivatives,” *J. Am. Chem. Soc.*, vol. 133, no. 16, pp. 6166–6169, Apr. 2011.
[24] F. Xu, D. Huang, C. Han, W. Shen, X. Lin, and Y. Wang, “SPINOL-Derived Phosphoric Acids: Synthesis and Application in Enantioselective Friedel−Crafts Reaction of Indoles with Imines,” *J. Org. Chem.*, vol. 75, no. 24, pp. 8677–8680, Dec. 2010.
[25] I. Čorić, S. Müller, and B. List, “Kinetic Resolution of Homoaldols via Catalytic Asymmetric Transacetalization,” *J. Am. Chem. Soc.*, vol. 132, no. 49, pp. 17370–17373, Dec. 2010.
[26] T. Hashimoto and K. Maruoka, “Design of Axially Chiral Dicarboxylic Acid for Asymmetric Mannich Reaction of Arylaldehyde N-Boc Imines and Diazo Compounds,” *J. Am. Chem. Soc.*, vol. 129, no. 33, pp. 10054–10055, Aug. 2007.
[27] D. Kampen, A. Ladépêche, G. Claßen, and B. List, “Brønsted Acid-Catalyzed Three-Component Hosomi–Sakurai Reactions,” *Advanced Synthesis & Catalysis*, vol. 350, no. 7, pp. 962–966, May 2008.
[28] M. Hatano, T. Maki, K. Moriyama, M. Arinobe, and K. Ishihara, “Pyridinium 1,1′-Binaphthyl-2,2′-disulfonates as Highly Effective Chiral Brønsted Acid−Base Combined Salt Catalysts for Enantioselective Mannich-Type Reaction,” *J. Am. Chem. Soc.*, vol. 130, no. 50, pp. 16858–16860, Dec. 2008.
[29] P. García-García, F. Lay, P. García-García, C. Rabalakos, and B. List, “A Powerful Chiral Counteranion Motif for Asymmetric Catalysis,” *Angewandte Chemie International Edition*, vol. 48, no. 24, pp. 4363–4366,

Jun. 2009.
[30] L.-Y. Chen, H. He, W.-H. Chan, and A. W. M. Lee, “Chiral Sulfonimide as a Brønsted Acid Organocatalyst for Asymmetric Friedel–Crafts Alkylation of Indoles with Imines,” *J. Org. Chem.*, vol. 76, no. 17, pp. 7141–7147, Sep. 2011.
[31] H. Ishibashi, K. Ishihara, and H. Yamamoto, “Chiral Proton Donor Reagents: Tin Tetrachloride?Coordinated Optically Active Binaphthol Derivatives,” *Chem. Record*, vol. 2, no. 3, pp. 177–188, Jun. 2002.
[32] H. Yamamoto and K. Futatsugi, “‘Designer Acids’: Combined Acid Catalysis for Asymmetric Synthesis,” *Angewandte Chemie International Edition*, vol. 44, no. 13, pp. 1924–1942, Mar. 2005.
[33] L. Duhamel, S. Fouquay, and J.-C. Plaquevent, “Ligand exchange in asymmetric reactions of lithium enolates : application to the deracemization of α-aminoacids,” *Tetrahedron Letters*, vol. 27, no. 41, pp. 4975–4978, 1986.
[34] M. B. Eleveld and H. Hogeveen, “Enantioselective deprotonation of two racemic cyclic carbonyl compounds by a chiral lithium amide,” *Tetrahedron Letters*, vol. 27, no. 5, pp. 631–634, 1986.
[35] K. Matsumoto, S. Tsutsumi, T. Ihori, and H. Ohta, “Enzyme-mediated enantioface-differentiating hydrolysis of .alpha.-substituted cycloalkanone enol esters,” *J. Am. Chem. Soc.*, vol. 112, no. 26, pp. 9614–9619, Dec. 1990.
[36] Y. Kume and H. Ohta, “Enzyme-mediated enantioface-differentiating hydrolysis of α-substituted sulfur-containing cyclic ketone enol esters,” *Tetrahedron Letters*, vol. 33, no. 42, pp. 6367–6370, 1992.
[37] I. Fujii, R. A. Lerner, and K. D. Janda, “Enantiofacial protonation by catalytic antibodies,” *J. Am. Chem. Soc.*, vol. 113, no. 22, pp. 8528–8529, Oct. 1991.
[38] K. Ishihara, M. Kaneeda, and H. Yamamoto, “Lewis Acid Assisted Chiral Bronsted Acid for Enantioselective Protonation of Silyl Enol Ethers and Ketene Bis(trialkylsilyl) Acetals,” *J. Am. Chem. Soc.*, vol. 116, no. 24, pp. 11179–11180, Nov. 1994.
[39] A. Burns and S. Iliffe, “Alzheimer's disease,” *BMJ*, vol. 338, 2009.
[40] G. Wenk, *Neuropathologic Changes in Alzheimer’s Disease*, vol. 64. 2003, pp. 7–10.
[41] R. S. Desikan, H. J. Cabral, C. P. Hess, W. P. Dillon, C. M. Glastonbury, M. W. Weiner, N. J. Schmansky, D. N. Greve, D. H. Salat, R. L. Buckner, B. Fischl, Alzheimer's Disease Neuroimaging Initiative, “Automated MRI measures identify individuals with mild cognitive impairment and Alzheimer's disease,” *Brain*, vol. 132, no. 8, pp. 2048–2057, Jul. 2009.
[42] C. Ballard, S. Gauthier, A. Corbett, C. Brayne, D. Aarsland, and E. Jones, “Alzheimer's disease,” *The Lancet*, vol. 377, no. 9770, pp. 1019–1031, Mar. 2011.
[43] A. Martorana, Z. Esposito, and G. Koch, “Beyond the Cholinergic Hypothesis: Do Current Drugs Work in Alzheimer's Disease?,” *CNS Neuroscience & Therapeutics*, vol. 16, no. 4, pp. 235–245, 2010.

[44] S. J. Rochfort, L. Towerzey, A. Carroll, G. King, A. Michael, G. Pierens, T. Rali, J. Redburn, J. Whitmore, and R. J. Quinn, "Latifolians A and B, Novel JNK3 Kinase Inhibitors from the Papua New Guinean Plant Gnetumlatifolium," *J. Nat. Prod.*, vol. 68, no. 7, pp. 1080–1082, Jul. 2005.

[45] S. O. Yoon, D. J. Park, J. C. Ryu, H. G. Ozer, C. Tep, Y. J. Shin, T. H. Lim, L. Pastorino, A. J. Kunwar, J. C. Walton, A. H. Nagahara, K. P. Lu, R. J. Nelson, M. H. Tuszynski, and K. Huang, "JNK3 Perpetuates Metabolic Stress Induced by Aβ Peptides," *Neuron*, vol. 75, no. 5, pp. 824–837, Sep. 2012.

[46] W. F. A. W. Kitching, "Spiroacetals in Insects," *Current Organic Chemistry*, vol. 5, no. 2, pp. 233–251, Aug. 2001.

[47] J. E. Aho, P. M. Pihko, and T. K. Rissa, "Nonanomeric Spiroketals in Natural Products: Structures, Sources, and Synthetic Strategies," *Chem. Rev.*, vol. 105, no. 12, pp. 4406–4440, Dec. 2005.

[48] M. Terada, H. Tanaka, and K. Sorimachi, "Enantioselective Direct Aldol-Type Reaction of Azlactone via Protonation of Vinyl Ethers by a Chiral Brønsted Acid Catalyst," *J. Am. Chem. Soc.*, vol. 131, no. 10, pp. 3430–3431, Mar. 2009.

[49] P. P. de Castro, A. G. Carpanez, and G. W. Amarante, "Azlactone Reaction Developments," *Chem. Eur. J.*, vol. 22, no. 30, pp. 10294–10318, Jun. 2016.

[50] S. Tsunehiko, T. Haruhiro, Y. Masaaki, and M. Teruaki, "Efficient Activation of Acetals, Aldehydes, and Imines toward Silylated Nucleophiles by the Combined Use of Catalytic Amounts of [Rh(COD)Cl]2 and TMS-CN under Almost Neutral Conditions," *Bulletin of the Chemical Society of Japan*, vol. 63, no. 11, pp. 3122–3131, 1990.

[51] C. D. Gheewala, B. E. Collins, and T. H. Lambert, "An aromatic ion platform for enantioselective Brønsted acid catalysis.," *Science*, vol. 351, no. 6276, pp. 961–965, Feb. 2016.

[52] J. Dietrich, V. Gokhale, X. Wang, L. H. Hurley, and G. A. Flynn, "Bioorganic & Medicinal Chemistry," *Bioorganic & Medicinal Chemistry*, vol. 18, no. 1, pp. 292–304, Jan. 2010.

[53] I. Suzuki, M. Yasuda, and A. Baba, "Zn(ii) chloride-catalyzed direct coupling of various alkynes with acetals: facile and inexpensive access to functionalized propargyl ethers," *Chem. Commun.*, vol. 49, no. 99, p. 11620, 2013.

[54] S. K. De and R. A. Gibbs, "Ruthenium(III) chloride-catalyzed chemoselective synthesis of acetals from aldehydes," *Tetrahedron Letters*, vol. 45, no. 44, pp. 8141–8144, Oct. 2004.

[55] S. G. Krasutsky, S. H. Jacobo, S. R. Tweedie, R. Krishnamoorthy, and A. S. Filatov, "Route Optimization and Synthesis of Taxadienone," *Org. Process Res. Dev.*, vol. 19, no. 1, pp. 284–289, Jan. 2015.

[56] G. A. Ramann and B. J. Cowen, "Quinoline synthesis by improved Skraup–Doebner–Von Miller reactions utilizing acrolein diethyl acetal," *Tetrahedron Letters*, vol. 56, no. 46, pp. 6436–6439, 2015.

[57] N. Costes, S. Michel, F. Tillequin, M. Koch, A. Pierré, and G. Atassi, "Chiral Dihydroxylation of Acronycine: Absolute Configuration of Natural cis-1,2-Dihydroxy-1,2-dihydroacronycine and Cytotoxicity of (1 R,2 R)- and (1 S,2 S)-1,2-Diacetoxy-1,2-dihydroacronycine," *J. Nat. Prod.*, vol. 62, no. 3, pp. 490–492, Mar. 1999.

[58] G. A. Cain and E. R. Holler, "Extended scope of in situ iodotrimethylsilane mediated selective reduction of benzylic alcohols," *Chem. Commun.*, no. 13, pp. 1168–1169, 2001.

[59] J.-H. Xie, L.-C. Guo, X.-H. Yang, L.-X. Wang, and Q.-L. Zhou, "Enantioselective Synthesis of 2,6- cis-Disubstituted Tetrahydropyrans via a Tandem Catalytic Asymmetric Hydrogenation/Oxa-Michael Cyclization: An Efficient Approach to (−)-Centrolobine," *Org. Lett.*, vol. 14, no. 18, pp. 4758–4761, Sep. 2012.

[60] A. Bartoszewicz, M. Kalek, J. Nilsson, R. Hiresova, and J. Stawinski, "A New Reagent System for Efficient Silylation of Alcohols: Silyl Chloride- N-Methylimidazole-Iodine," *Synlett*, no. 1, pp. 37–40, Jan. 2008.

[61] C. B. Rao, B. Chinnababu, and Y. Venkateswarlu, "An Efficient Protocol for Alcohol Protection Under Solvent- and Catalyst-Free Conditions," *J. Org. Chem.*, vol. 74, no. 22, pp. 8856–8858, Nov. 2009.

[62] T. Akiyama, " Catalyst for asymmetric synthesis with chiral Bronsted acid and asymmetric synthesis method using said catalyst," WO/2004/096753.

[63] S. Hoffmann, M. Nicoletti, and B. List, "Catalytic Asymmetric Reductive Amination of Aldehydes via Dynamic Kinetic Resolution," *J. Am. Chem. Soc.*, vol. 128, no. 40, pp. 13074–13075, Oct. 2006.

[64] J. Zhou and B. List, "Organocatalytic Asymmetric Reaction Cascade to Substituted Cyclohexylamines," *J. Am. Chem. Soc.*, vol. 129, no. 24, pp. 7498–7499, Jun. 2007.

[65] J. Seayad, A. M. Seayad, and B. List, "Catalytic Asymmetric Pictet−Spengler Reaction," *J. Am. Chem. Soc.*, vol. 128, no. 4, pp. 1086–1087, Feb. 2006.

[66] M. Terada and K. Sorimachi, "Enantioselective Friedel−Crafts Reaction of Electron-Rich Alkenes Catalyzed by Chiral Brønsted Acid," *J. Am. Chem. Soc.*, vol. 129, no. 2, pp. 292–293, Jan. 2007.

[67] Y.-X. Jia, J. Zhong, S.-F. Zhu, C.-M. Zhang, and Q.-L. Zhou, "Chiral Brønsted Acid Catalyzed Enantioselective Friedel–Crafts Reaction of Indoles and α-Aryl Enamides: Construction of Quaternary Carbon Atoms," *Angewandte Chemie International Edition*, vol. 46, no. 29, pp. 5565–5567, Jul. 2007.

[68] T. Akiyama, Y. Tamura, J. Itoh, H. Morita, and K. Fuchibe, "Enantioselective Aza-Diels-Alder Reaction Catalyzed by a Chiral Brønsted Acid: Effect of the Additive on the Enantioselectivity," *Synlett*, no. 1, pp. 0141–0143, Aug. 2006.

[69] W.-J. Liu, X.-H. Chen, and L.-Z. Gong, "Direct Assembly of Aldehydes, Amino Esters, and Anilines into Chiral Imidazolidines via Brønsted Acid

Catalyzed Asymmetric 1,3-Dipolar Cycloadditions," *Org. Lett.*, vol. 10, no. 23, pp. 5357–5360, Dec. 2008.
[70] J. Lacour and D. Moraleda, "Chiral anion-mediated asymmetric ion pairing chemistry," *Chem. Commun.*, vol. 41, no. 46, p. 7073, 2009.
[71] X. Wang and B. List, "Asymmetric Counteranion-Directed Catalysis for the Epoxidation of Enals," *Angewandte Chemie International Edition*, vol. 47, no. 6, pp. 1119–1122, Jan. 2008.
[72] N. J. A. Martin and B. List, "Highly Enantioselective Transfer Hydrogenation of α,β-Unsaturated Ketones," *J. Am. Chem. Soc.*, vol. 128, no. 41, pp. 13368–13369, Oct. 2006.
[73] X. Wang, C. M. Reisinger, and B. List, "Catalytic Asymmetric Epoxidation of Cyclic Enones," *J. Am. Chem. Soc.*, vol. 130, no. 19, pp. 6070–6071, May 2008.
[74] G. L. Hamilton, E. J. Kang, M. Mba, and F. D. Toste, "A Powerful Chiral Counterion Strategy for Asymmetric Transition Metal Catalysis," *Science*, vol. 317, no. 5837, pp. 496–499, Jul. 2007.
[75] S. Mukherjee and B. List, "Chiral Counteranions in Asymmetric Transition-Metal Catalysis: Highly Enantioselective Pd/Brønsted Acid-Catalyzed Direct α-Allylation of Aldehydes," *J. Am. Chem. Soc.*, vol. 129, no. 37, pp. 11336–11337, Sep. 2007.
[76] V. Komanduri and M. J. Krische, "Enantioselective Reductive Coupling of 1,3-Enynes to Heterocyclic Aromatic Aldehydes and Ketones via Rhodium-Catalyzed Asymmetric Hydrogenation: Mechanistic Insight into the Role of Brønsted Acid Additives," *J. Am. Chem. Soc.*, vol. 128, no. 51, pp. 16448–16449, Dec. 2006.
[77] C. Li, C. Wang, B. Villa-Marcos, and J. Xiao, "Chiral Counteranion-Aided Asymmetric Hydrogenation of Acyclic Imines," *J. Am. Chem. Soc.*, vol. 130, no. 44, pp. 14450–14451, Nov. 2008.
[78] C. Li, B. Villa-Marcos, and J. Xiao, "Metal−Brønsted Acid Cooperative Catalysis for Asymmetric Reductive Amination," *J. Am. Chem. Soc.*, vol. 131, no. 20, pp. 6967–6969, May 2009.
[79] M. Klussmann, "Asymmetric Reductive Amination by Combined Brønsted Acid and Transition-Metal Catalysis," *Angewandte Chemie International Edition*, vol. 48, no. 39, pp. 7124–7125, Sep. 2009.
[80] X.-Y. Liu and C.-M. Che, "Highly Enantioselective Synthesis of Chiral Secondary Amines by Gold(I)/Chiral Brønsted Acid Catalyzed Tandem Intermolecular Hydroamination and Transfer Hydrogenation Reactions," *Org. Lett.*, vol. 11, no. 18, pp. 4204–4207, Sep. 2009.
[81] M. Klussmann, L. Ratjen, S. Hoffmann, V. Wakchaure, R. Goddard, and B. List, "Synthesis of TRIP and Analysis of Phosphate Salt Impurities," *Synlett*, no. 14, pp. 2189–2192, Jul. 2010.
[82] M. Terada, K. Sorimachi, and D. Uraguchi, "Phosphorodiamidic Acid as a Novel Structural Motif of Brønsted Acid Catalysts for Direct Mannich Reaction of N-Acyl Imines with 1,3-Dicarbonyl Compounds," *Synlett*, no. 1,

pp. 0133–0136, 2006.
[83] D. Nakashima and H. Yamamoto, “Design of Chiral N-Triflyl Phosphoramide as a Strong Chiral Brønsted Acid and Its Application to Asymmetric Diels−Alder Reaction,” *J. Am. Chem. Soc.*, vol. 128, no. 30, pp. 9626–9627, Aug. 2006.
[84] C. H. Cheon and H. Yamamoto, “Super Brønsted acid catalysis,” *Chem. Commun.*, vol. 47, no. 11, p. 3043, 2011.
[85] M. Rueping, B. J. Nachtsheim, W. Ieawsuwan, and I. Atodiresei, “Modulating the Acidity: Highly Acidic Brønsted Acids in Asymmetric Catalysis,” *Angewandte Chemie International Edition*, vol. 50, no. 30, pp. 6706–6720, Jun. 2011.
[86] C. H. Cheon and H. Yamamoto, “A Brønsted Acid Catalyst for the Enantioselective Protonation Reaction,” *J. Am. Chem. Soc.*, vol. 130, no. 29, pp. 9246–9247, Jul. 2008.
[87] S. Vellalath, I. Čorić, and B. List, “N-Phosphinyl Phosphoramide-A Chiral Brønsted Acid Motif for the Direct Asymmetric N,O-Acetalization of Aldehydes,” *Angewandte Chemie International Edition*, vol. 49, no. 50, pp. 9749–9752, Nov. 2010.
[88] D. M. Knotter, D. M. Grove, W. J. J. Smeets, A. L. Spek, and G. Van Koten, “A new class of organocopper and organocuprate compounds derived from copper(I) arenethiolates,” *J. Am. Chem. Soc.*, vol. 114, no. 9, pp. 3400–3410, Apr. 1992.
[89] M. V. Klaveren, F. Lambert, D. J. F. M. Eijkelkamp, D. M. Grove, and G. Van Koten, “Arenethiolatocopper(I) complexes as homogeneous catalysts for Michael addition reactions,” *Tetrahedron Letters*, vol. 35, no. 33, pp. 6135–6138, 1994.
[90] M. van Klaveren, E. S. M. Persson, A. del Villar, D. M. Grove, J.-E. Bäckvall, and G. Van Koten, “Chiral arenethiolatocopper(I) catalyzed substitution reactions of acyclic allylic substrates with Grignard reagents,” *Tetrahedron Letters*, vol. 36, no. 17, pp. 3059–3062, 1995.
[91] A. M. Masdeu, A. Orejón, A. Ruiz, S. Castillón, and C. Claver, “New hydroformylation rhodium catalysts with dithiolate chiral ligands,” *Journal of Molecular Catalysis*, vol. 94, no. 2, pp. 149–156, 1994.
[92] D. Fabbri, S. Pulacchini, and S. Gladiali, “Synthesis of Atropisomeric Heterotopic S-Donor Ligands through Asymmetrization of C2-Symmetry 2,2’-Disubstituted 1,1’-Binaphthalene Derivatives,” no. 11, pp. 1054–1056, Aug. 1996.
[93] J. N. Harvey, J. Jover, G. C. Lloyd-Jones, J. D. Moseley, P. Murray, and J. S. Renny, “The Newman-Kwart Rearrangement of O-Aryl Thiocarbamates: Substantial Reduction in Reaction Temperatures through Palladium Catalysis,” *Angewandte Chemie International Edition*, vol. 48, no. 41, pp. 7612–7615, Sep. 2009.
[94] A. J. Perkowski, C. L. Cruz, and D. A. Nicewicz, “Ambient-Temperature Newman–Kwart Rearrangement Mediated by Organic Photoredox

Catalysis," *J. Am. Chem. Soc.*, vol. 137, no. 50, pp. 15684–15687, Dec. 2015.

[95] P. S. Selig and S. J. Miller, "Tetrahedron Letters," *Tetrahedron Letters*, vol. 52, no. 17, pp. 2148–2151, Apr. 2011.

[96] A. Nishiguchi, K. Maeda, and S. Miki, "Sulfonyl Chloride Formation from Thiol Derivatives by N-Chlorosuccinimide Mediated Oxidation," *Synthesis*, vol. 2006, no. 24, pp. 4131–4134, Dec. 2006.

[97] J. L. Romera, J. M. Cid, and A. A. Trabanco, "Potassium iodide catalysed monoalkylation of anilines under microwave irradiation," *Tetrahedron Letters*, vol. 45, no. 48, pp. 8797–8800, Nov. 2004.

[98] R. H. Grubbs, S. J. Miller, and G. C. Fu, "Ring-Closing Metathesis and Related Processes in Organic Synthesis," *Acc. Chem. Res.*, vol. 28, no. 11, pp. 446–452, May 1995.

[99] N. Mittal, D. X. Sun, and D. Seidel, "Conjugate-Base-Stabilized Brønsted Acids: Catalytic Enantioselective Pictet–Spengler Reactions with Unmodified Tryptamine," *Org. Lett.*, vol. 16, no. 3, pp. 1012–1015, Jan. 2014.

[100] E. Mons, M. J. Wanner, S. Ingemann, J. H. van Maarseveen, and H. Hiemstra, "Organocatalytic Enantioselective Pictet–Spengler Reactions for the Syntheses of 1-Substituted 1,2,3,4-Tetrahydroisoquinolines," *J. Org. Chem.*, vol. 79, no. 16, pp. 7380–7390, Aug. 2014.

APPENDIX A. ^{1}H NMR SPECTRA

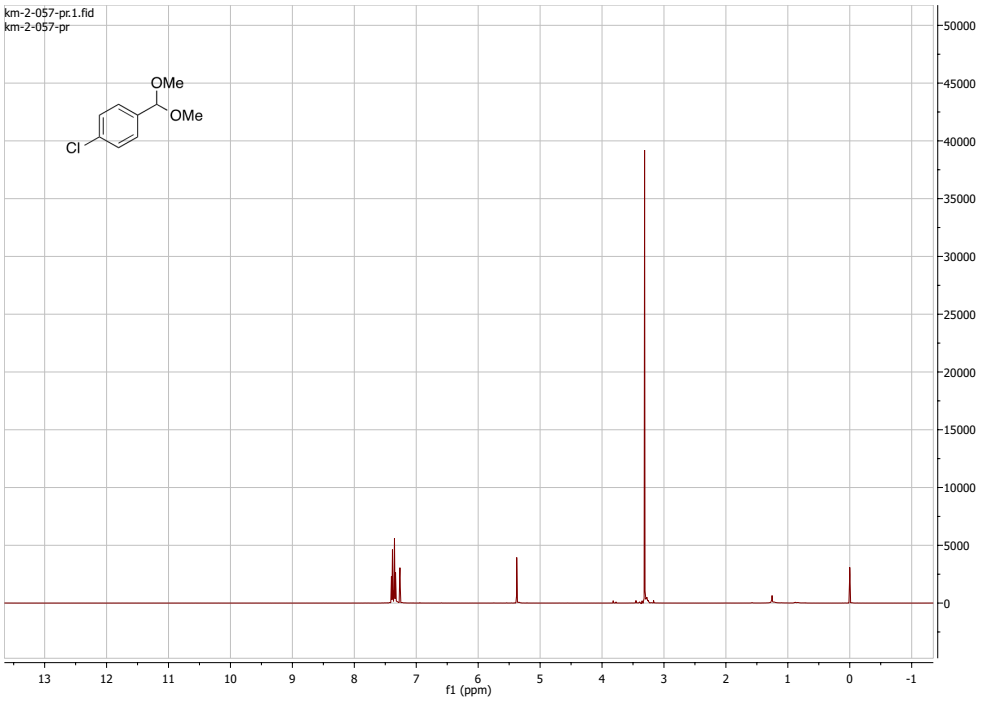

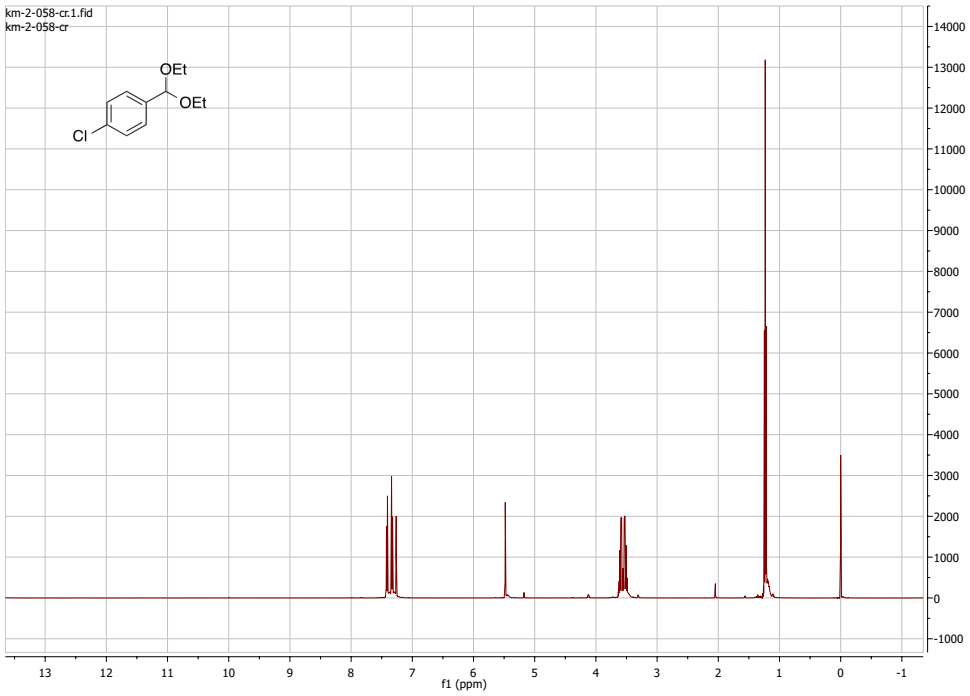

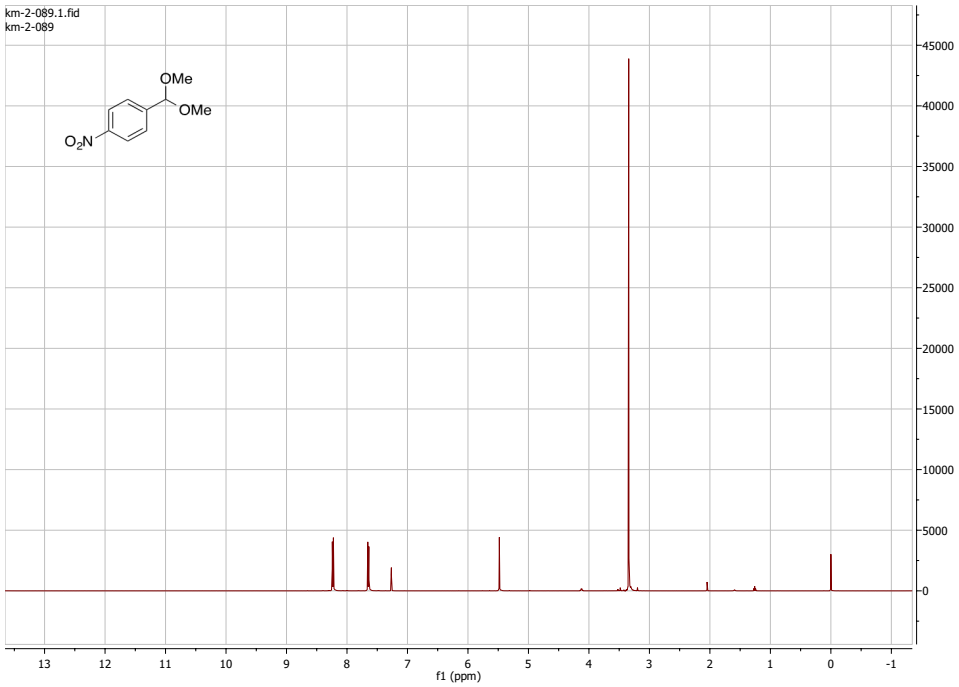
km-2-089.1.fid
km-2-089
OMe
OMe
O2N
45000
40000
35000
30000
25000
20000
15000
10000
5000
0
13
12
11
10
9
8
7
6
5
4
3
2
1
0
-1
f1 (ppm)

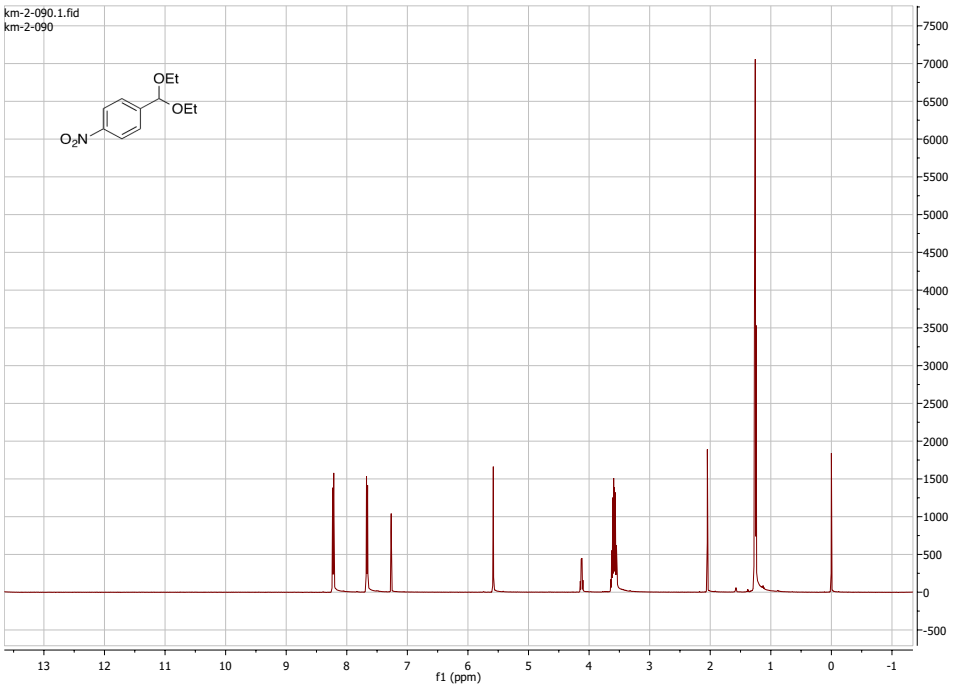
km-2-090.1.fid
km-2-090
OEt
OEt
O2N
7500
7000
6500
6000
5500
5000
4500
4000
3500
3000
2500
2000
1500
1000
500
0
-500
13
12
11
10
9
8
7
6
5
4
3
2
1
0
-1
f1 (ppm)

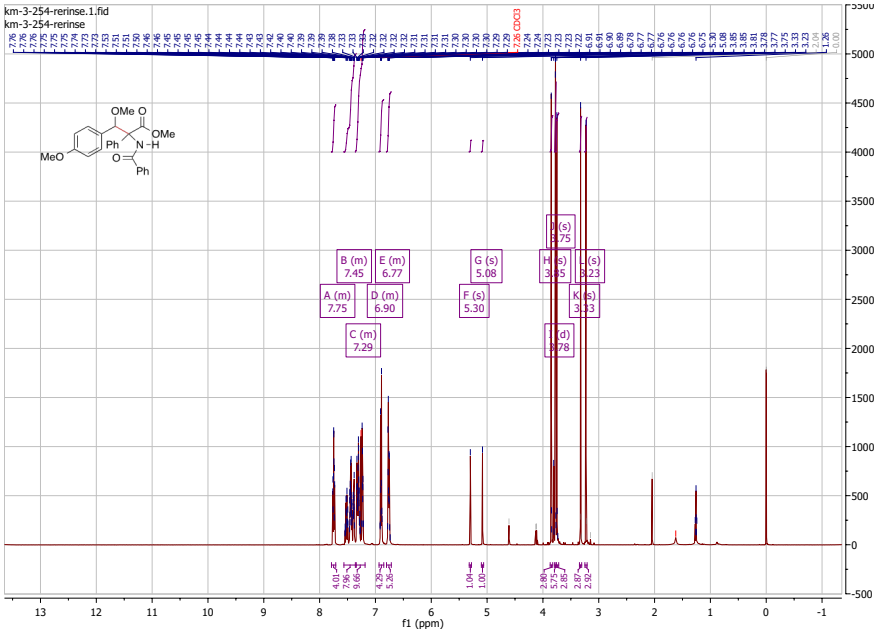
km-3-254-rerinse.1.fid
km-3-254-rerinse
OMe O
OMe
Ph
N
H
O
MeO
Ph
B (m) 7.45
E (m) 6.77
G (s) 5.08
I (s) 3.75
H (s) 3.65
L (s) 3.23
A (m) 7.75
D (m) 6.90
F (s) 5.30
K (s) 3.23
C (m) 7.29
J (d) 2.78
f1 (ppm)

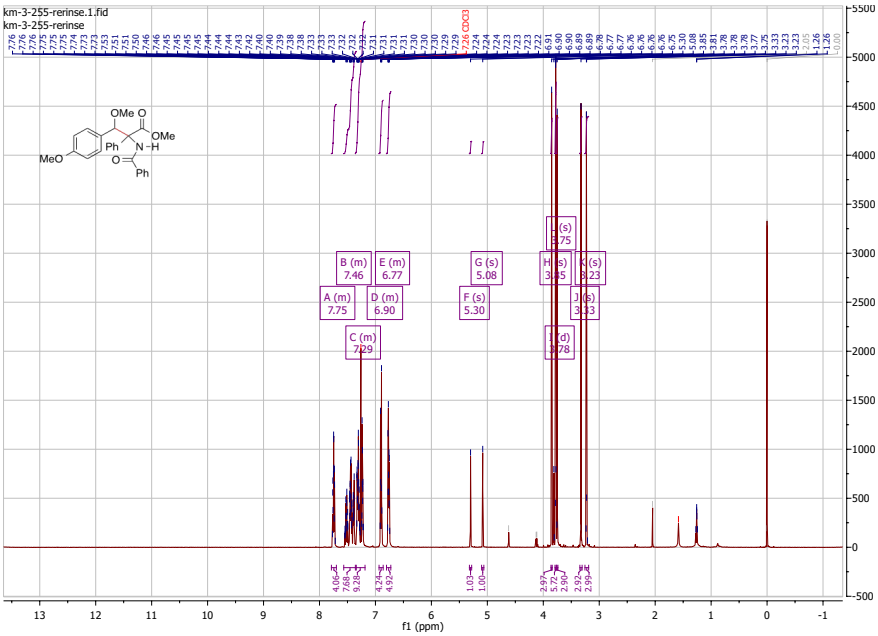
km-3-255-rerinse.1.fid
km-3-255-rerinse
OMe O
OMe
Ph
N
H
O
MeO
Ph
B (m) 7.46
E (m) 6.77
G (s) 5.08
I (s) 3.75
H (s) 3.65
L (s) 3.23
A (m) 7.75
D (m) 6.90
F (s) 5.30
K (s) 3.23
C (m) 7.29
J (d) 2.78
f1 (ppm)

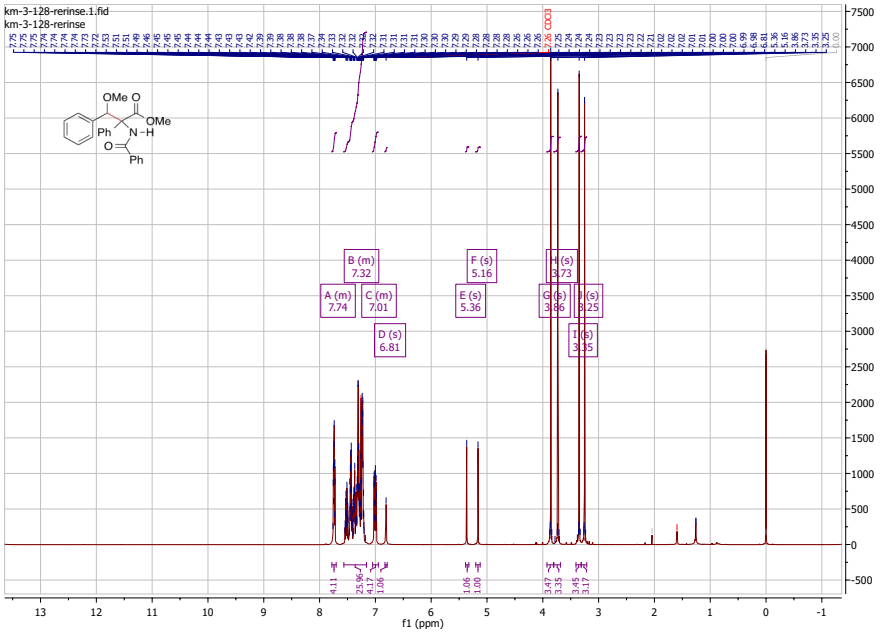
km-3-128-rerinse.1.fid
km-3-128-rerinse
OMe O
OMe
Ph
N–H
O
Ph
B (m) 7.32
A (m) 7.74
C (m) 7.01
D (s) 6.81
F (s) 5.16
E (s) 5.36
G (s) 3.86
H (s) 3.73
I (s) 3.25
J (s) 3.35
f1 (ppm)

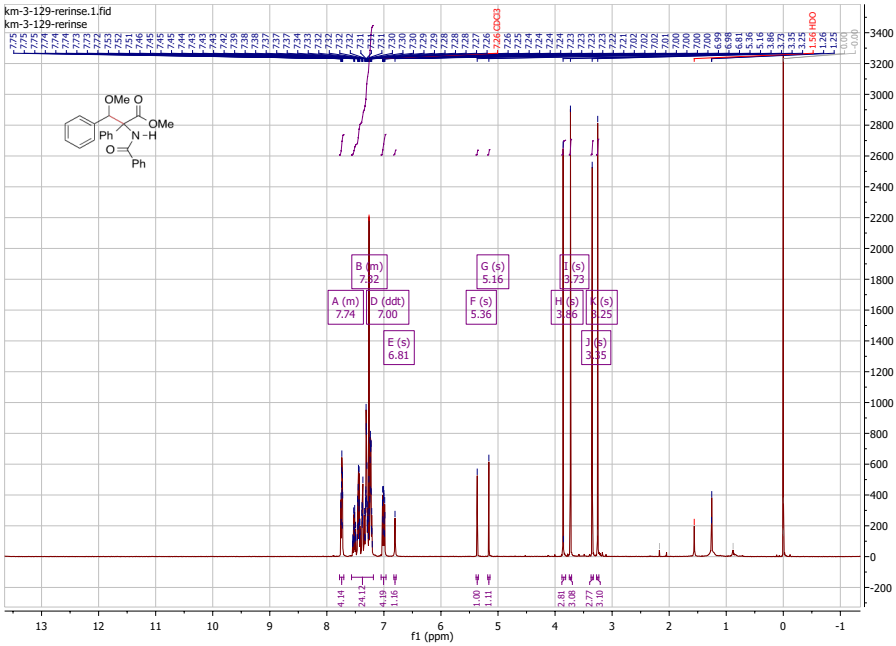
km-3-129-rerinse.1.fid
km-3-129-rerinse
OMe O
OMe
Ph
N–H
O
Ph
B (m) 7.32
A (m) 7.74
D (ddt) 7.00
E (s) 6.81
G (s) 5.16
F (s) 5.36
H (s) 3.73
I (s) 3.86
K (s) 3.25
J (s) 3.35
f1 (ppm)

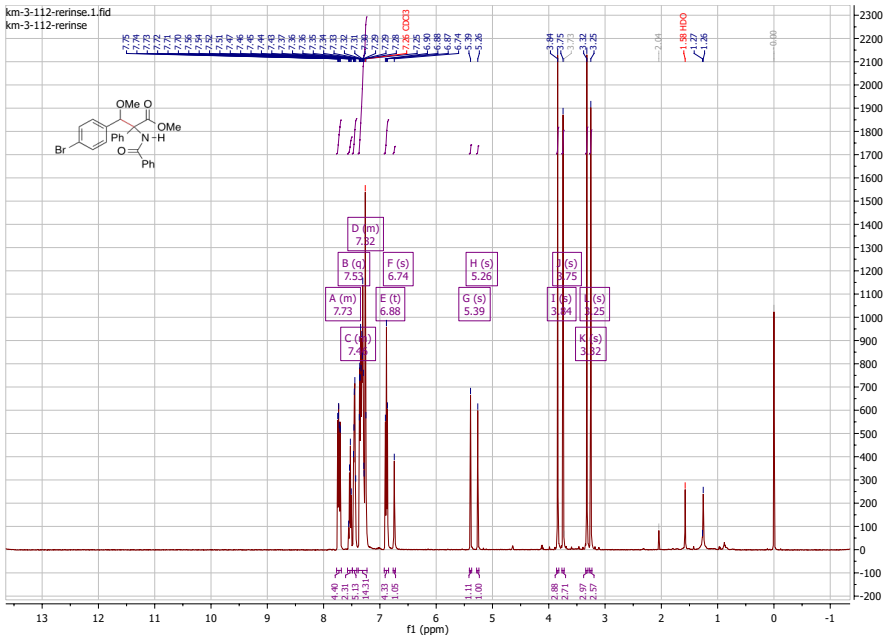
km-3-112-rerinse.1.fid
km-3-112-rerinse
OMe O
OMe
Ph
N
H
O
Br
Ph
D (m) 7.82
B (q) 7.53
F (s) 6.74
H (s) 5.26
J (s) 3.75
A (m) 7.73
E (t) 6.88
G (s) 5.39
I (s) 3.44
K (s) 3.32
C (m) 7.49
f1 (ppm)

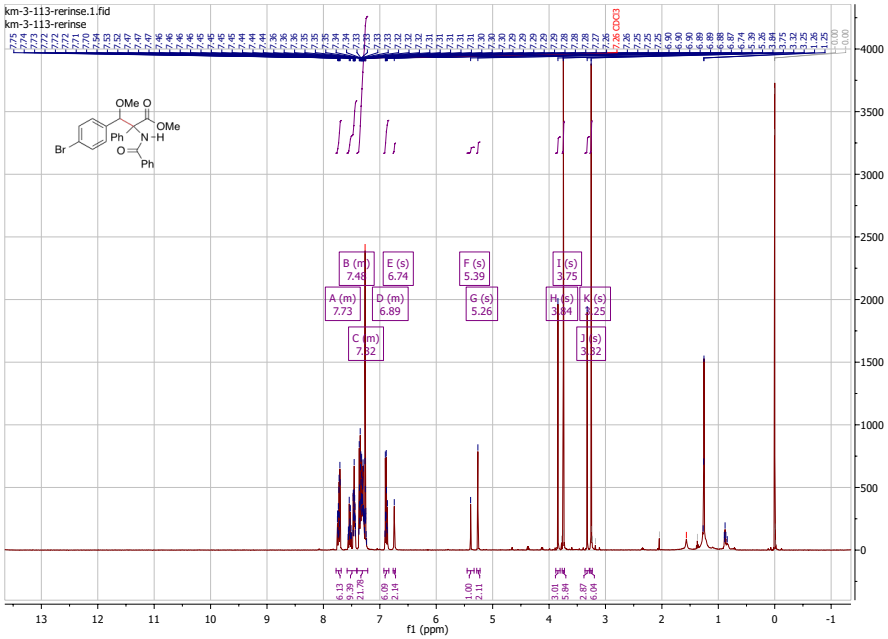
km-3-113-rerinse.1.fid
km-3-113-rerinse
OMe O
OMe
Ph
N
H
O
Br
Ph
B (m) 7.48
E (s) 6.74
F (s) 5.39
I (s) 3.75
A (m) 7.73
D (m) 6.89
G (s) 5.26
H (s) 3.44
K (s) 3.25
C (m) 7.82
J (s) 3.32
f1 (ppm)

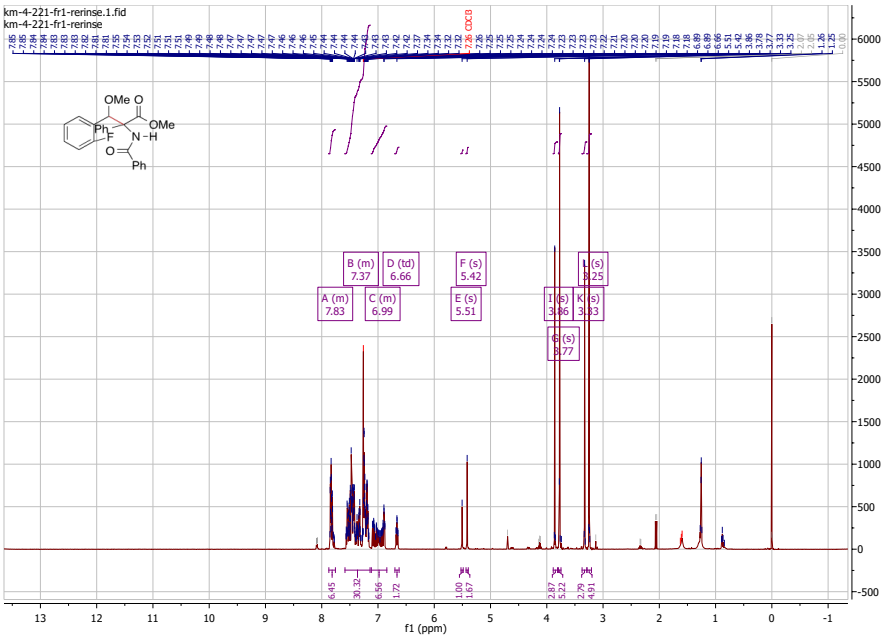
km-4-221-fr1-rerinse.1.fid
km-4-221-fr1-rerinse
OMe O
OMe
Ph
F
N–H
O
Ph
B (m) 7.37
D (td) 6.66
F (s) 5.42
A (m) 7.83
C (m) 6.99
E (s) 5.51
I (s) 3.86
K (s) 3.33
G (s) 3.77
f1 (ppm)

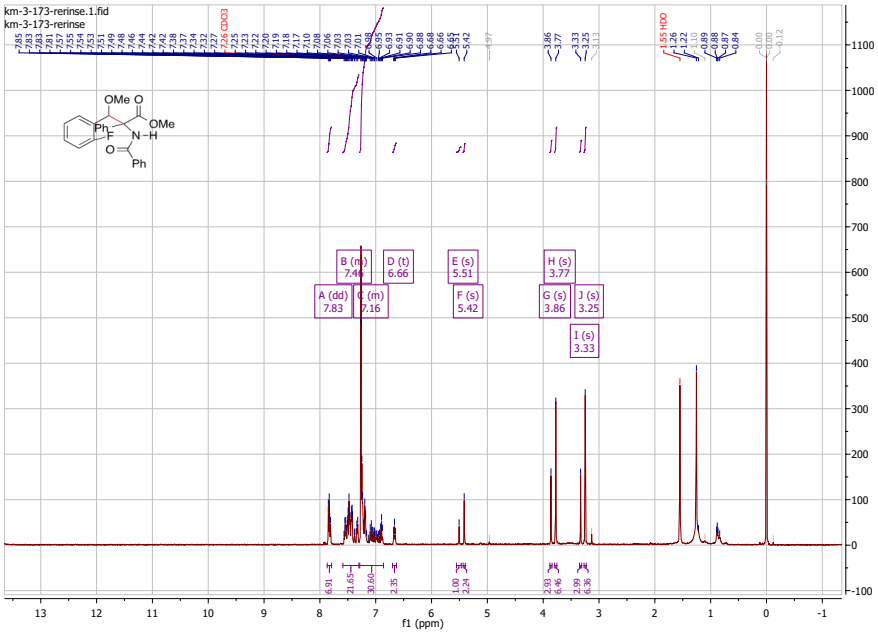
km-3-173-rerinse.1.fid
km-3-173-rerinse
OMe O
OMe
Ph
F
N–H
O
Ph
B (m) 7.46
D (t) 6.66
E (s) 5.51
H (s) 3.77
A (dd) 7.83
C (m) 7.16
F (s) 5.42
G (s) 3.86
J (s) 3.25
I (s) 3.33
f1 (ppm)

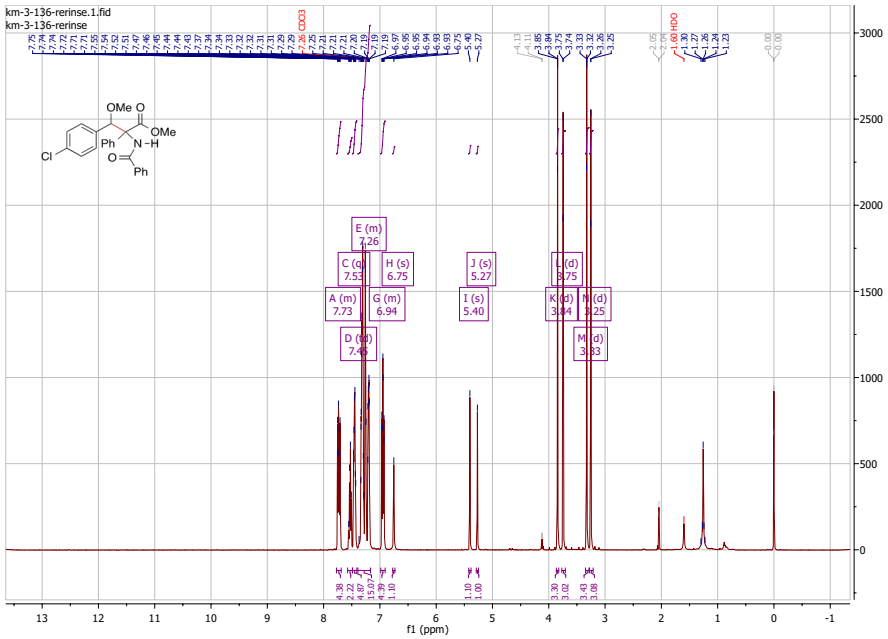
km-3-136-rerinse.1.fid
km-3-136-rerinse
OMe O
OMe
Ph
N-H
Cl
O
Ph
E (m)
7.26
C (q)
7.53
H (s)
6.75
J (s)
5.27
L (d)
3.75
A (m)
7.73
G (m)
6.94
I (s)
5.40
K (d)
3.44
N (d)
3.25
D (m)
7.49
M (d)
3.33
f1 (ppm)

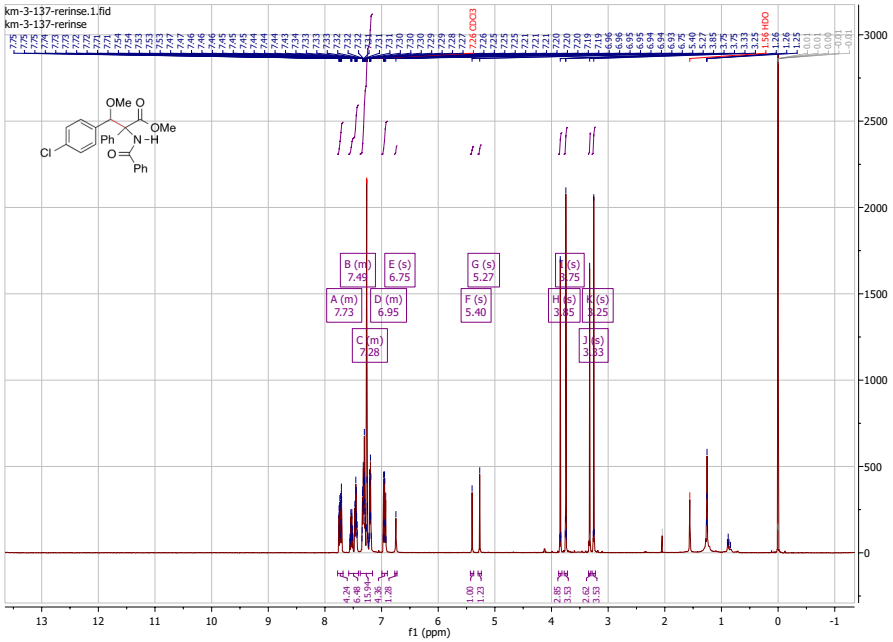
km-3-137-rerinse.1.fid
km-3-137-rerinse
OMe O
OMe
Ph
N-H
Cl
O
Ph
B (m)
7.49
E (s)
6.75
G (s)
5.27
I (s)
3.75
A (m)
7.73
D (m)
6.95
F (s)
5.40
H (s)
3.65
K (s)
3.25
C (m)
7.28
J (s)
3.33
f1 (ppm)

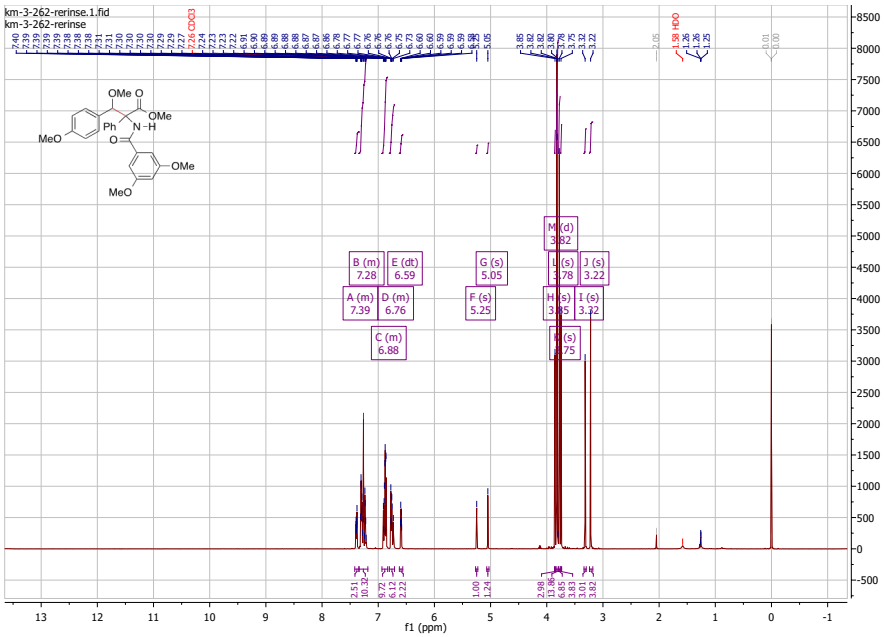
km-3-262-rerinse.1.fid
km-3-262-rerinse
OMe O
OMe
Ph
N-H
O
MeO
OMe
MeO
M (d) 3.82
B (m) 7.28
E (dt) 6.59
G (s) 5.05
L (s) 3.78
J (s) 3.22
A (m) 7.39
D (m) 6.76
F (s) 5.25
H (s) 3.85
I (s) 3.32
C (m) 6.88
K (s) 3.75
f1 (ppm)

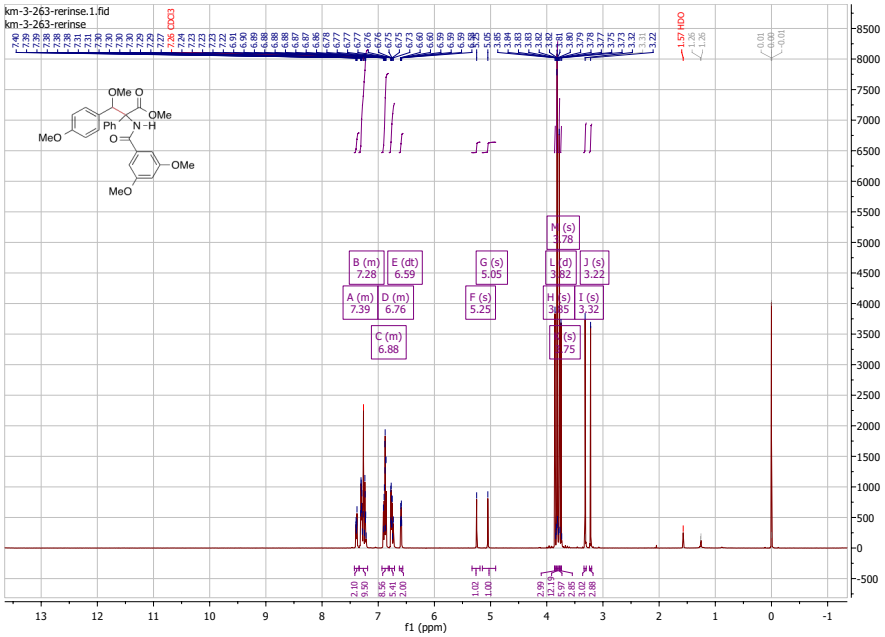
km-3-263-rerinse.1.fid
km-3-263-rerinse
OMe O
OMe
Ph
N-H
O
MeO
OMe
MeO
M (s) 3.78
B (m) 7.28
E (dt) 6.59
G (s) 5.05
L (d) 3.82
J (s) 3.22
A (m) 7.39
D (m) 6.76
F (s) 5.25
H (s) 3.85
I (s) 3.32
C (m) 6.88
K (s) 3.75
f1 (ppm)

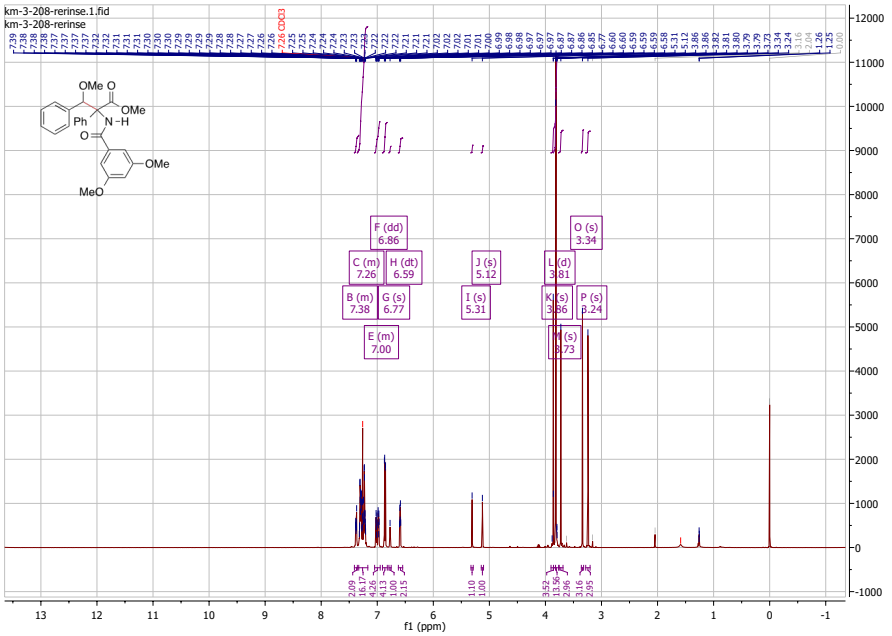
km-3-208-rerinse.1.fid
km-3-208-rerinse
OMe O
OMe
Ph
N–H
O
OMe
MeO
F (dd) 6.86
O (s) 3.34
C (m) 7.26
H (dt) 6.59
J (s) 5.12
L (d) 3.81
B (m) 7.38
G (s) 6.77
I (s) 5.31
K (s) 3.86
P (s) 3.24
E (m) 7.00
N (s) 3.73
f1 (ppm)

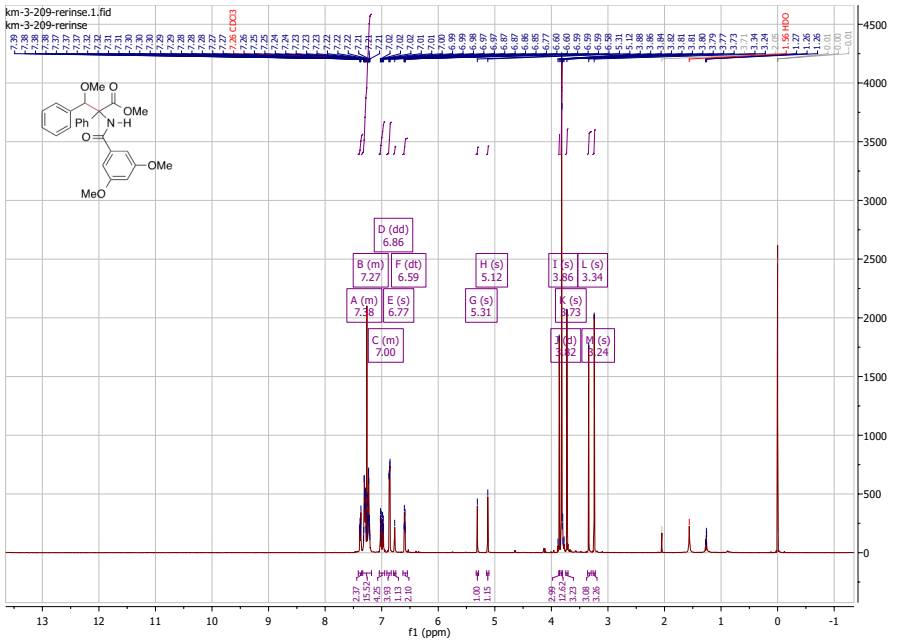
km-3-209-rerinse.1.fid
km-3-209-rerinse
OMe O
OMe
Ph
N–H
O
OMe
MeO
D (dd) 6.86
B (m) 7.27
F (dt) 6.59
H (s) 5.12
I (s) 3.86
L (s) 3.34
A (m) 7.38
E (s) 6.77
G (s) 5.31
K (s) 3.73
C (m) 7.00
J (d) 3.82
M (s) 3.24
f1 (ppm)

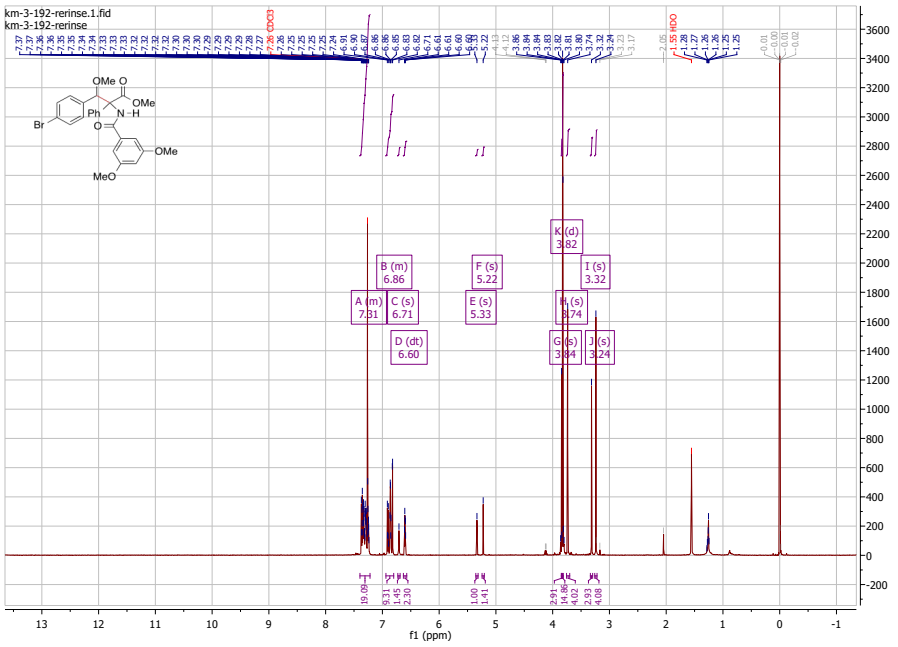
km-3-192-rerinse.1.fid
km-3-192-rerinse
OMe O
OMe
Ph
N–H
O
Br
OMe
MeO
B (m) 6.86
A (m) 7.31
C (s) 6.71
D (dt) 6.60
F (s) 5.22
E (s) 5.33
K (d) 3.82
H (s) 3.74
I (s) 3.32
G (s) 3.84
J (s) 3.24
f1 (ppm)

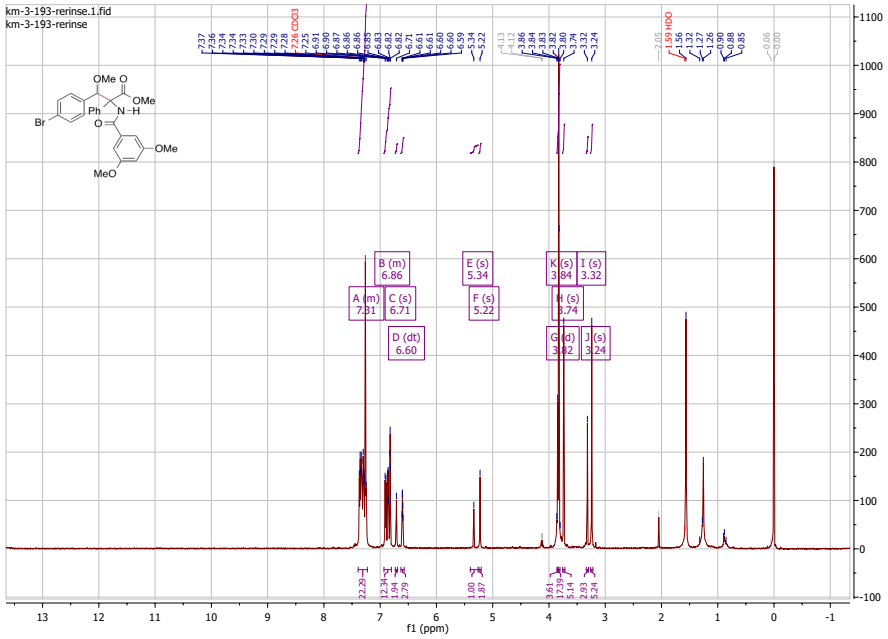
km-3-193-rerinse.1.fid
km-3-193-rerinse
OMe O
OMe
Ph
N–H
O
Br
OMe
MeO
B (m) 6.86
A (m) 7.31
C (s) 6.71
D (dt) 6.60
E (s) 5.34
F (s) 5.22
K (s) 3.84
I (s) 3.32
H (s) 3.74
G (d) 3.82
J (s) 3.24
f1 (ppm)

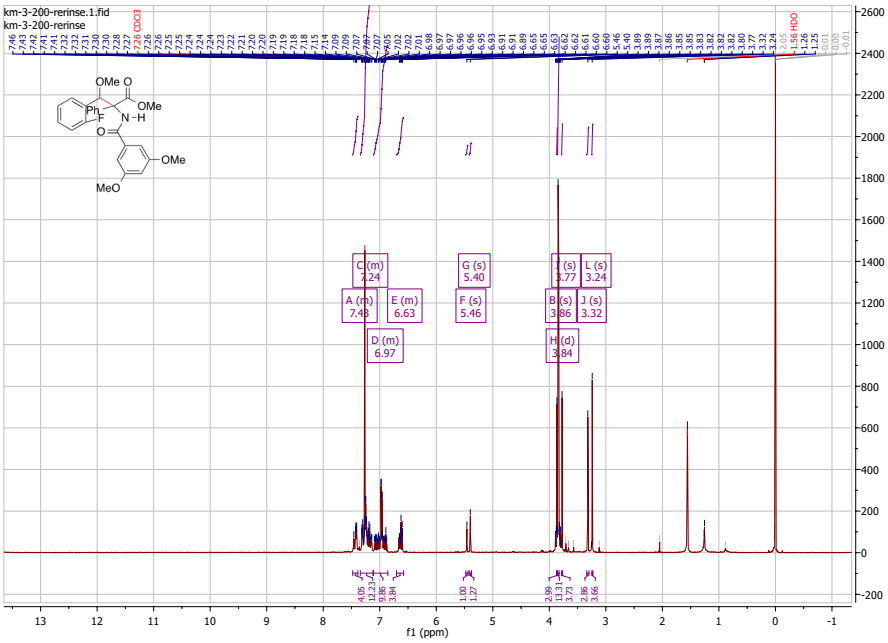
km-3-200-rerinse.1.fid
km-3-200-rerinse
f1 (ppm)

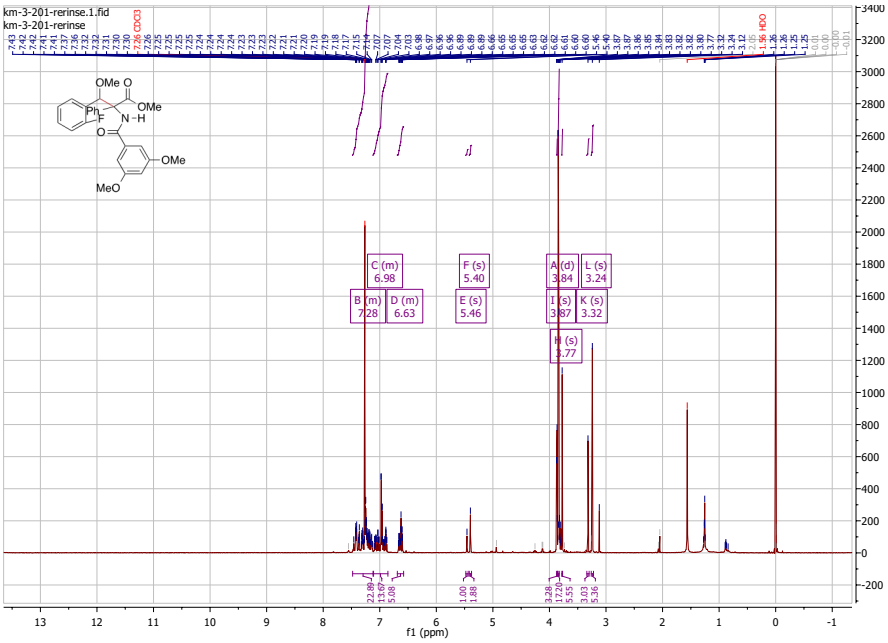
km-3-201-rerinse.1.fid
km-3-201-rerinse
f1 (ppm)

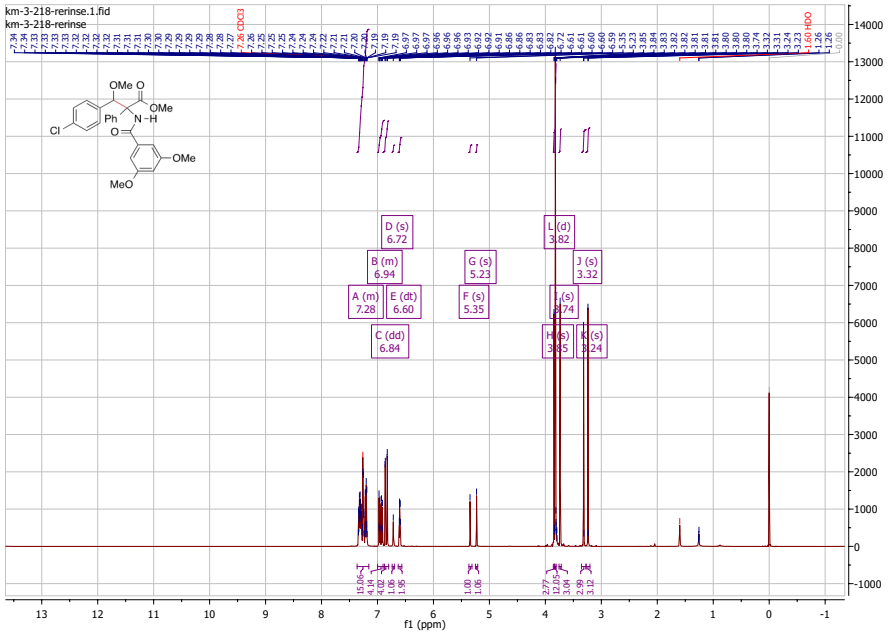
km-3-218-rerinse.1.fid
km-3-218-rerinse
OMe O
OMe
Ph
N–H
Cl
O
OMe
MeO
D (s) 6.72
B (m) 6.94
A (m) 7.28
E (dt) 6.60
C (dd) 6.84
G (s) 5.23
F (s) 5.35
L (d) 3.82
J (s) 3.32
H (s) 3.85
K (s) 3.24
f1 (ppm)

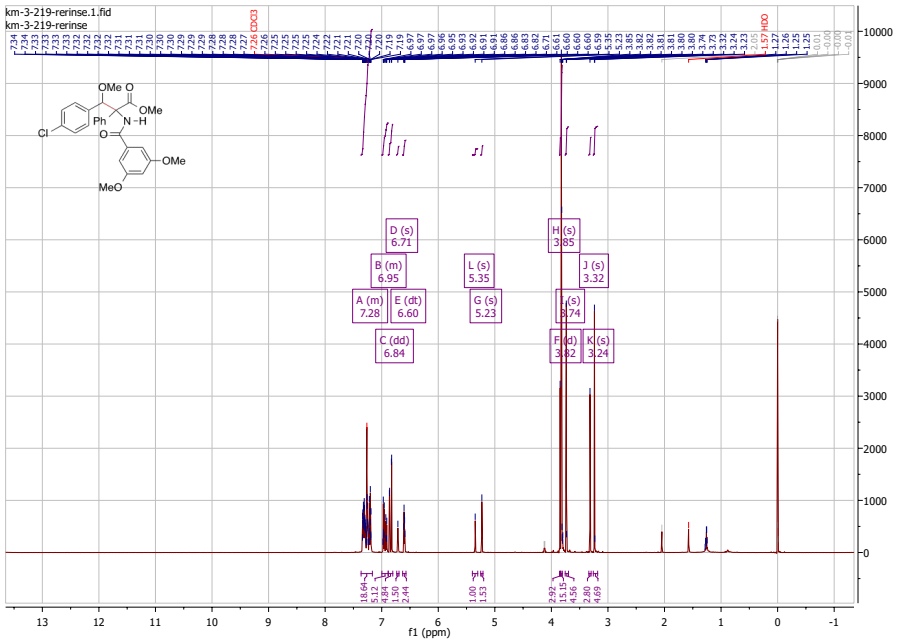
km-3-219-rerinse.1.fid
km-3-219-rerinse
OMe O
OMe
Ph
N–H
Cl
O
OMe
MeO
D (s) 6.71
B (m) 6.95
A (m) 7.28
E (dt) 6.60
C (dd) 6.84
L (s) 5.35
G (s) 5.23
H (s) 3.85
J (s) 3.32
F (d) 3.82
K (s) 3.24
f1 (ppm)

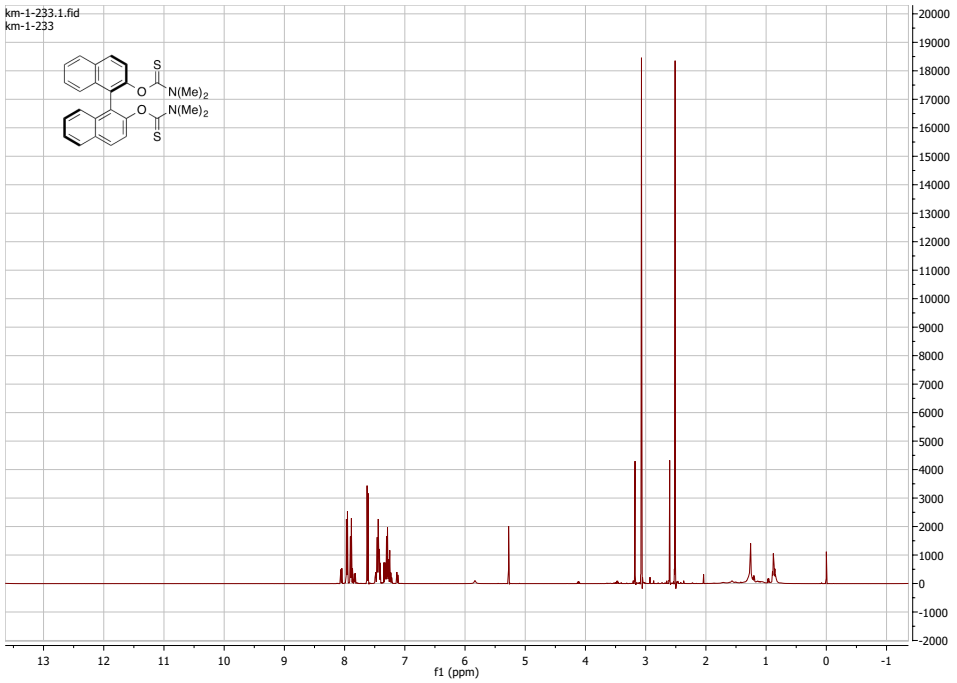
km-1-233.1.fid
km-1-233
S
O
N(Me)2
O
N(Me)2
S
f1 (ppm)

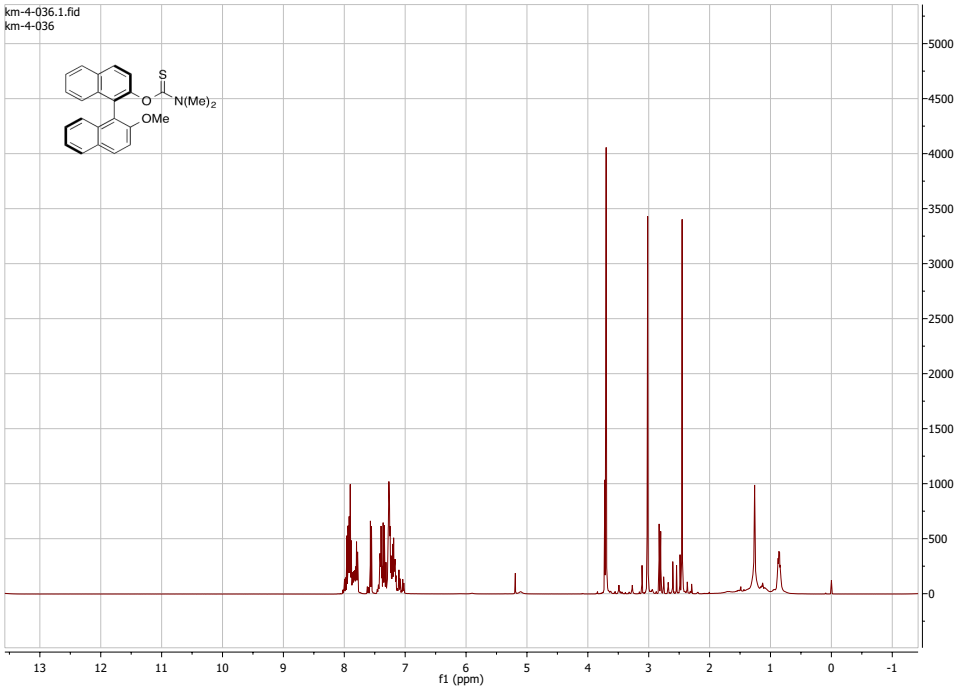
km-4-036.1.fid
km-4-036
S
O
N(Me)2
OMe
f1 (ppm)

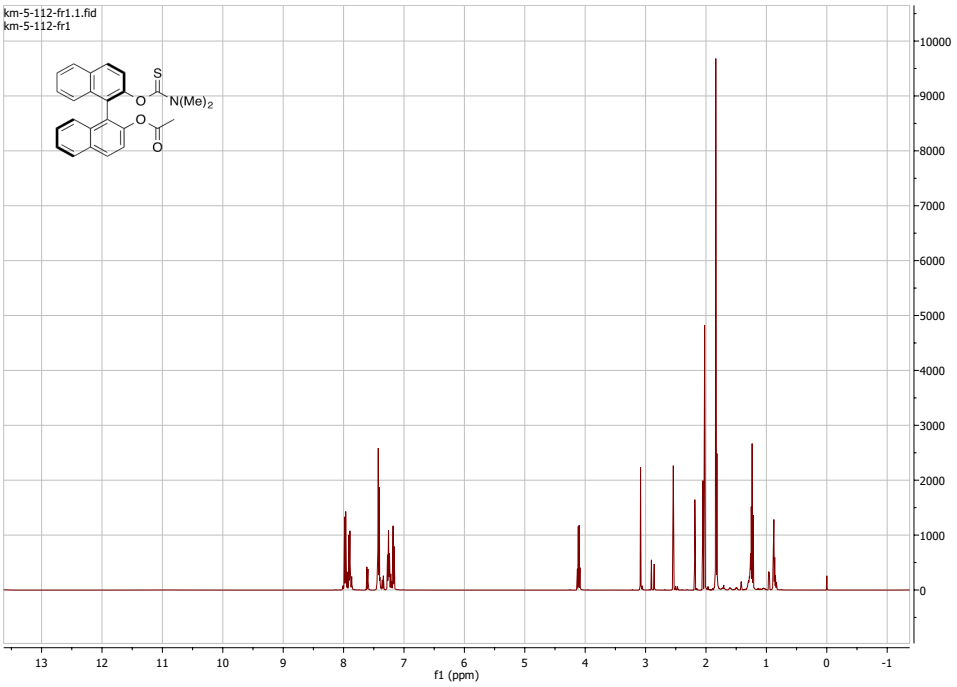
km-5-112-fr1.1.fid
km-5-112-fr1
S
O
N(Me)2
O
O
f1 (ppm)

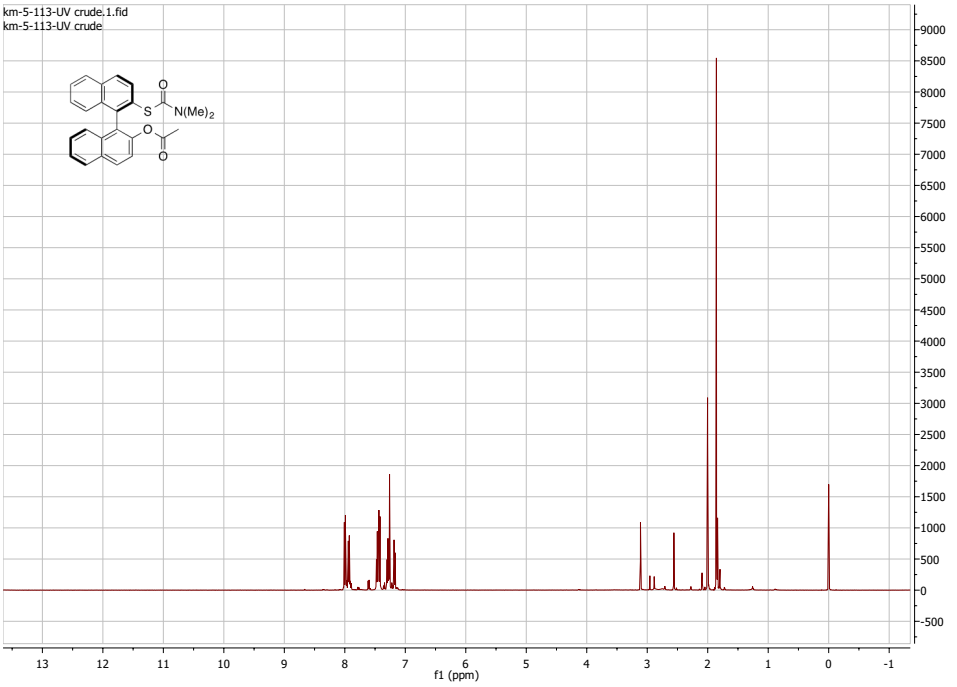
km-5-113-UV crude.1.fid
km-5-113-UV crude
O
S
N(Me)2
O
O
f1 (ppm)

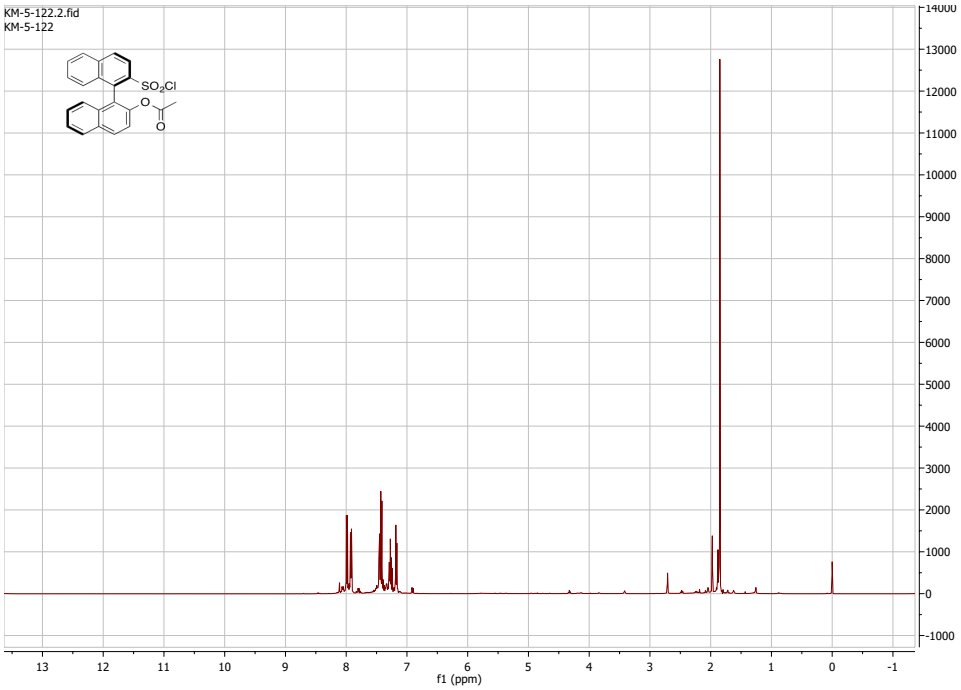
KM-5-122.2.fid
KM-5-122
SO2Cl
O
O
f1 (ppm)

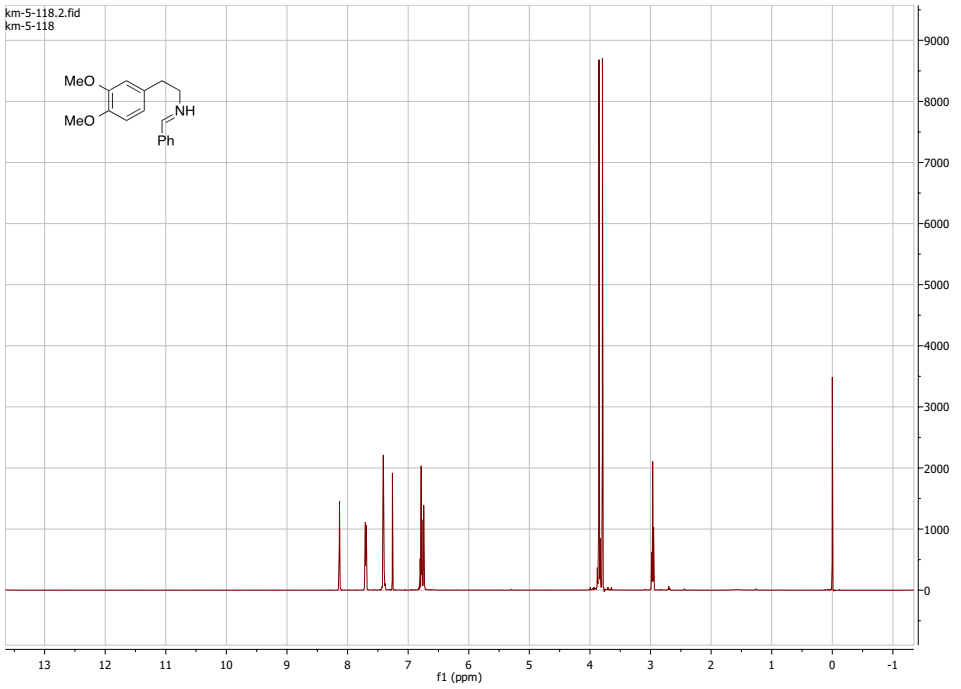
km-5-118.2.fid
km-5-118
MeO
MeO
NH
Ph
f1 (ppm)

APPENDIX B. ^{13}C NMR SPECTRA

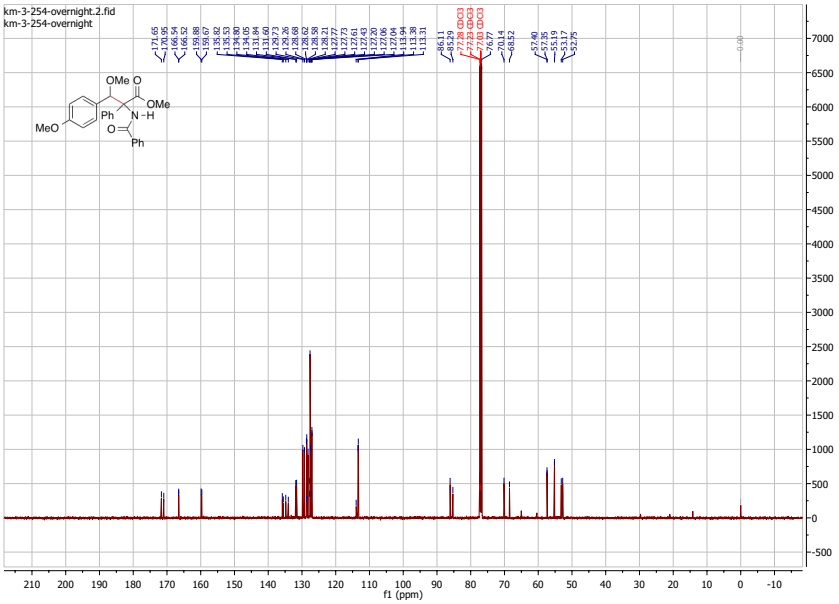

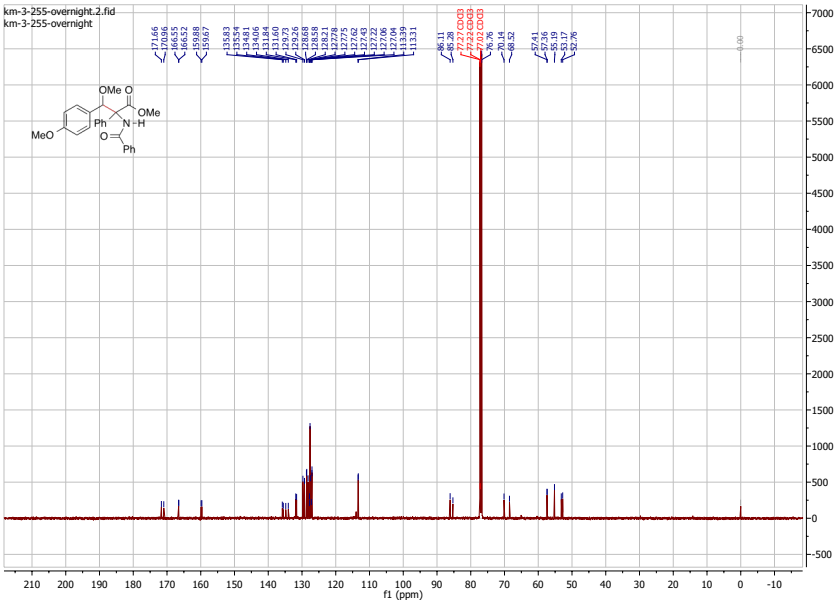

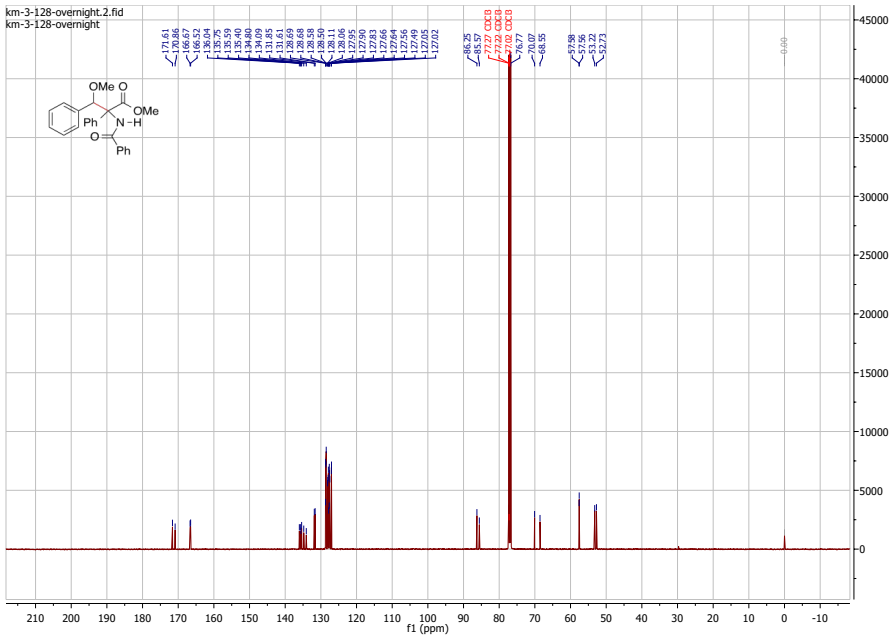
km-3-128-overnight.2.fid
km-3-128-overnight
f1 (ppm)

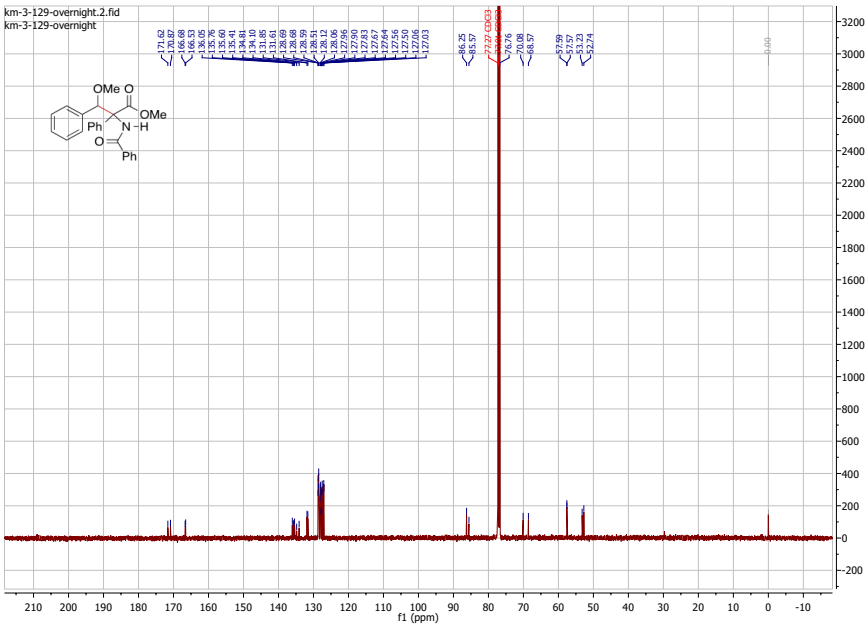
km-3-129-overnight.2.fid
km-3-129-overnight
f1 (ppm)

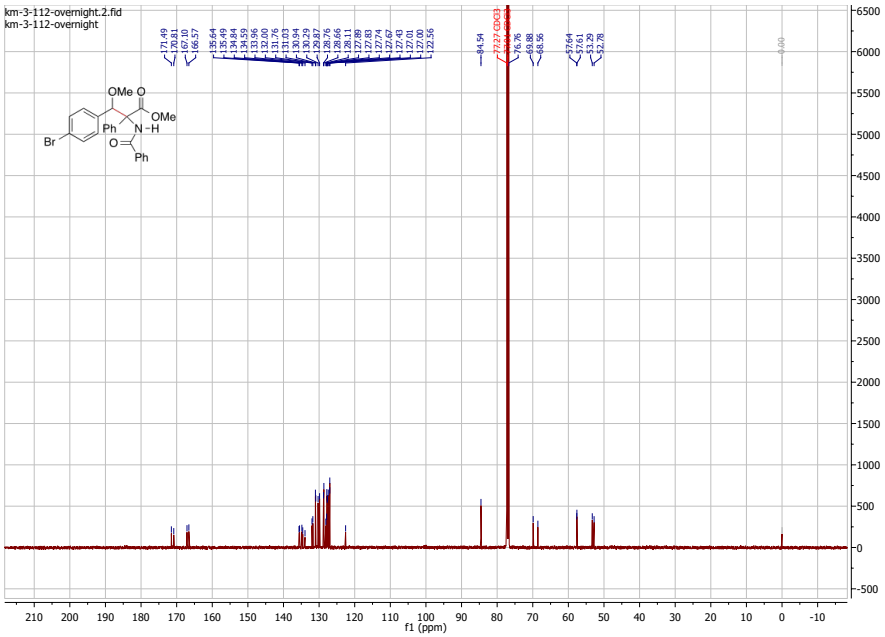
km-3-112-overnight.2.fid
km-3-112-overnight
f1 (ppm)

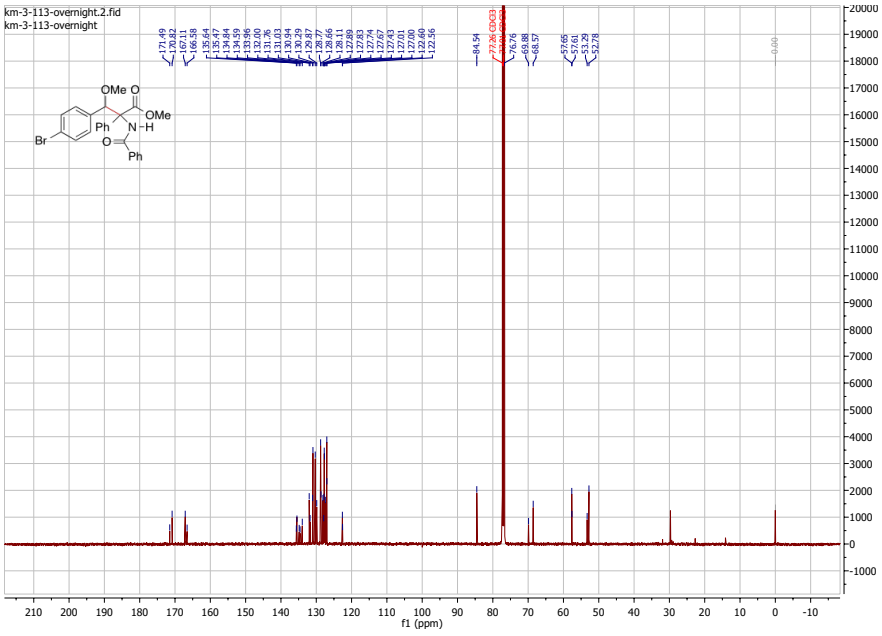
km-3-113-overnight.2.fid
km-3-113-overnight
f1 (ppm)

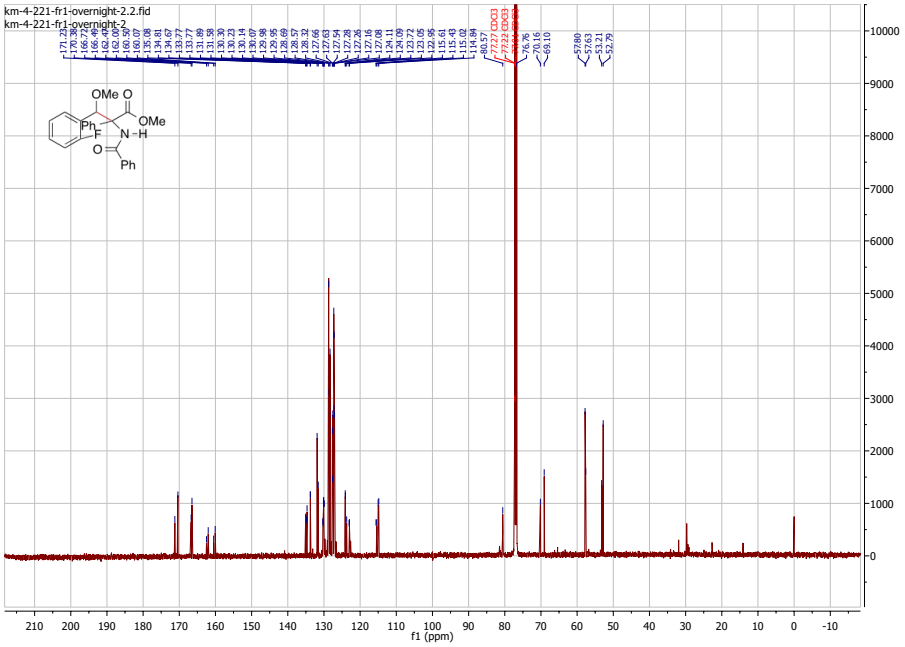
km-4-221-fr1-overnight-2.2.fid
km-4-221-fr1-overnight-2
OMe O
OMe
Ph
F
N–H
O
Ph
f1 (ppm)

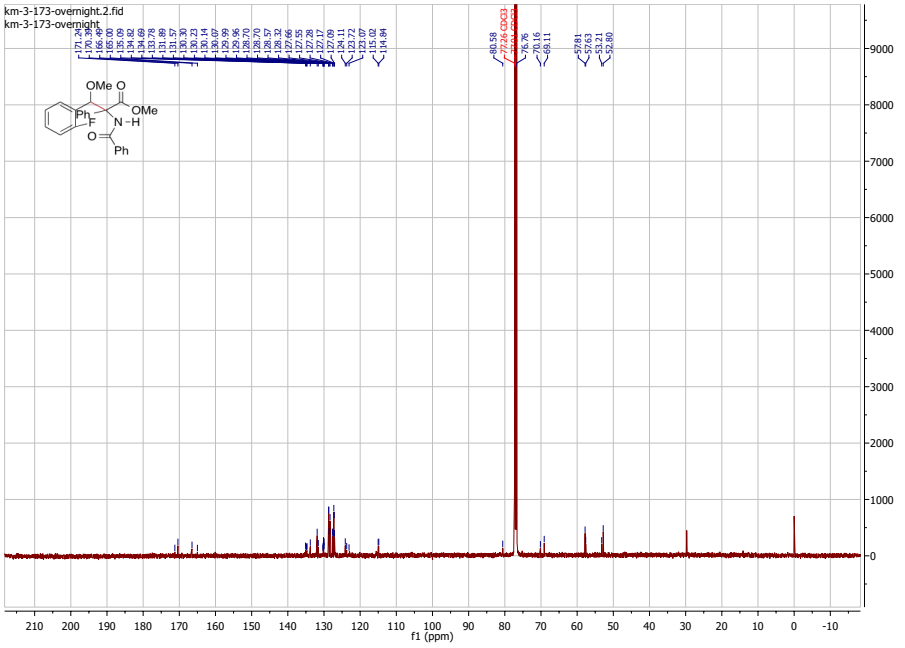
km-3-173-overnight.2.fid
km-3-173-overnight
OMe O
OMe
Ph
F
N–H
O
Ph
f1 (ppm)

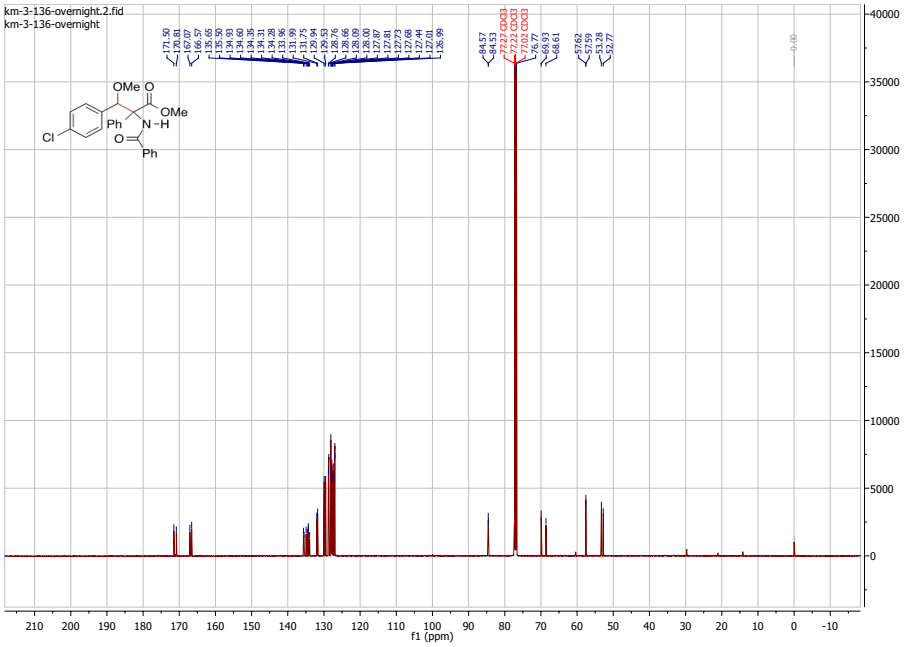
km-3-136-overnight.2.fid
km-3-136-overnight
f1 (ppm)

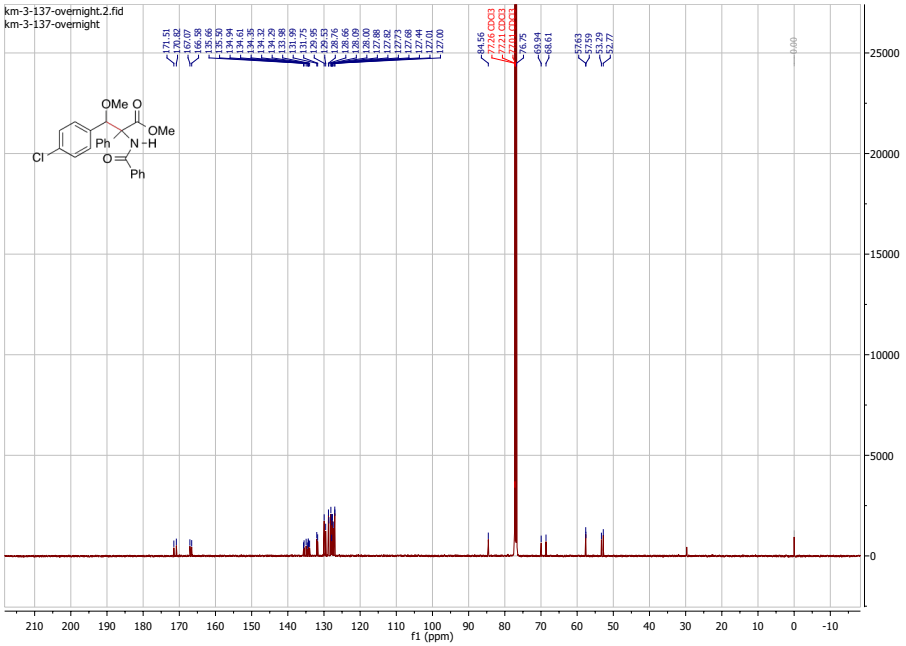
km-3-137-overnight.2.fid
km-3-137-overnight
f1 (ppm)

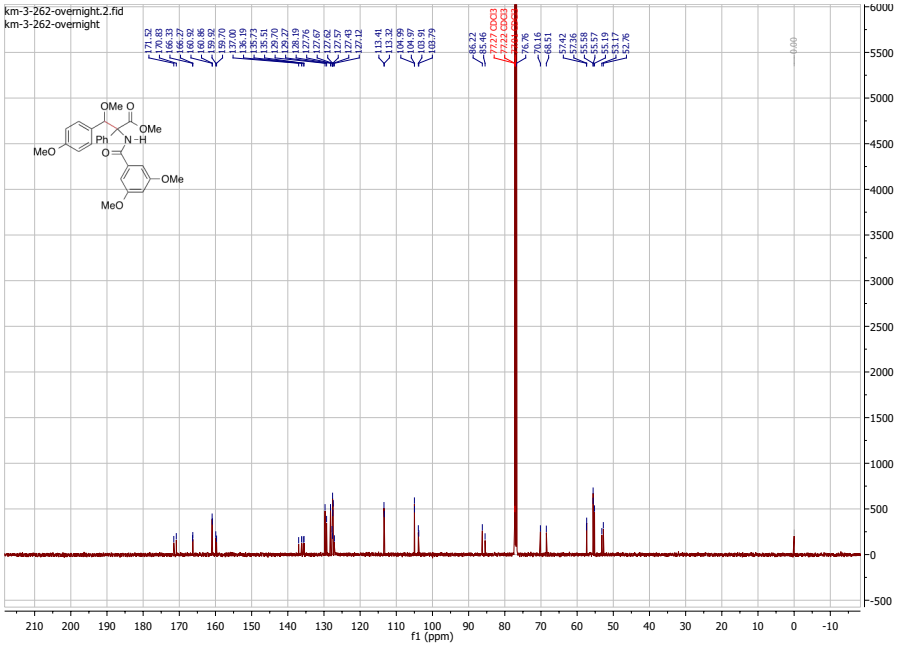
km-3-262-overnight.2.fid
km-3-262-overnight
f1 (ppm)

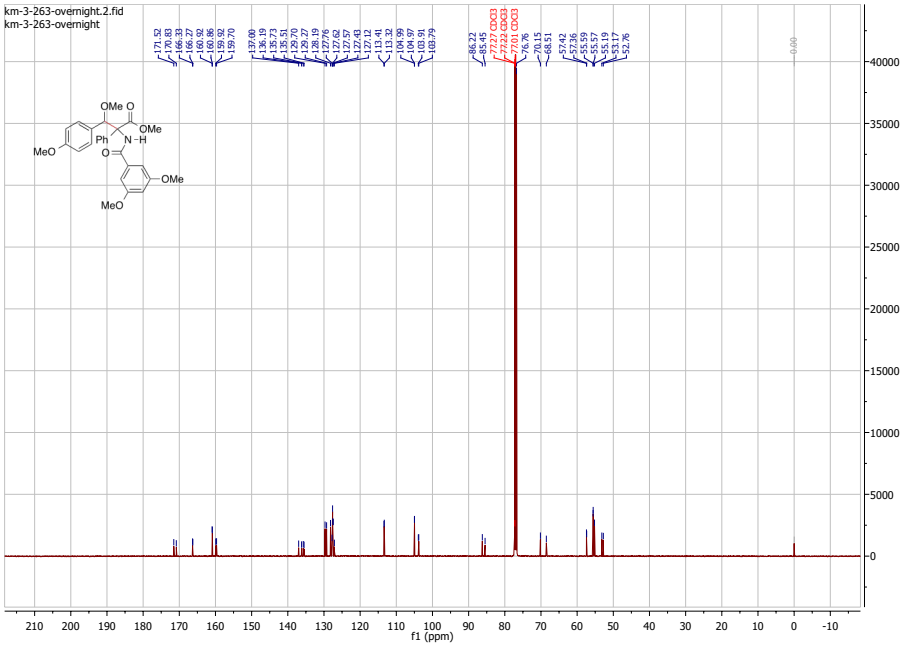
km-3-263-overnight.2.fid
km-3-263-overnight
f1 (ppm)

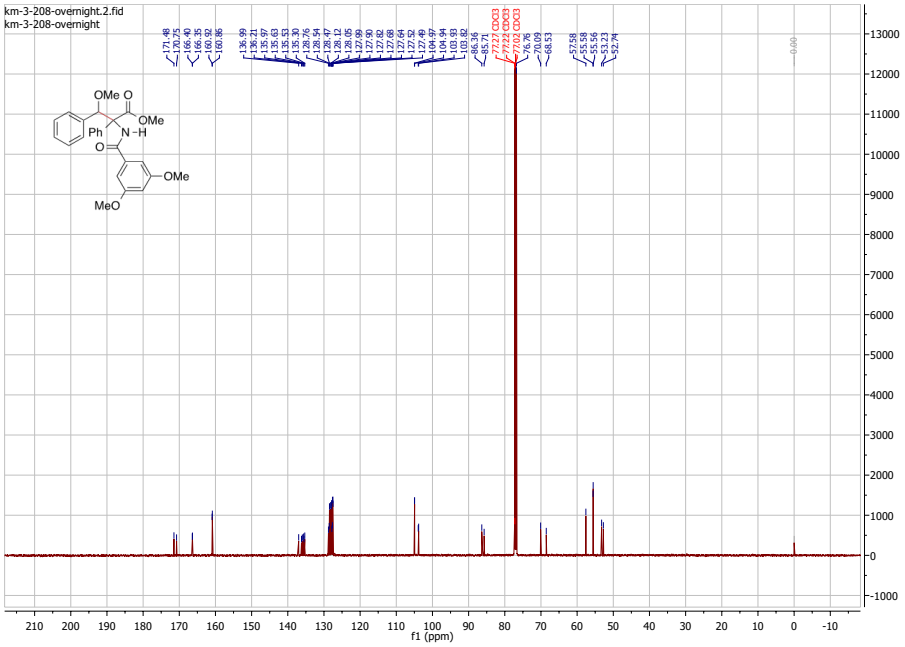
km-3-208-overnight.2.fid
km-3-208-overnight
OMe O
OMe
Ph
N
H
O
OMe
MeO
f1 (ppm)

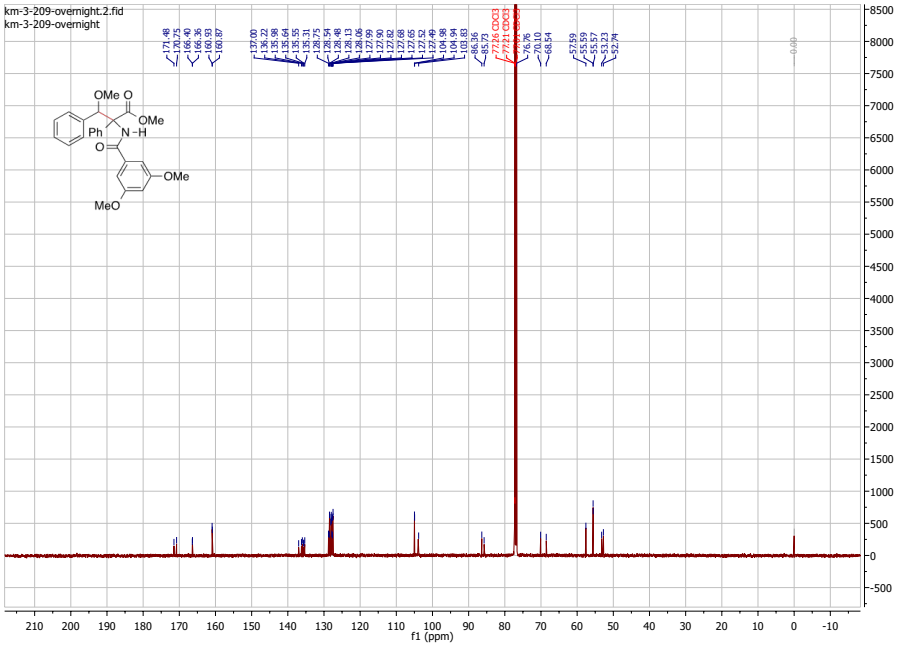
km-3-209-overnight.2.fid
km-3-209-overnight
OMe O
OMe
Ph
N
H
O
OMe
MeO
f1 (ppm)

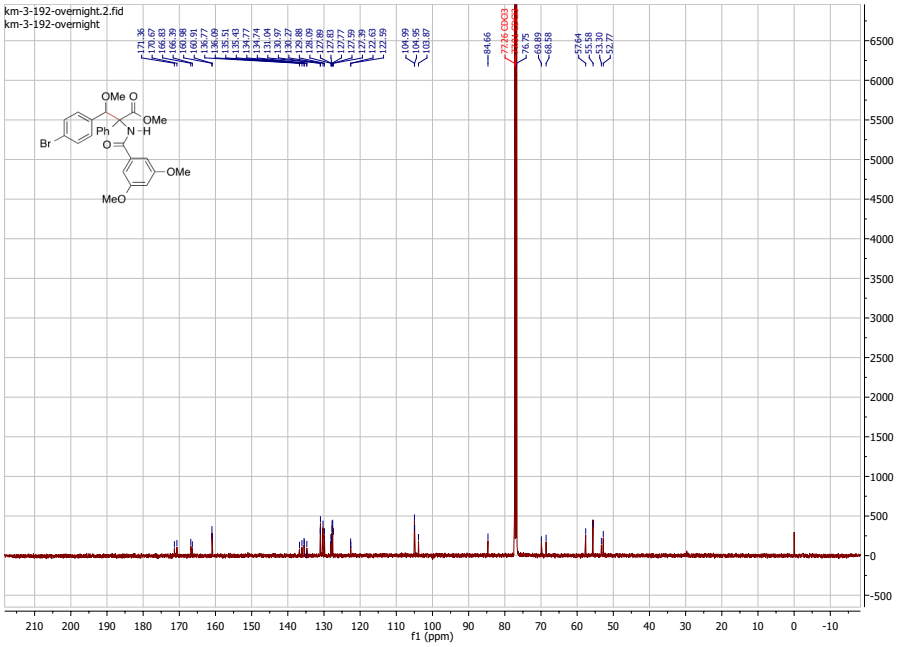
km-3-192-overnight.2.fid
km-3-192-overnight
f1 (ppm)

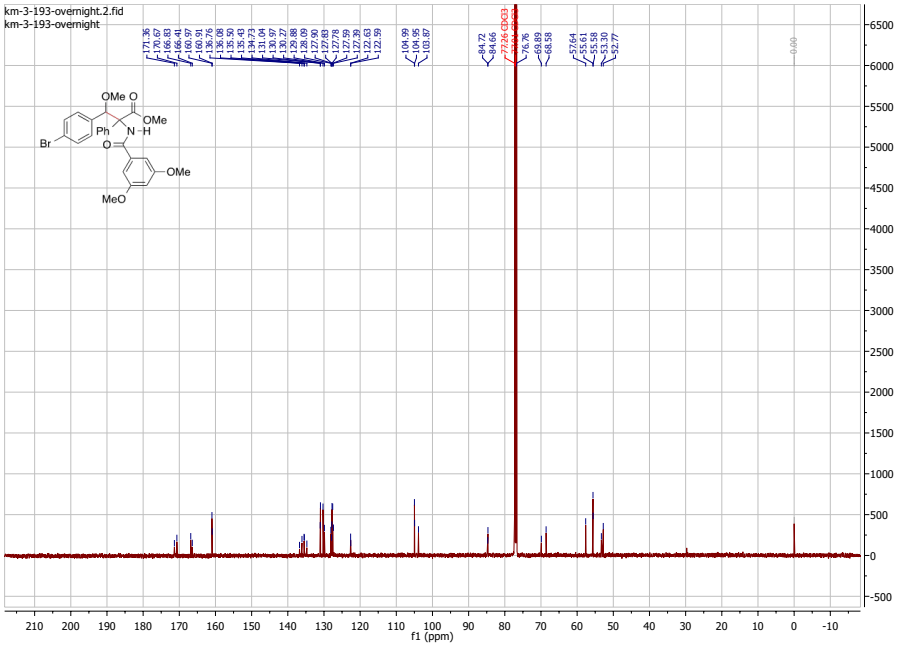
km-3-193-overnight.2.fid
km-3-193-overnight
f1 (ppm)

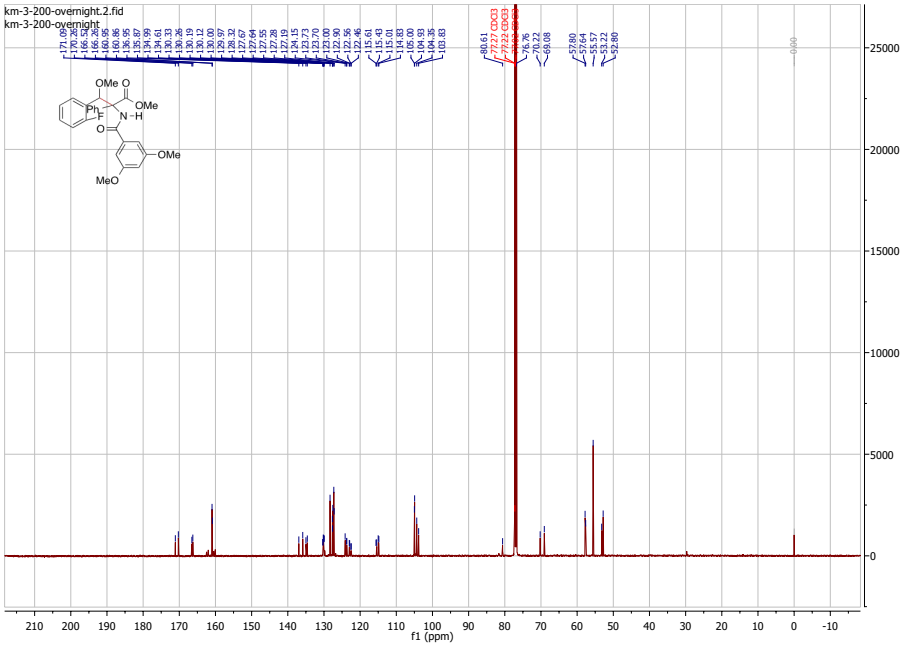
km-3-200-overnight.2.fid
km-3-200-overnight
f1 (ppm)

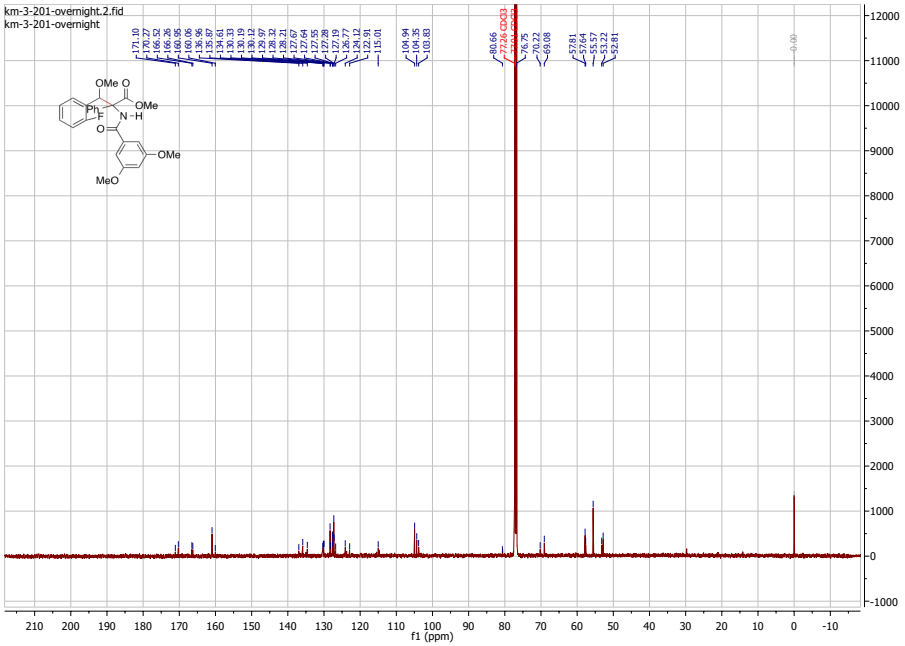
km-3-201-overnight.2.fid
km-3-201-overnight
f1 (ppm)

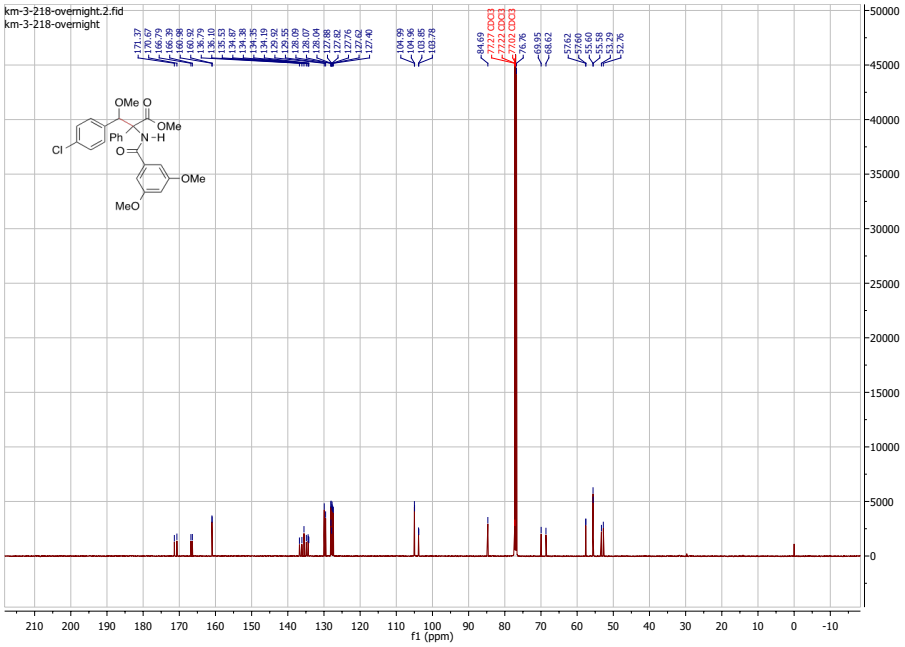
km-3-218-overnight.2.fid
km-3-218-overnight
f1 (ppm)

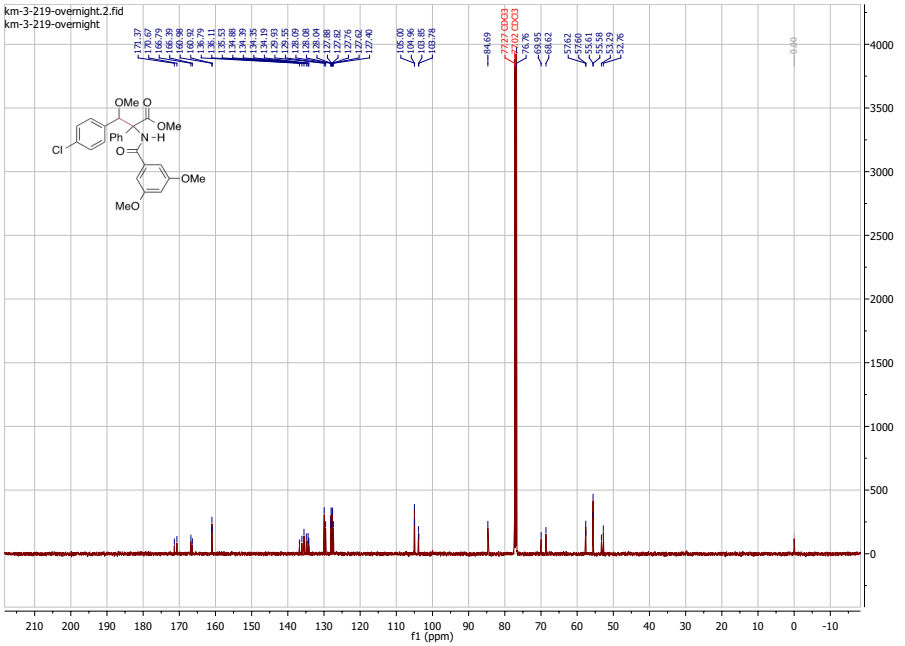
km-3-219-overnight.2.fid
km-3-219-overnight
f1 (ppm)